Title
Analysis of Signal Transduction Pathways in Induced Pluripotent Stem Cell Reprogramming

Author
Fritz, Ashley Linn

Publication Date
2013

Peer reviewed|Thesis/dissertation

Analysis of Signal Transduction Pathways in Induced Pluripotent Stem Cell Reprogramming

By

Ashley Linn Fritz

A dissertation submitted in partial satisfaction of the

requirements for the degree of

Doctor of Philosophy

in

Chemical Engineering

in the

Graduate Division

of the

University of California, Berkeley

Committee in charge:

Professor David Schaffer, Chair
Professor Danielle Tullman Ercek
Professor Lin He

Fall 2013

Abstract

Analysis of Signal Transduction Pathways in Induced Pluripotent Stem Cell Reprogramming

by

Ashley Linn Fritz

Doctor of Philosophy in Chemical Engineering

University of California, Berkeley

Professor David V. Schaffer, Chair

Embryonic stem cells have immense biomedical potential, since they are pluripotent and thus have the capability to form any cell type in the adult body. Human embryonic stem cell derivation, however, involves destroying "leftover" embryos - a non-ideal scenario both ethically and as the embryonic stem cells may not be representative of, or "tissue compatible" with, the general patient population. In 2006, researchers discovered a way to "reprogram" an adult cell into an embryonic-like cell by expressing only four genes, the "Yamanaka factors" (*c-Myc*, *Klf4*, *Oct4*, *Sox2*), work that was awarded the 2012 Nobel Prize in Medicine. The resultant embryonic-like cells were termed induced pluripotent stem (iPS) cells. With this technology, cell-replacement therapies, where a diseased cell type in an individual is replaced with stem cell-derived cells, will be able to utilize a patient's own cells. Additionally, biopsies from patients will allow for researchers to study and culture diseased cells, a benefit especially if the cause of the disease is unknown and the diseased cells are not easily isolated.

However, two limitations hinder the applications of iPS cell technology. First, the formation of iPS cells is very inefficient, with only 0.01-0.1% of cells converting back to an embryonic-like state. Second, there is an increased risk of cell abnormalities and cancer. The delivery of the factors to cells is mediated by viral delivery, which can modify the genome and activate cancer-causing genes. Additionally, the proteins KLF4 and C-MYC are oncogenes, or have the potential to cause cancer. Typically, replacing a factor or changing the gene delivery method from viral gene delivery results in an even lower efficiency and has remained a challenge for iPS cell technology.

Signal transduction, the relay of an input from outside the cell to the DNA inside the nucleus, is mediated through protein-protein interactions, and has been shown to be a central regulator of cell behavior. Signal transduction proteins directly affect the activation of transcription factors (such as C-MYC, KLF4, OCT4, and SOX2), which then bind to DNA to regulate gene expression. Because signal transduction proteins are more easily manipulated through small molecules (drugs) and external proteins, I have developed a way to study signal transduction during iPS cell reprogramming.

I have created a library of 38 genes encoding signal transduction proteins that can upregulate and downregulate major signaling pathways within the cell. The library can be used in a modular approach to study reprogramming using mouse cells. First, the library can be used by itself to see if there are any combinations of signaling proteins that can replace the Yamanaka factors. Second, the library can be used in conjunction with the Yamanaka factors to see how

signaling proteins affect reprogramming. Third, the library can be used to see if any signaling proteins can replace OCT4, SOX2, and KLF4.

The second aim of the library, to see how each signaling protein affects reprogramming, resulted in a group of genes that aided in reprogramming, a group that had no effect on reprogramming, and a group that was deleterious to reprogramming. Importantly, the results from the library showed that previously published results aligned with our data, verifying our methods to study reprogramming. Additionally, I identified several GTPases that improve or hinder iPS cell reprogramming, factors that to date have not been largely studied in reprogramming.

To learn more about the individual signaling proteins and their role in reprogramming, I performed studies looking if each signaling protein could replace OCT4, SOX2, and KLF4. The most promising results were in replacing OCT4, which to date has been the most difficult to replace as SOX2, KLF4, and c-MYC have published small molecule replacements. I discovered an activated cell surface receptor, GNAS, that could replace OCT4 with approximately 8% of the efficiency of OCT4, SOX2, KLF4, and C-MYC. Forskolin, a small molecule that mimicked the activity of the receptor could also replace OCT4 with a 2.1-fold increase in reprogramming efficiency. To illustrate these cells are pluripotent, I did immunostaining to probe for the presence of embryonic stem cell markers, SSEA1, OCT4, and NANOG. The cells were able to differentiate into the three germ layers, resulting in cells from the brain, muscle, liver, and heart. Additionally, I have determined that forskolin acts via the EPAC signaling pathway and is necessary and sufficient to induce colony formation. Forskolin also increases epithelial gene expression, decreases mesenchymal gene expression, and increases cell proliferation to replace OCT4 during reprogramming

To date, this work shows a small molecule can replace OCT4 to result in pluripotent cells. Not only does this aid the understanding of reprogramming biology, but it is an initial step in finding a method to reprogram without viruses or oncogenes, which is ideal for downstream applications such as cell-replacement therapies and disease studies.

TABLE OF CONTENTS

List of Tables and Figures iv
Acknowledgments vii

Chapter 1: Introduction 1
Embryonic and Induced Pluripotent Stem Cells 1
Intracellular Signal Transduction and Induced Pluripotent Stem Cells 3
Signal Transduction Library 5
References 5

Chapter 2: A Medium-Throughput Analysis of Signaling Involved in Early Stages of Stem Cell Reprogramming 9
Abstract 9
Introduction 9
Materials and Methods 10
Cell Culture and Plasmid Construction 10
Viral Production and Titering 11
iPS Cell Reprogramming and Analysis 11
Results 12
Discussion 18
References 19

Chapter 3: Analysis of Smoothened, Ras, and Notch Signal Transduction Pathways During Induced Pluripotent Stem Cell Reprogramming 23
Abstract 23
Introduction 23
Materials and Methods 24
Cell Culture and Plasmid Construction 24
Viral Production and Titering 25
iPS Cell Reprogramming – Factor Replacement 25
Sonic Hedgehog Reprogramming 25
NANOG Analysis 26
Cell Line Isolation and Pluripotency Immunostaining 26
Embryoid Body Differentiation 26
Results 27
Screening for OCT4, KLF4, or SOX2 Replacements Results in Minimal Reprogramming 27
External Activation of the Sonic Hedgehog Pathway Minimally Improves Reprogramming 30
Activation of the MAPK Pathway Can Replace KLF4 or OCT4 to Result in NANOG Positive Colonies 31
Notch1 Activates Pluripotency Markers in the Absence of OCT4 but Fails to Induce Ectoderm Differentiation 33
Discussion 34
References 35

Chapter 4: cAMP and EPAC Signaling Can Functionally Replace OCT4 During Induced Pluripotent Stem Cell Reprogramming **38**
Abstract 38
Introduction 38
Materials and Methods 39
Cell Culture 39
Viral Production and Titer 39
iPS Cell Reprogramming and Efficiency Calculations 40
Cell Line Isolation and Pluripotency Immunostaining 40
Embryoid Body Differentiation 41
Small Molecule Reprogramming Assay 41
Proliferation Assay 42
Quantitative RT-PCR 42
Results 42
Adenylyl Cyclase Activators Produce OCT4 Positive Colonies in the Absence of the Oct4 Transgene 42
cAMP Activation with 2i Inhibition Results in Pluripotency without the Oct4 Transgene 44
cAMP Acts Through the EPAC-RAP1 Pathway to Induce Reprogramming 47
cAMP Signaling Increases Cellular Division Rates and Regulates Genes Involved in the Mesenchymal to Epithelial Transition to Replace OCT4 48
Discussion 50
References 52

Appendix A: Gene Information **56**

Appendix B: Cloning Primer Information **62**

Appendix C: Colony Counting Code **64**

Appendix D: Supplemental Figures for Chapter 2 **72**

Appendix E: Supplemental Information for Chapter 3 **77**
Supplemental Figures 77
Supplemental Tables 80
Supplemental Methods 81
OSKM Replacement Reprogramming 81

Appendix F: Supplemental Information for Chapter 4 **82**
Supplemental Figures 82
Supplemental Tables 89
Supplemental Methods 89
Toxicity Measurements 89
Mouse Ear Fibroblast Reprogramming 90
Complete Factor Replacement with Small Molecules 90

References 90

Appendix G: Supplemental Protocols **91**
General Protocol for Reprogramming 91
Mouse iPSC Colony Selection 94
Mouse iPS Cell Culturing Protocol 97
Immunocytochemistry Protocol (Pluripotency and Differentiation Markers) 100
Mouse Embryoid Body Differentiation – Hanging Drop Protocol 102

LIST OF TABLES AND FIGURES

Chapter 1: Introduction

Figure 1: Induced pluripotent stem cell applications 3
Figure 2: Simplified schematics of signal transduction from the cell membrane to the nucleus 4

Chapter 2: A Medium-Throughput Analysis of Signaling Pathways Involved in the Early Stages of Stem Cell Reprogramming

Table I: Signal transduction genes used in the study 12
Figure 1: Lentiviral titering 14
Figure 2: Analysis of alkaline phosphatase expression for induced pluripotent colonies 15
Figure 3: Number of alkaline phosphatase positive colonies 9 days post-infection with a signal transduction gene and Oct4, Sox2, Klf4, and c-Myc as determined by high-content imaging and analysis 16
Figure 4: Total area of alkaline phosphatase positive colonies 9 days post-infection with a signal transduction gene and Oct4, Sox2, Klf4, and c-Myc as determined by high-content imaging and analysis 17

Chapter 3: Analysis of Smoothened, Ras, and Notch Signal Transduction Pathways During Induced Pluripotent Stem Cell Reprogramming

Table I: Reprogramming factor replacement 27
Figure 1: Signaling pathways can induce alkaline phosphatase colonies in the absence of KLF4 28
Figure 2: Signaling pathways can induce alkaline phosphatase colonies in the absence of SOX2 29
Figure 3: Signaling pathways can induce alkaline phosphatase colonies in the absence of OCT4 30
Figure 4: External modulation of the sonic hedgehog signaling pathway does not strongly affect OSKM reprogramming 31
Figure 5: Constitutively-active HRAS can induce NANOG expression without the Klf4 or Oct4 transgene 32
Figure 6: The small molecule, SC1, can induce NANOG expression without the Oct4 transgene 32
Figure 7: Activating Notch1 expression activates endogenous pluripotency genes 33
Figure 8: Constitutively-active Notch1 cell lines form embryoid bodies and produce two germ layers in vitro 34

Chapter 4: cAMP and EPAC Signaling Can Functionally Replace OCT4 During Induced Pluripotent Stem Cell Reprogramming

Figure 1: The cAMP activators, constitutively-active GNAS and forskolin, induce OCT4 positive colonies in the absence of the Oct4 transgene 43
Table I: Normalized reprogramming efficiencies 44
Figure 2: cAMP signaling induces morphological changes and activates pluripotent gene expression with 2i and without the Oct4 transgene 45

Figure 3: Forskolin 2i cell lines form embryoid bodies and produce three germ layers in vitro 46
Figure 4: The EPAC-RAP1 pathway is necessary for replacement of OCT4 47
Figure 5: cAMP activation induces cell division changes and gene expression changes to lower the barrier to reprogramming 49

Appendix A: Gene Information
Table AI: Plasmid information, retroviral library 56
Table AII: Database and cloning information 58
Table AIII: Gene size and homology 60

Appendix B: Cloning Primer Information
Table BI: Quikchange and cloning primers 62
Table BII: Sequencing primers 63
Table BIII: Cloning oligos used in the pHIV IG loxP cloning 63

Appendix D: Supplemental Figures for Chapter 2
Figure D1: Lentiviral titers from the cassette virus, STEMCCA loxP, which expresses Oct4, Sox2, Klf4, and c-Myc 72
Figure D2: Number of alkaline phosphatase positive colonies 9 days post-infection with cDNA encoding a signal transduction factor, as well as Oct4, Sox2, Klf4, and c-Myc, as determined by high-throughput imaging and analysis 73
Figure D3: Total area of alkaline phosphatase positive colonies 9 days post-infection with cDNA encoding a signal transduction factor, as well as Oct4, Sox2, Klf4, and c-Myc, as determined by high-throughput imaging and analysis 74
Figure D4: Constitutively-active ACVR1 condition 75
Figure D5: Constitutively-active HRAS conditions 76

Appendix E: Supplemental Figures for Chapter 3
Figure E1: STEMCCA loxP viral vectors 77
Figure E2: Activated HRAS induces alkaline phosphatase positive colonies in the absence of Klf4 but not Oct4 77
Figure E3: Constitutively-active HRAS induces morphologically different NANOG positive colonies without the Klf4 or Oct4 transgene, respectively 78
Figure E4: HRAS-mediated Oct4 replacement may be improved through the addition of CHIR99021 only or 2i addition earlier in reprogramming 79
Figure E5: Growth factors may increase the number of NANOG positive colonies in SC1 SKM induced reprogramming 79
Figure E6: 2i inhibitors hinder constitutively-active Notch1-mediated Oct4 replacement 80
Table EI: Genes affecting reprogramming 80
Table EII: Different combinations to replace OSKM 80

Appendix F: Supplemental Figures for Chapter 4
Figure F1: Negative controls have little OCT4 expression 82

Figure F2: The number of infected cells plated in each condition can be used in determining the efficiency of reprogramming 82
Figure F3: Serum-free conditions and PD 0325901 improve the reprogramming efficiency for OCT4 replacement 83
Figure F4: Measuring larger OCT4 colonies results in similar trends in reprogramming efficiency 84
Figure F5: NANOG staining revels similar trends for forskolin conditions, but fewer colonies compared to OCT4 staining 84
Figure F6: SKM FK 2i-01 cell line expresses pluripotency markers, SSEA1, OCT4, and NANOG 85
Figure F7: SKM FK 2i-06 cell line expresses pluripotency markers, SSEA1, OCT4, and NANOG in feeder and feeder-free conditions 86
Figure F8: SKM FK 2i-06 maintains embryonic stem cell colony morphology 19 passages after isolation 87
Figure F9: SKM FK 2i-02 produces three germ layers in vitro 87
Figure F10: GGTI-298 is toxic to mouse embryonic fibroblasts at higher concentrations 88
Figure F11: Small molecules increase the number of OCT4 positive cells in adult mouse ear fibroblasts with SKM and forskolin 88
Table FI: Primers used for qPCR 89
Table FII: Combinations of small molecules for complete factor replacement 89

ACKNOWLEDGMENTS

This work could not be done alone, and there are almost too many people to thank. First, I would like to thank my advisor, David Schaffer, who drove me to being a better scientist but gave me a lot of freedom in the process. He also created a lab filled with amazing individuals, and I cannot imagine my life during or after graduate school without them. I would also like to thank my committee members, Danielle Tullman Ercek and Lin He for their suggestions and support throughout the years.

I would like to acknowledge those brave souls who also decided to pursue reprogramming experiments, especially in the early years of the field, and they were always there for helpful discussions or protocols: Shawdee Eshghi, Yong Jin Choi, Teppei Yamaguchi, and Timothy Downing.

To those who make things happen: Wanichaya Ramey for being an amazing lab manager and keeping us sane, Mary West for running the stem cell center and her eagerness to help out on this project, Paula Gedraitis for her support with the colony counting code (over several years even), Nicol Wilson for her kindness and support, and Lily Mirels for her support with the journal club and always being someone to talk with.

I would also like to thank my undergraduates: Sunnie Mao and Kevin Huang. While Sunnie only worked a little over a semester in lab, her unparalleled drive was amazing to channel into research. Among many things, she helped me culture an unfathomable number of cell lines, and for that, I cannot thank her enough since I could actually take a weekend off. Kevin worked with me at the end of my project, and his work was not presented here, but I would like to thank him for his eagerness to learn and to take on his own projects.

To the lab members who got me started, Joseph Peltier and Albert Keung, thank you. Thank you to the following lab members who went above and beyond supporting me: Joe Peltier (Pooky!), Lauren Little, Daniel Stone, Jamie Bergen, Jonathan Foley, Melissa Kotterman, Lukasz Bugaj, Albert Keung, Phung Gip, Prajit Limsirichai, Dawn Spelke, Sisi Chen, and Tandis Vazin. I would especially like to mention, John Weinstein, who was my classmate in lab. I doubt we had a choice in becoming ‘besties,’ and now he’s my brother even though I never asked for one (thank you).

To my adopted family, Joe Peltier and Nick Perry: thank you for your friendship and love and introducing me and Matt to the Forbidden Island Tiki Bar, which I am positive also helped me survive grad school. I cannot wait to have more Macadamia Nut Chi Chis and Monkeypods with you both and see where life takes us. To Suzanne Miller, my friend from high school who ended up living four blocks away, thank you for always being there and reminding me of the world outside science.

To Matthew Dodd, my support, thank you. I know I couldn’t have done this without him. To his parents and sisters, my father, and my grandmother, thank you for being there. To the many friends I forgot to thank and the Schaffer lab past and present, thank you.

CHAPTER 1

INTRODUCTION

Embryonic and Induced Pluripotent Stem Cells

Embryonic stem cells (ESCs) are endowed with the pluripotency of an early stage embryo, i.e. the capacity to differentiate into all cell types within the adult body. Additionally, ESCs can divide indefinitely in an immature state, a process known as self-renewal. In 1981, embryonic stem cells were first generated from mouse embryos[1, 2], and seventeen years later human embryonic stem cells (hESCs) were successfully created (from human embryos that would otherwise be discarded at in vitro fertilization clinics) and cultured[3]. Since hESCs can potentially differentiate into any cell type, cell replacement therapies – where cells lost due to disease or injury are replaced with healthy cells derived from hESCs – have been a major focus for hESC research. However, there are numerous major challenges to such efforts, including immune responses, since differentiated cells derived from a general hESC will not be "tissue matched" to a particular patient recipient. Some research has shown that ESCs and their derivatives do not activate the immune system[4, 5], but other studies have shown the opposite[6-8], potentially requiring patients undergoing hESC treatments to suppress their immune system, as illustrated in a landmark clinical trial. On January 23, 2009, the FDA approved the first hESC cell replacement therapy clinical trial for treatment of spinal cord injury[9]. Geron Corporation, in collaboration with the University of California, Irvine, showed that hESC-derived "oligodendrocyte progenitors" implanted into a spinal cord injury site in rat models could restore locomotion[10, 11], which in part provided the basis for human trials. During the clinical trial, patients must undergo immune suppression for 60 days, a potential drawback for treating patients. Creating pluripotent, embryonic-like stem cells from a patient could enable the generation of "tissue matched" cells, thereby avoiding immune response issues.

Another powerful application for hESCs is to study processes of human development, and in addition, introducing disease-associated genetic mutations into the cells offers opportunities to study mechanisms of human disease and models for developing new medical therapies[12]. However, one major challenge is that many molecular mechanisms underlying human disease are unknown, and it is difficult to know in advance whether a particular hESC would harbor genetic or other modifications that would result in a disease, given that the embryo did not have the opportunity to develop and exhibit that disease. It is thus difficult to generate hESC-based models of many forms of human disease. Therefore, despite the promise of hESCs, biomedical limitations and some ethical concerns remain.

In parallel to work with hESCs, the stem cell and development fields have been exploring whether it is possible to endow mature or differentiated cells with the capacity for pluripotency and self-renewal, i.e. to reprogram them to an "embryonic" state. Such reprogramming has been previously achieved through the use of somatic cell nuclear transfer (SCNT), a process where the nucleus of a differentiated cell is transferred into an egg cell whose own nucleus has been removed, which can result in "rebooting" the cell to a pluripotent cell (the process that led to Dolly the sheep). However, while SCNT has established that reprogramming is possible, the molecular factors in the egg that were responsible for initiating the nuclear reprogramming process were unclear[13]. In 2006, Kazutoshi Takahashi and Shinya Yamanaka remarkably discovered that a small set of factors was sufficient to reprogram cells and thereby generate "induced" pluripotent stem (iPS) cells. Specifically, when genes encoding four transcription

factors – *c-Myc*, *Klf4*, *Oct4*, and *Sox2* – were introduced into fibroblasts (differentiated cells from connective tissue) to overproduce or "overexpress" those factors, the cells reverted back to a pluripotent state replete with the differentiation potential and self renewal of an ESC[14]. The year after this groundbreaking work, iPS cells were created from differentiated human cell lines using the four "Yamanaka factors" (*c-Myc*, *Klf4*, *Oct4*, and *Sox2*), as well as an alternate set of 4 genes (*Lin28*, *Nanog*, *Oct4*, and *Sox2*)[15, 16], indicating that multiple "paths" can lead to a pluripotent state.

To establish their differentiation potential, numerous cell types have been created from iPS cells and compared to the corresponding ES-derived, differentiated cells. In particular, cardiovascular cells[17-21], leukocytes[22], hematopoietic cells[23], adipocytes[24], and neurons[25] have been generated from iPS cells. Also, in a proof-of-principle experiment for cell replacement therapy using iPS cells, Hanna *et al.* isolated tail-tip fibroblasts from a sickle cell anemia mouse model, created an iPS cell line, and introduced genes to correct the mutated β-globin gene. When replacing diseased cells with the corrected cells derived from the iPS cell lines, the mice had a reduction of the sickle-shaped blood cells, increased urine concentration, decreased respiration, and increased weight, which were all comparable to the non-sickle cell anemia control animals[26].

Importantly, iPS cells have potential as systems for studying mechanisms of human disease via isolating a readily accessible cell type from a diseased person (an option not available for hESCs), reprogramming the cell type to form iPS lines, and differentiating the iPS cell line into the diseased cell type present in the patient's body (Figure 1). Not only does this method allow for culturing diseased cell types that are inaccessible through surgeries or biopsies (e.g. brain tissue), but differentiation of iPS cells into the diseased state can yield valuable information about the progression and pathology of the disease. Using biopsied skin cells from two patients suffering from the neurodegenerative disease amyotrophic lateral sclerosis (ALS or Lou Gehrig's disease), Dimos *et al.* reprogrammed the cells to iPSC and then differentiated them to motor neurons, the diseased cell type in ALS[27]. An iPS culture model for ALS will enable high throughput screening to aid in pharmaceutical development. For diseases that have multiple mutations, no associated mutation, or are influenced by environmental effects, iPS culture models could also allow the study of various environmental perturbations and the effect on disease progression and prognosis.

While iPS cells hold great promise for medical therapies and research, numerous issues with reprogramming remain. Currently, the efficiency of reprogramming is exceedingly low; for every 10,000 mouse embryonic fibroblasts infected with retroviral vectors (viruses modified to carry genes inside of cells) containing the Yamanaka genes, 1-10 fully reprogrammed colonies are expected[28], and the efficiency with human cells is lower. Small molecules[29-31], microRNAs[32], and different starting cell types[33] have been used to enhance reprogramming, but the efficiency is still low. Furthermore, the process of reprogramming is time intensive, taking approximately 2 weeks to isolate mouse iPS colonies and 3-4 weeks to isolate human iPS colonies[34]. Since much is still unknown about the mechanism of reprogramming, screening methodologies could potentially discover new empirical means to increase reprogramming efficiency, increase the rate of iPS conversion, and further elucidate reprogramming mechanisms.

In addition to efficiency, when using iPS cells for human therapy, safety is a concern. The reprogramming process most often involves inserting the reprogramming genes into the genome, which could potentially disrupt key genes and damage the cell, and additionally, one of the Yamanaka genes, *c-Myc*, is an oncogene, which when activated promotes cancer formation[35].

Several efforts have been made to overcome these limitations: by using a viral vector less likely to integrate into the genome[36]; using small molecules[37]; reducing the number of integrations into the genome[38, 39]; delivering non-integrating plasmid DNA[40-42]; (repeatedly) delivering of proteins rather than of DNA into cells[43]; removing c-myc from the Yamanaka genes[44, 45]; and excising the integrated DNA after reprogramming has occurred[41, 46, 47]. These methods, however, usually lower the efficiency of reprogramming even further. Identifying additional factors that aid reprogramming may yield a deeper understanding of the underlying mechanism as well as result in new approaches for efficient and safe reprogramming.

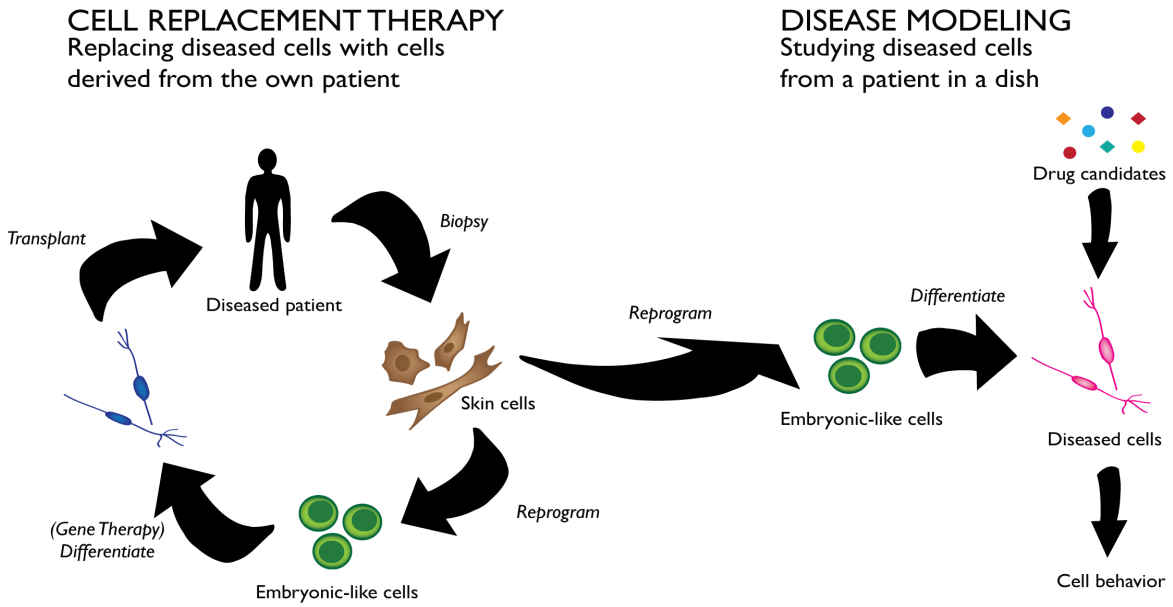

Figure 1. Induced pluripotent stem cell applications. Induced pluripotent stem cells have potential for cell replacement therapies, where a diseased patient's cells are reprogrammed to an embryonic state, corrected via gene therapy if necessary, differentiated into the diseased phenotype, and then transplanted back into the patient. iPS cells can also be used for disease modeling, where reprogrammed cells are differentiated into the diseased phenotype and can be used to screen therapeutic drugs.

Intracellular Signal Transduction and Induced Pluripotent Stem Cells

During normal embryonic development, a cell receives cues from environmental signaling molecules, cell-cell contacts, the extracellular matrix, and mechanical forces acting on the cell surface, which first govern cell fate by interacting with receptor proteins primarily on the cell surface. These receptors in turn activate pathways of proteins inside the cell, in a process known as "signal transduction." The resulting signals then reach the nucleus and modulate the activation of transcription factors, key proteins that then activate or represses the expression (messenger RNA production) of specific genes, which then execute changes in cell behavior (Figure 2)[48]. This process of sensing and processing environmental signals regulates nearly all cell behavior, such as the ability of a stem cell to differentiate to a particular cell type, become quiescent, self-renew, or die[49]. In contrast to normal development, the viral vector introduction of the four Yamanaka factors is sufficient to reverse cellular differentiation, originally specified through the various environmental cues, resulting in induced pluripotent stem cells. However,

the field has primarily focused its efforts on reprogramming though the introduction of transcription factors, and it is largely unknown whether pluripotent cells can also be obtained by instead manipulating signal transduction pathways, or by manipulating the external environment of the cell.

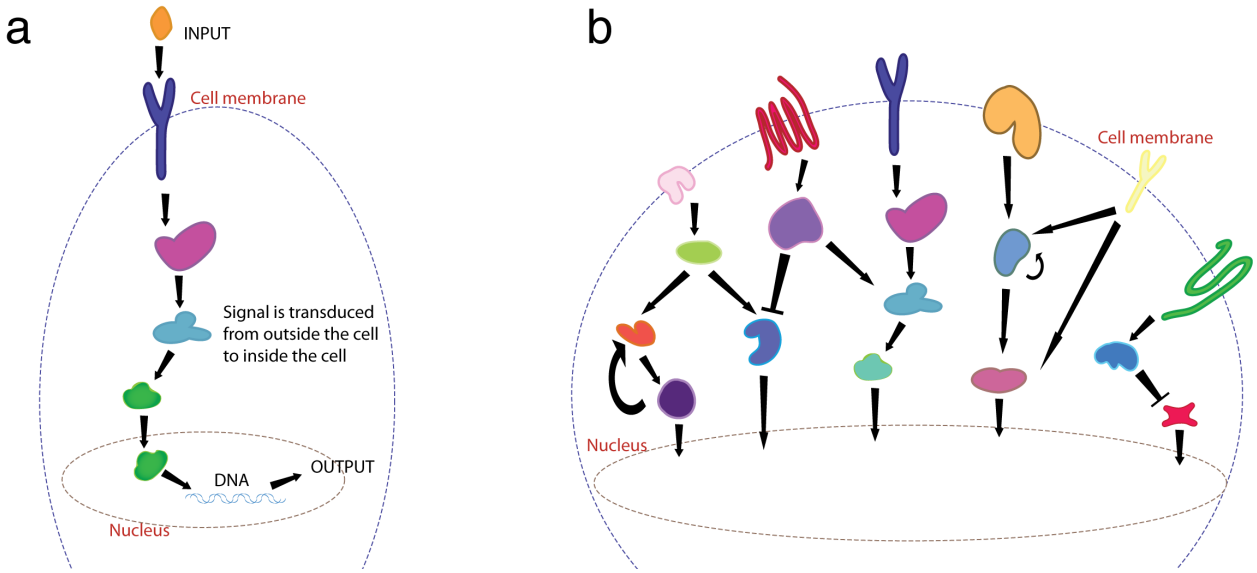

Figure 2. Simplified schematics of signal transduction from the cell membrane to the nucleus. (a) An input signal external to the cell is first transduced into the cell via cell surface receptors spanning the cell membrane. A series of protein-protein interactions transduce the signal to transcription factors in the nucleus. Transcription factors bind DNA to initiate gene transcription and expression changes, which could result in cell behavior. (b) Signal transductions are complex, with many downstream effectors and feedback loops and crosstalk possible between pathways.

Important work has quantitatively studied how external signaling inputs are propagated through signal transduction networks to effect changes in cell behavior, i.e. the input-output relationships of signal transduction. For instance, Janes *et al*. studied signaling regulation on a form of cell death known as apoptosis. Cells were experimentally perturbed with combinations of three extracellular signaling molecules: TNF to induce death vs. EGF or insulin to inhibit death. Subsequently, both the activity of 19 intracellular proteins known to be involved in the apoptotic signal transduction pathways and the progression of apoptosis were measured. Using mathematical modeling to find the most important variables leading to apoptosis resulted in three important conclusions. First, knowledge of the activity of any individual protein was not sufficient to predict cellular output behavior, in this case apoptosis. Second, intracellular signal transduction proteins more accurately predicted the progression of apoptosis than the extracellular signaling molecules (94% to 45% accuracy, respectively). Third, knowledge of the activity of 3-7 signal transduction proteins was sufficient to predict cell apoptosis. Cell behavior could thus be predicted by and presumably depended upon the cellular state of signal transduction, i.e. the repertoire of active and inactive signal transduction proteins[50]. Therefore, studying and manipulating signal transduction proteins could be useful in inducing other cell behavior, such as inducing pluripotency. While the focus in the reprogramming field has been on analysis of transcription factors, we propose to study whether inducing pluripotent stem cells may be aided by perturbing cellular signal transduction using a library-based approach. In

addition, building on the idea that multiple paths can lead to pluripotency, as evident in the fact that two distinct sets of transcription factors are capable of reprogramming a cell[15, 16], we will explore whether signal transduction proteins are also sufficient to induce pluripotency.

Signal transduction is necessary for maintaining ESC pluripotency and self-renewal. As one of many examples, hESCs require a high level of ERK signaling, whereas mESCs require inhibition of ERK activity[51-53]. Unsurprisingly, research has also implicated a relationship between signal transduction pathways and reprogramming. Silva *et al*. have shown that the addition of two chemical inhibitors, specific to ERK and GSK3β, can fully reprogram neural stem cells overexpressing KLF4 and OCT4[29]. Similarly, three chemical inhibitors, specific to ERK, GSK3β, and ALK5, were necessary to propagate and maintain rat iPS cells infected with the Yamanaka factors[54]. Additionally, the estrogen receptor ESRRB was able to reprogram mouse embryonic fibroblasts in combination with only OCT4 and SOX2[55], and kenpaullone, a non-specific inhibitor of kinases (proteins that add phosphate groups onto target molecules), was able to replace KLF4 in reprogramming[56]. Finally, the extracellular signaling protein WNT3A promotes reprogramming of mouse embryonic fibroblasts overexpressing KLF4, OCT4, and SOX2[57]. While the concept that manipulating signal transduction can aid or enhance reprogramming shows promise, few signal transduction pathways necessary for reprogramming have been determined, and most efforts to discern signal transduction proteins have been through inhibitory screens, which can only decrease activity of signaling proteins even though activation of some may play a role in inducing pluripotency.

Signal Transduction Library

By sampling more signal transduction states, both through inhibition and activation of signal transduction proteins, we will explore the hypothesis that signal transduction proteins can enhance or even replace transcription factor mediated reprogramming, with the ultimate goal of replacing all four transcription factors. Furthermore, perturbing the signal transduction pathways to achieve reprogramming would further our understanding of the reprogramming process, could alleviate the risk of manipulating the genome, and may lead to increases in reprogramming efficiency.

References

1. Evans, M.J. & Kaufman, M.H. Establishment in culture of pluripotential cells from mouse embryos. (1981).
2. Martin, G.R. Isolation of a pluripotent cell line from early mouse embryos cultured in medium conditioned by teratocarcinoma stem cells. *Proc Natl Acad Sci U S A* **78**, 7634-7638 (1981).
3. Thomson, J.A. et al. Embryonic stem cell lines derived from human blastocysts. *SCIENCE* **282**, 1145-1147 (1998).
4. Drukker, M. et al. Human embryonic stem cells and their differentiated derivatives are less susceptible to immune rejection than adult cells. *Stem Cells* **24**, 221-229 (2006).
5. Li, L. et al. Human embryonic stem cells possess immune-privileged properties. *Stem Cells* **22**, 448-456 (2004).
6. Swijnenburg, R.-J. et al. Immunosuppressive therapy mitigates immunological rejection of human embryonic stem cell xenografts. *Proc Natl Acad Sci U S A* **105**, 12991-12996 (2008).

7. Swijnenburg, R.-J. et al. Embryonic stem cell immunogenicity increases upon differentiation after transplantation into ischemic myocardium. *Circulation* **112**, I166-172 (2005).
8. Toriumi, H. et al. Treatment of Parkinson's disease model mice with allogeneic embryonic stem cells: necessity of immunosuppressive treatment for sustained improvement. *Neurol Res* **31**, 220-227 (2009).
9. Alper, J. Geron gets green light for human trial of ES cell-derived product. *Nat Biotechnol* **27**, 213-214 (2009).
10. Keirstead, H.S. et al. Human embryonic stem cell-derived oligodendrocyte progenitor cell transplants remyelinate and restore locomotion after spinal cord injury. *J Neurosci* **25**, 4694-4705 (2005).
11. Nistor, G.I., Totoiu, M.O., Haque, N., Carpenter, M.K. & Keirstead, H.S. Human embryonic stem cells differentiate into oligodendrocytes in high purity and myelinate after spinal cord transplantation. *Glia* **49**, 385-396 (2005).
12. Hook, L., O'Brien, C. & Allsopp, T. ES cell technology: an introduction to genetic manipulation, differentiation and therapeutic cloning. *Adv Drug Deliv Rev* **57**, 1904-1917 (2005).
13. Gurdon, J.B. & Melton, D.A. Nuclear reprogramming in cells. *Science* **322**, 1811-1815 (2008).
14. Takahashi, K. & Yamanaka, S. Induction of pluripotent stem cells from mouse embryonic and adult fibroblast cultures by defined factors. *Cell* **126**, 663-676 (2006).
15. Takahashi, K. et al. Induction of pluripotent stem cells from adult human fibroblasts by defined factors. *Cell* **131**, 861-872 (2007).
16. Yu, J. et al. Induced pluripotent stem cell lines derived from human somatic cells. *Science* **318**, 1917-1920 (2007).
17. Mauritz, C. et al. Generation of functional murine cardiac myocytes from induced pluripotent stem cells. *Circulation* **118**, 507-517 (2008).
18. Narazaki, G. et al. Directed and systematic differentiation of cardiovascular cells from mouse induced pluripotent stem cells. *Circulation* **118**, 498-506 (2008).
19. Taura, D. et al. Induction and Isolation of Vascular Cells From Human-Induced Pluripotent Stem Cells. *Arterioscler Thromb Vasc Biol* (2009).
20. Xie, C. et al. A Comparison of Murine Smooth Muscle Cells Generated from Embryonic versus Induced Pluripotent Stem Cells. *Stem Cells Dev* (2008).
21. Zhang, J. et al. Functional Cardiomyocytes Derived From Human Induced Pluripotent Stem Cells. *Circ Res* (2009).
22. Senju, S. et al. Characterization of Dendritic Cells and Macrophages Generated by Directed Differentiation from Mouse Induced Pluripotent Stem Cells. *Stem Cells* **27**, 1021-1031 (2009).
23. Choi, K.-D. et al. Hematopoietic and Endothelial Differentiation of Human Induced Pluripotent Stem Cells. *Stem Cells* **27**, 559-567 (2009).
24. Taura, D. et al. Adipogenic differentiation of human induced pluripotent stem cells: Comparison with that of human embryonic stem cells. *FEBS Lett* (2009).
25. Karumbayaram, S. et al. Directed Differentiation of Human-Induced Pluripotent Stem Cells Generates Active Motor Neurons. *Stem Cells* **27**, 806-811 (2009).
26. Hanna, J. et al. Treatment of sickle cell anemia mouse model with iPS cells generated from autologous skin. *Science* **318**, 1920-1923 (2007).

27. Dimos, J.T. et al. Induced pluripotent stem cells generated from patients with ALS can be differentiated into motor neurons. *Science* **321**, 1218-1221 (2008).
28. Hochedlinger, K. & Plath, K. Epigenetic reprogramming and induced pluripotency. *Development* **136**, 509-523 (2009).
29. Silva, J. et al. Promotion of reprogramming to ground state pluripotency by signal inhibition. *PLoS Biol* **6**, e253 (2008).
30. Huangfu, D. et al. Induction of pluripotent stem cells by defined factors is greatly improved by small-molecule compounds. *Nat Biotechnol* **26**, 795-797 (2008).
31. Mikkelsen, T.S. et al. Dissecting direct reprogramming through integrative genomic analysis. *Nature* **454**, 49-55 (2008).
32. Judson, R.L., Babiarz, J.E., Venere, M. & Blelloch, R. Embryonic stem cell-specific microRNAs promote induced pluripotency. *Nat Biotechnol* (2009).
33. Aasen, T. et al. Efficient and rapid generation of induced pluripotent stem cells from human keratinocytes. *Nat Biotechnol* **26**, 1276-1284 (2008).
34. Maherali, N. & Hochedlinger, K. Guidelines and techniques for the generation of induced pluripotent stem cells. *Cell Stem Cell* **3**, 595-605 (2008).
35. Zhao, R. & Daley, G.Q. From fibroblasts to iPS cells: induced pluripotency by defined factors. *J Cell Biochem* **105**, 949-955 (2008).
36. Okita, K., Nakagawa, M., Hyenjong, H., Ichisaka, T. & Yamanaka, S. Generation of mouse induced pluripotent stem cells without viral vectors. *Science* **322**, 949-953 (2008).
37. Shi, Y. et al. Induction of pluripotent stem cells from mouse embryonic fibroblasts by Oct4 and Klf4 with small-molecule compounds. *Cell Stem Cell* **3**, 568-574 (2008).
38. Carey, B.W. et al. Reprogramming of murine and human somatic cells using a single polycistronic vector. *Proc Natl Acad Sci U S A* **106**, 157-162 (2009).
39. Shao, L. et al. Generation of iPS cells using defined factors linked via the self-cleaving 2A sequences in a single open reading frame. *Cell Res* (2009).
40. Gonzalez, F. et al. Generation of mouse-induced pluripotent stem cells by transient expression of a single nonviral polycistronic vector. *Proc Natl Acad Sci U S A* (2009).
41. Kaji, K. et al. Virus-free induction of pluripotency and subsequent excision of reprogramming factors. *Nature* (2009).
42. Yu, J. et al. Human Induced Pluripotent Stem Cells Free of Vector and Transgene Sequences. *Science* (2009).
43. Kim, D. et al. (2009).
44. Nakagawa, M. et al. Generation of induced pluripotent stem cells without Myc from mouse and human fibroblasts. *Nat Biotechnol* **26**, 101-106 (2008).
45. Wernig, M., Meissner, A., Cassady, J.P. & Jaenisch, R. c-Myc is dispensable for direct reprogramming of mouse fibroblasts. *Cell Stem Cell* **2**, 10-12 (2008).
46. Chang, C.-W. et al. Polycistronic Lentiviral Vector for "Hit and Run" Reprogramming of Adult Skin Fibroblasts to Induced Pluripotent Stem Cells. *Stem Cells* **27**, 1042-1049 (2009).
47. Woltjen, K. et al. piggyBac transposition reprograms fibroblasts to induced pluripotent stem cells. *Nature* (2009).
48. Downward, J. The ins and outs of signalling. *Nature* **411**, 759-762 (2001).
49. Metallo, C.M. et al. Engineering the stem cell microenvironment. *Biotechnol Prog* **23**, 18-23 (2007).

50. Janes, K.A. et al. A systems model of signaling identifies a molecular basis set for cytokine-induced apoptosis. *SCIENCE* **310**, 1646-1653 (2005).
51. Li, J. et al. MEK/ERK signaling contributes to the maintenance of human embryonic stem cell self-renewal. *Differentiation* **75**, 299-307 (2007).
52. James, D., Levine, A.J., Besser, D. & Hemmati-Brivanlou, A. TGFbeta/activin/nodal signaling is necessary for the maintenance of pluripotency in human embryonic stem cells. *Development* **132**, 1273-1282 (2005).
53. Okita, K. & Yamanaka, S. Intracellular signaling pathways regulating pluripotency of embryonic stem cells. *Curr Stem Cell Res Ther* **1**, 103-111 (2006).
54. Li, W. et al. Generation of rat and human induced pluripotent stem cells by combining genetic reprogramming and chemical inhibitors. *Cell Stem Cell* **4**, 16-19 (2009).
55. Feng, B. et al. Reprogramming of fibroblasts into induced pluripotent stem cells with orphan nuclear receptor Esrrb. *Nat Cell Biol* (2009).
56. Lyssiotis, C.A. et al. Reprogramming of murine fibroblasts to induced pluripotent stem cells with chemical complementation of Klf4. *Proc Natl Acad Sci U S A* (2009).
57. Marson, A. et al. Wnt Signaling Promotes Reprogramming of Somatic Cells to Pluripotency. *Cell Stem Cell* **3**, 132-135 (2008).

CHAPTER 2

A MEDIUM-THROUGHPUT ANALYSIS OF SIGNALING PATHWAYS INVOLVED IN EARLY STAGES OF STEM CELL REPROGRAMMING

Abstract

The induction of pluripotent stem cells from adult cells has enormous potential in regenerative medicine. While initial efforts to study mechanisms and improve the efficiency of induced pluripotent stem (iPS) reprogramming focused on the direct roles of transcriptional regulators, increasing evidence indicates that cellular signal transduction pathways can modulate induced pluripotency. Here, we present a medium-throughput system to study the effect of signaling pathways on the early stages of reprogramming. We have generated a set of lentiviral vectors encoding 38 genes that upregulate or downregulate major signal transduction pathways. In combination with the four Yamanaka factors OCT4, SOX2, KLF4, and C-MYC, we have quantified each signaling factor's effect on reprogramming. This approach confirmed the role of several factors previously implicated in reprogramming, as well as identified several GTPases that improve or hinder iPS cell reprogramming, factors that to date have not been largely studied in reprogramming, as well as a possible pathway involving GNAQ and MAP2K6 that blocks reprogramming. In addition to identifying potential relationships between signal transduction and reprogramming, this methodology is useful in determining new targets for increasing reprogramming efficiency and/or cell differentiation.

Introduction

Yamanaka's groundbreaking work found that expression of only four transcription factors – OCT4, SOX2, KLF4 and, C-MYC (OSKM) – was sufficient to revert differentiated adult cells to embryonic phenotypes[1]. The resulting induced pluripotent stem (iPS) cells, which have the capacity to form all three germ layers and subsequently all cell types in an adult organism – offer immense biomedical potential including the use of patient-derived iPS cells for cell-replacement therapies or for *in vitro* models of human disease. However, further understanding of reprogramming mechanisms is necessary for this relatively new technology, particularly to develop safer and potentially more efficient reprogramming methodologies for downstream applications.

Signal transduction, the relay of a microenvironmental input into the interior of a cell, is mediated through protein-protein and second messenger interactions and is a central regulator of nearly all facets of cell behavior. In many cases, these signaling pathways can modulate the activity of key transcription factors, including the Yamanaka factors and other factors involved in pluripotency, strongly suggesting that signaling may modulate reprogramming. For instance, leukemia inhibitor factor (LIF) and bone morphogenic protein 4 (BMP4) activate signaling pathways and downstream effectors such as STAT3, which in turn activates C-MYC, as well as Inhibitor of Differentiation (ID) proteins to maintain murine embryonic stem cell pluripotency[2-7]. To date several signaling pathways have indeed been implicated in the reprogramming process. For example, early work demonstrated that a small molecule inhibitor of TGFβ signaling could replace SOX2, BMP signaling is important in the early state mesenchymal to epithelial transition[8], and exogenous WNT3A could create pluripotent colonies in the absence of C-MYC[9].

Guided by the candidate approach that originally led to the identification of the Yamanaka factors, we have systematically investigated additional upstream signal transducers that may modulate reprogramming, including numerous pathways whose activity can readily be manipulated with small molecules and/or exogenous proteins. Specifically, we generated a set of lentiviral vectors encoding 38 constitutively-active, dominant-negative, or wild-type versions of signal transduction genes to probe several intracellular signaling pathways. By measuring the effect of each on reprogramming in a medium-throughput, quantitative manner, we have both validated the methodology by comparison to previously published results as well as discovered new roles for GTPase-mediated signal transduction pathways in early stages of reprogramming.

Materials and Methods

Cell Culture and Plasmid Construction

HEK293T cells were maintained in IMDM with 10% FBS and 1% penicillin/streptomycin. 129 MEF cells were a kind gift of Lin He (University of California, Berkeley), isolated as previously described[10]. MEFs were maintained in DMEM (high glucose), 10% FBS, 1% GlutaMAX, and 1% penicillin/streptomycin (Invitrogen). Cells undergoing reprogramming were maintained in mouse embryonic stem cell conditions: DMEM (high glucose), 15% FBS (Hyclone, SH3007003E), 0.5% penicillin/streptomycin, 1% GlutaMAX, 1% Sodium Pyruvate, 1% MEM NEAA, 0.1 mM 2-mercaptoethanol (Invitrogen), and 1000 U/mL LIF (Millipore, ESG1106). Cells were maintained at 37°C with 5% CO_2.

Plasmids were obtained from several sources. STEMCCA-loxP was a kind gift of Gustavo Mostoslavsky (Boston University)[11]. The following plasmids were obtained from Addgene: pHIV EGFP (plasmid 21373)[12], pCMV5 ALK-2 Q207D (plasmid 11740)[13], pRC/RSV Flag MKK3(glu) (plasmid 14670)[14], and pCDNA3-Flag MKK6(glu) (plasmid 13518)[14]. pCDNA3.1+ Gαi1 Q204L pCDNA3.1+ Gα12 Q231L, pCDNA3.1+ Gαq Q209L, and pCDNA3.1+ Gαs Q227L were obtained from Missouri S&T cDNA Resource Center (www.cdna.org). CLGPIT myc DN RhoA T19N, CLGPIT myc CA RhoA Q63L, CLGPIT CA Rac1(Q61L), CLGPIT DN Rac1(T17N), CLGPIT CA Cdc42(Q61L), CLGPIT DN Cdc42(T17N), pBS SK SP Smo, pEN RelA, CLGPIT Akt1, and CLGPIT Akt AAA were described previously[15-18]. CLPIT GSK3β K85R, CLPIT GSK3β R96A, and CLPIT GSK3β S9A, cloned from rat cDNA and mutagenized, were kind gifts from Smita Agrawal. MIG STAT3 and MIG DN STAT3 were kind gifts from Il-Hoan Oh[19]. pCS2-ICV-6MT mNICD was a kind gift of Raphael Kopan (Washington University)[20], and CLPIT mNICD was a kind gift of Smita Agrawal. pEN IkBa, cloned from cDNA, was a kind gift of Kathryn Miller-Jensen (Yale University). Wild-type constructs containing CaMKII, CaMKIIN, and CaMKIV were a kind gift of Thomas Soderling (Oregon Health & Science University)[21, 22], and CLGPIT CaMKII T286D, CLGPIT CaMKIIN, CLGPIT CaMKIV were a kind gift from Joseph Peltier. The RasG12V construct was a kind gift of Paul Khavari (Stanford University)[23], and CLGPIT HRas G12V was a kind gift of Joseph Peltier. CLGPIT Akt DD and CLGPIT HRas S17N, were mutagenized from WT Akt and HRas G12V constructs, respectively, and were kind gifts of Joseph Peltier. CLPIT CTNNB1 was a kind gift from Anand Asthagiri (Northeastern University). pRK5F FLAG TbRI T202D was a kind gift from Rik Derynck (UCSF)[24]. pCDNA3.1+ HIF ΔODD was a kind gift from David Young (UCSF)[25]. pCEP4 ERK1, pCEP4 ERK1 K71R, 3XFLAG-CMV7 ERK2, and 3XFLAG-CMV7 ERK2 K52R were kind gifts from Melanie Cobb (University of Texas Southwestern Medical Center)[26]. Plasmids containing *CTNNB1*, *Hif1a*, *NFKBIA*, *Smo*, and *STAT3* required site directed mutagenesis following the QuikChange protocol (Strategene).

Using standard cloning techniques, all genes were inserted into the murine leukemia virus (MLV) retroviral vector CLGPIT[27] and subsequently transferred to the lentiviral vector, pHIV IG loxP. pHIV IG loxP was created by insertion of three oligo constructs into the pHIV EGFP backbone[12]. The oligos encoded the lox66 site, a multiple cloning site, or the lox71 site. DNA was prepared with QIAGEN Plasmid Midi Kit per manufacturer's instructions. Plasmid sequences were verified by restriction enzyme digest and sequencing.

Viral Production and Titering

For the signal transduction vectors, lentiviral supernatant was produced by HEK293T cells in 6 well plates using calcium phosphate transfection as previously described[28]. Supernatant was collected 48 hours post transfection, aliquoted, and stored at -80°C. For the reprogramming cassette, STEMCCA loxP, the lentiviral transfection and centrifugation were performed as previously described[11, 28]. STEMCCA loxP is a second-generation lentivirus, and CLPIT Tat-mCherry[29] was thus added during transfection to promote viral genomic mRNA expression. 0.45 μm bottle top filters (Thermo Scientific, 09-740-28D) were used to filter the virus, and no sucrose layer was used in ultracentrifugation. The concentrated virus was aliquoted and stored at -80°C. Aliquots were only thawed once.

To quantify the amount of virus produced, 1,600 MEF or HEK293T cells were plated in black-walled 96 well plates (E+K Scientific) coated with gelatin or poly-D-lysine, respectively. After the cells attached, virus was added to the media.

Vector-mediated gene expression was analyzed 72 hours post-infection. For the signal transduction viruses, HEK293T cells were incubated with Hoescht stain (Sigma-Aldrich, B2261) to visualize nuclei. MEF cells were fixed in 4% paraformaldehyde for 15 minutes. The cells were blocked and permeabilized with 5% donkey serum with 0.3% Triton X-100 in PBS. The anti-GFP primary antibody (Invitrogen, A-11122, 1:500 dilution) was incubated overnight at 4°C. The secondary antibody (Invitrogen, A-21206, 1:250 dilution) was incubated for 2 hours at room temperature. DAPI (Invitrogen, 1:2000 dilution) was used as a nuclear stain. For STEMCCA-loxP virus, both cell types were fixed and stained. An anti-Oct4 antibody (Santa Cruz Biotechnology, sc-5279, 1:100 dilution) and a secondary antibody (Invitrogen, A-21235, 1:250 dilution) were used. GFP or OCT4 expression was imaged with the Molecular Devices ImageXpress Micro and analyzed with MetaXpress software. Infectious titers were calculated as previously described[28].

iPS Cell Reprogramming and Analysis

7,500 passage 3 MEF cells were plated into 48 well plates. One signal transduction virus (85-500 μL) and 14.3 μL of STEMCCA-loxP virus were added to each well 8 hours after plating. The following day, the media were replaced with fresh MEF media. 48 hours post-infection, each 48 well was split into triplicate onto MEF feeder layers (GlobalStem, GSC-6101M) in mouse embryonic stem cell media. Media were changed every day.

9 days post-infection, cells were fixed with 4% paraformaldehyde for 15 minutes. Alkaline phosphatase expression was assayed using the ELF Phosphatase Detection Kit (ATCC, SCRR-3010) per manufacturer's instructions. (Note that ATCC kit has been discontinued, and we have found the ELF 97 Endogenous Phosphatase Detection Kit (Invitrogen, E-6601) to be an appropriate substitute). HCS NuclearMask Red stain (Invitrogen, H10326, 1:1000 dilution) was used to visualize nuclei.

The 24 well plates were imaged with a Molecular Devices ImageXpress Micro high-throughput imager. A custom filter cube (Semrock BrightLine filters, Excitation: FF01-377/50-25, Dichroic: FF409-Di03-25x36, Emission: FF01-536/40-25) was necessary to detect alkaline phosphatase expression. For image analysis, a custom journal was created in the MetaXpress software to merge the images and identify colonies/regions of alkaline phosphatase expression. Significance was measured in Prism software (GraphPad) using ANOVA with post-hoc Dunnett tests.

Results

To study the effect of signaling pathways on OSKM iPS cell reprogramming, we first inserted 38 genes encoding signal transduction proteins into the lentiviral vector pHIV IG loxP, a modified version of the self-inactivating vector pHIV-EGFP[12] (Fig. 1a). The 38 cDNAs encoding signaling factors (Table I) are representative of several pathways important in mammalian cell biology: calcium-modulated, cytoskeletal, G-protein receptor-mediated, hypoxia-mediated, JAK-STAT, canonical tyrosine kinase receptor-mediated, NFκB, Notch, Hedgehog, TGFβ , and Wnt-β-catenin signaling pathways.

Table I. Signal transduction genes used in the study.

Gene Symbol		Common Name	Accession	Species	Modifications
CA	*ACVR1*	ALK2	NP_001096	Human	Q207D
CA	*MAP2K3*	MEK3	NP_002747	Human	S189E, T193E, FLAG N-term (E312K mutation)
CA	*MAP2K6*	MEK6	NP_002749	Human	S207E, T211E, FLAG N-term
DN	*RHOA*	RhoA	NP_001655	Human	T19N, Myc epitope N-terminus
CA	*RHOA*	RhoA	NP_001655	Human	Q63L, Myc epitope N-terminus
CA	*RAC1*	Rac1	NP_008839	Human	Q61L
DN	*RAC1*	Rac1	NP_008839	Human	T17N
CA	*CDC42*	CDC42	NP_001782	Human	Q61L
DN	*CDC42*	CDC42	NP_001782	Human	T17N
WT	*Akt1*	Akt1	NP_033782	Mouse	
DN	*Akt1*	Akt1	NP_033782	Mouse	T308A, S473A, K179A
CA	*Akt1*	Akt1	NP_033782	Mouse	T308D, S473D
CA	*Camk2a*	CaMKII	NP_037052	Rat	T286D
WT	*Camk2n2*	CaMKIIN	NP_067710	Rat	
WT	*Camk4*	CaMKIV	NP_036859	Rat	
CA	*HRAS*	H-Ras	NP_005334	Human	G12V
DN	*HRAS*	H-Ras	NP_005334	Human	S17N
CA	*CTNNB1*	b-Catenin	NP_001895	Human	S374G, 2xFLAG C-terminus
WT	*RELA*	RelA	NP_068810	Human	
CA	*NFKBIA*	IkBa	NP_065390	Human	S32A, S36A
CA	*Tgfbr1*	ALK5	P80204	Rat	GSM after N148, T202D, FLAG N-terminus
CA	*Hif1a*	HIF1a	Q61221	Mouse	M1-L400, Q614-STOP(837)

WT	*MAPK3*	ERK1	NP_002737	Human	HA tag N-terminus
DN	*MAPK3*	ERK1	NP_002737	Human	K71R, HA tag N-terminus
WT	*Mapk1*	ERK2	NP_446294	Rat	
DN	*Mapk1*	ERK2	NP_446294	Rat	K52R
CA	*GNAI1*	Gai1	NP_002060	Human	Q204L
CA	*GNA12*	Ga12	NP_031379	Human	Q231L
CA	*GNAQ*	Gaq	NP_002063	Human	Q209L
CA	*GNAS*	Gas	NP_000507	Human	Q227L
CA	*Notch1*	Notch1	EDL08321	Mouse	V1744-S2184, 6 Myc epitopes (C-terminus)
CA	*Smo*	Smo	NP_036939	Rat	W539L
CA	*STAT3*	STAT3	NP_003141	Human	A662C, N664C
DN	*STAT3*	STAT3	NP_644805	Human	M1-K685
KD,DN	*Gsk3b*	Gsk3b	NP_114469	Rat	K85R
DN	*Gsk3b*	Gsk3b	NP_114469	Rat	R96A
CA	*Gsk3b*	Gsk3b	NP_114469	Rat	S9A
DN	*TGFBR2*	TGFb-RII	NP_003233	Human	M1-I219
Abbreviations: CA, constitutively-active; DN, dominant-negative; KD, kinase-dead; WT, wild-type					

After separately packaging vectors encoding the signaling factors, viral titer was determined using GFP expression on either HEK293T or MEF cells as previously described[28]. Briefly, 72 hours after infection, viral transgene expression was assayed with high-content imaging and analysis to measure GFP expression (Fig. 1b-c). GFP fluorescence levels within the MEF cells were lower than in HEK293Ts, presumably due to differences in cell shape/volume or promoter strength, and immunocytochemistry was necessary to amplify GFP expression for high-content imaging.

The resultant infectious viral titers illustrate that in most cases, the differences in titer between cell lines and batches were not substantial. However, with constitutively-active *HRAS*, the calculated titer was considerably higher on MEF cells than HEK293T cells, which – given that *HRAS* is a known oncogene – could reflect differential effects on the cell cycle of MEFs compared to immortalized HEK293T cells. For the full study, vectors were titered on HEK293Ts for use in reprogramming experiments.

Similar to the quantification of viral titer for those encoding signal transduction genes, – the cassette virus expressing *Oct4*, *Sox2*, *Klf4*, and *c-Myc*, STEMCCA-loxP[11] – was titered by immunocytochemistry to quantify Oct4 expression in HEK293T and MEF cells (Fig. D1). However, unlike the viruses encoding signaling factors, the STEMCCA titer was much lower (approximately 7.5-fold) on MEF cells than HEK293Ts (6.9×10^4 versus 5.2×10^5 infectious units/mL, respectively). The viral titer for STEMCCA-loxP on MEF cells was thus used in subsequent experiments.

To investigate each gene's effect on reprogramming, 7,500 MEF cells at passage 3 were plated into 48 well plates. To equalize vector dosages based on the measured titers, virus was added to the supernatant at a multiplicity of infection (MOI) of 1 (resulting in approximately 63% of the cells infected) for the signaling factors. As the sole exception, cells were infected with vector encoding constitutively-active *GNAQ*, which had the lowest viral titer, at an MOI of 0.83 (56% of the cells infected). In all cases, cells were infected with the STEMCCA virus at a MOI of 0.13 (~12% of the cells infected).

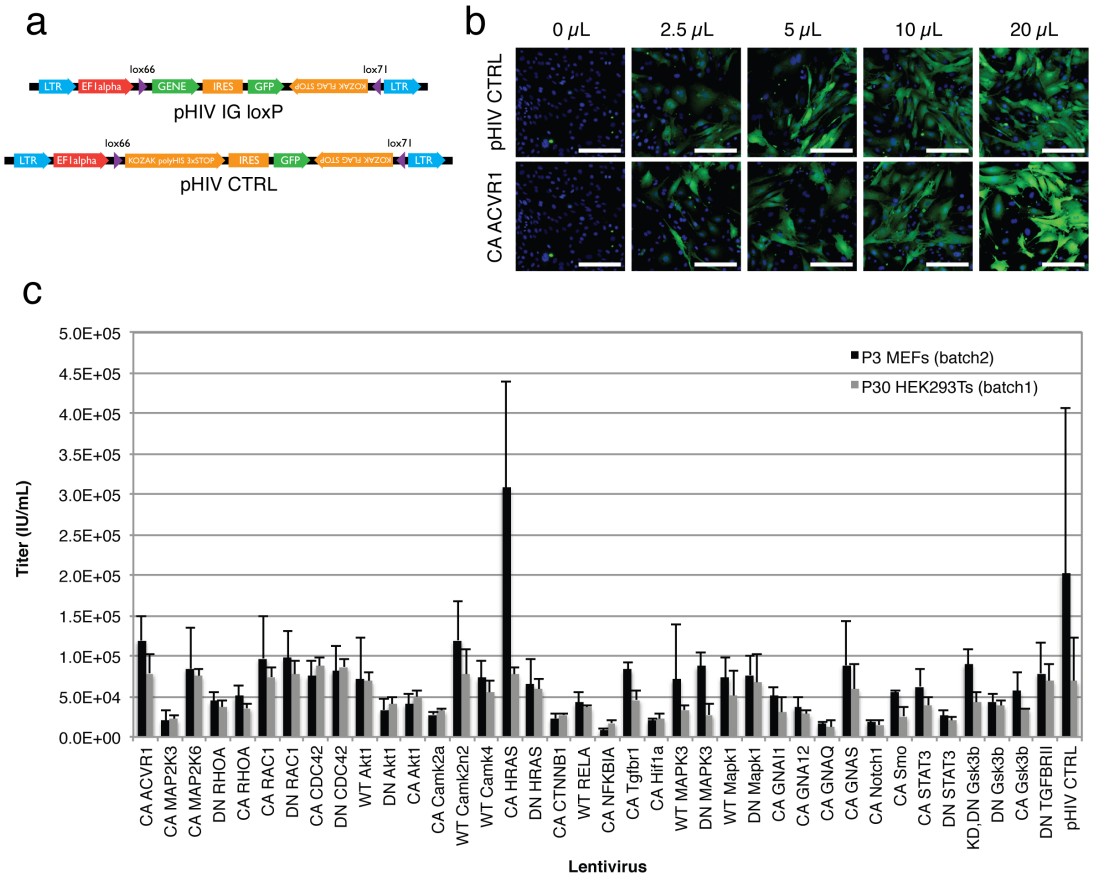

Figure 1. Lentiviral titering. (a) Schematic of the lentiviral vectors used for the reprogramming study. pHIV IG loxP is a self-inactivating lentiviral vector in which a signal transduction gene and GFP are transcribed from an EF1a promoter. pHIV CTRL is an empty vector used as an infection control. (b) Example images from titering the control virus and a virus containing a constitutively-active *ACVR1* on MEF cells. GFP signal was amplified through immunostaining. Nuclei were stained with DAPI. Scale bars are 200 μm. (c) Titers from two batches for signal transduction gene packaged into lentivirus. Cells were assayed for GFP expression 72 hours post-infection by high-throughput imaging and analysis. Error bars represent 95% confidence interval.

Forty-eight hours post-infection, each well was split into triplicate and plated on mitomycin c-treated MEF feeder layers in mouse embryonic stem cell conditions. Nine days post-infection, the cells were fixed and stained for alkaline phosphatase activity, an early marker of reprogramming[30]. Utilizing high-content imaging, 71% of each well was imaged and analyzed for alkaline phosphatase positive colonies (Fig. 2c). We created custom analysis software that allowed for the identification of colonies based on a minimum threshold of alkaline phosphatase expression and threshold of colony area. Additionally, this analysis measured individual colony metrics, such as colony area, intensity ranges, and shape factor (Fig. 2b). Example images from wells infected with the control virus (pHIV CTRL), constitutively-active *GNAQ*, or dominant-negative *Mapk1* are presented in Figure 2c.

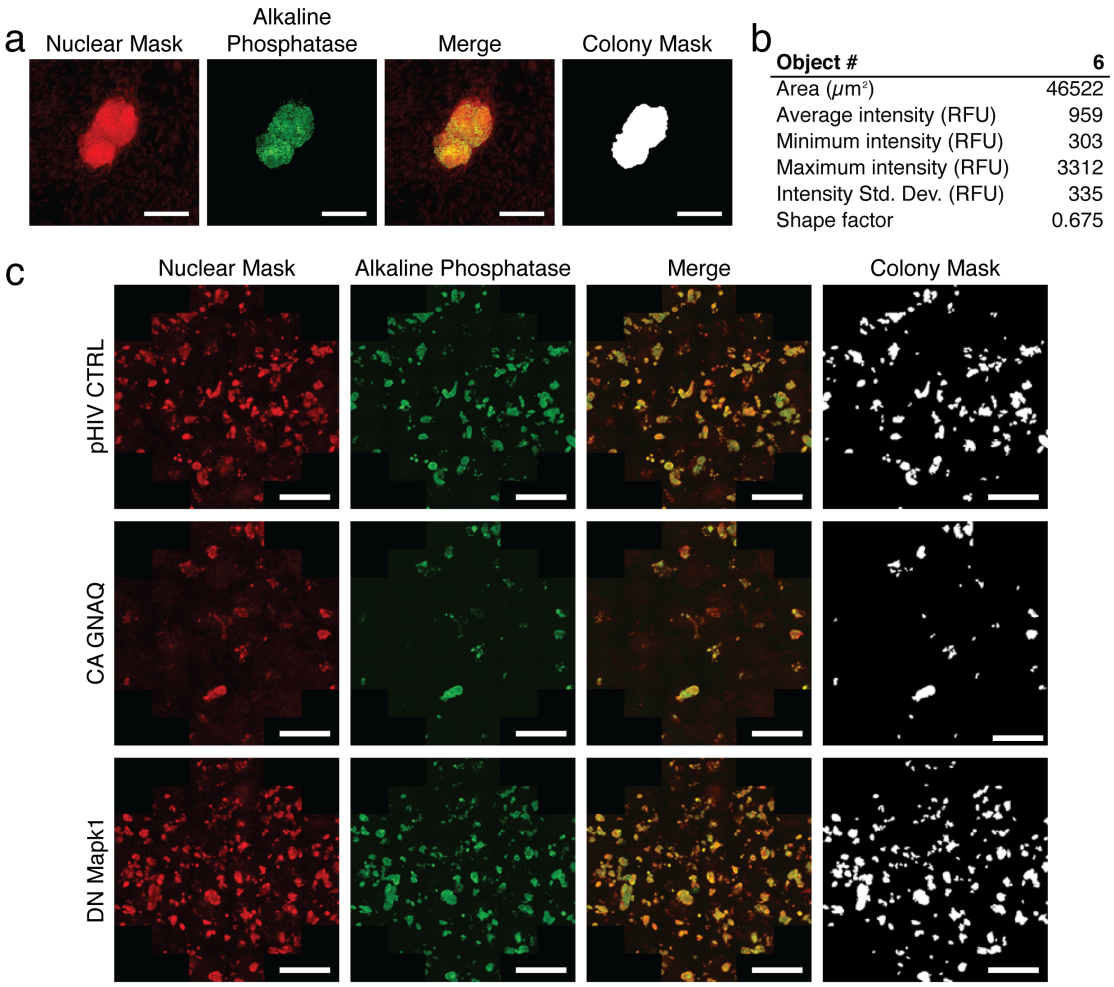

Figure 2. Analysis of alkaline phosphatase expression for induced pluripotent colonies. (a) Example of a stained colony from the wild-type *Akt1* condition. The nucleus was stained with HCS Nuclear Mask red stain. The alkaline phosphatase was stained with a fluorescent enzymatic-based kit (name manufacturer here). The images are shown individually and merged, and the resultant computer-generated mask from the analysis software from which the area and intensity metrics are measured is shown. Scale bars are 200 μm. (b) Example of individual colony metrics from the analysis. (c) Three wells are shown: the control pHIV CTRL condition, the constitutively-active *GNAQ* condition, and the dominant-negative *Mapk1* condition. Constitutively-active *GNAQ* and dominant-negative *Mapk1* represent extreme changes in reprogramming efficiency. The minimum colony size measured in the colony mask was 15,000 μm^2. Scale bars are 3 mm.

Numbers of alkaline phosphatase positive colonies for each condition are shown in Figure 3. While an exact efficiency – i.e., the fraction of cells infected on day 0 that subsequently underwent reprogramming – cannot be calculated due to conceivable differences in cell division rates among cells expressing different transgenes, an increase in colony number likely corresponds to an increase in reprogramming efficiency. In particular, constitutively-active *MAP2K3*, constitutively-active *NFKBIA*, constitutively-active *Hif1a*, dominant-negative *Mapk1*, constitutively-active *GNAI1*, and constitutively-active *Smo* exhibited a significant ($p<0.05$) increase in colony number compared to the control virus sample. Three of these signaling

pathways have been previously implicated in reprogramming biology. First, PD 0325901, a small molecule inhibitor of MAP2K1 and MAP2K2, has been found to help stabilize the pluripotent state when added with a GSK3β inhibitor[31]. MAP2K1 and MAP2K2 are activators of MAPK1, and as shown in Fig. 3, inhibition of *Mapk1* increased the colony number. Inhibition of MAPK1 and inhibition of MAP2K1 and MAP2K2 during reprogramming may thus act similarly by preventing differentiation[32].

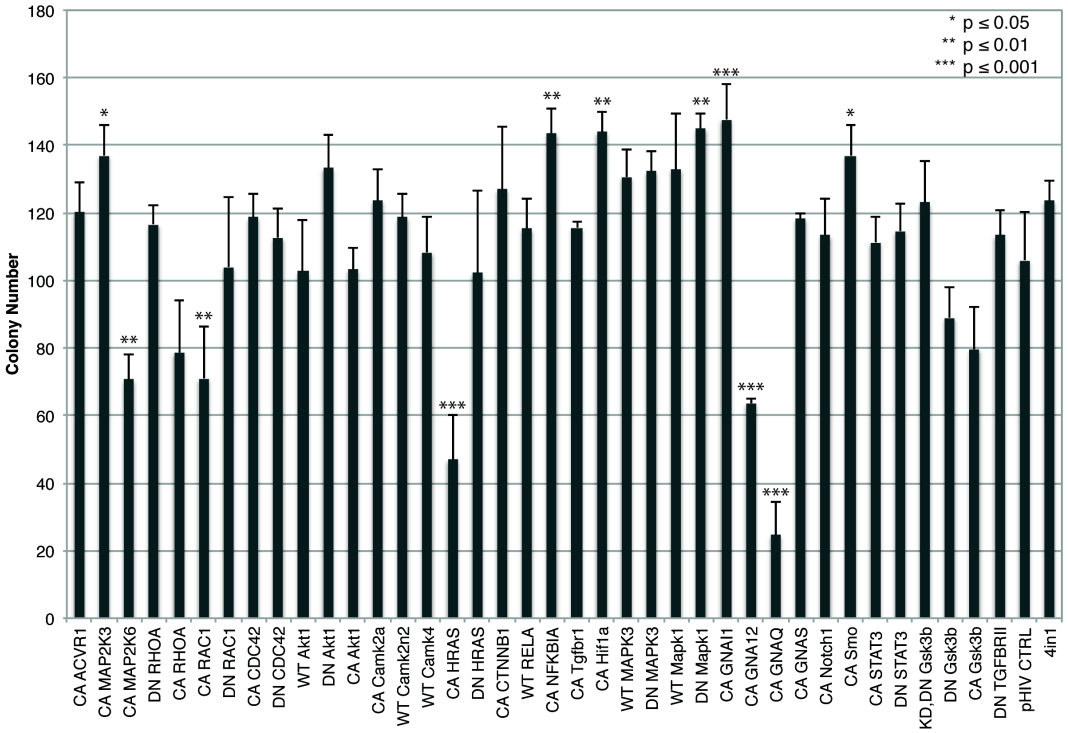

Figure 3. Number of alkaline phosphatase positive colonies 9 days post-infection with a signal transduction gene and *Oct4*, *Sox2*, *Klf4*, and *c-Myc* as determined by high-content imaging and analysis. Statistical significance was measured using ANOVA with a post-hoc Dunnett test relative to the infection control, pHIV CTRL. The minimum colony size measured was 15,000 μm^2. Error bars represent standard deviation.

Second, hypoxia has been previously found to increase reprogramming efficiency[33]. Analogously, a constitutively-active *Hif1a*, which mimics a hypoxic environment, increased the number of alkaline phosphatase colonies (Fig. 3). Third, soluble SHH in combination with OCT4 was able to induce pluripotent stem cells by enhancing an intermediate neural stem cell (NSC)-like state[34]. While it is unclear whether MEF reprogramming similarly proceeds through a NSC state, in our study a constitutively-active *Smo*, which activates the SHH signaling pathway, similarly increased the number of alkaline phosphatase colonies (Fig. 3).

Figure 3 also highlights signaling pathways that are detrimental to reprogramming. Constitutively-active versions of *MAP2K3*, *RAC1*, *HRAS*, *GNA12*, and *GNAQ* all led to significant reductions in alkaline phosphatase colonies. While none of the factors has been directly implicated in reprogramming, their signaling pathways offer interesting implications for reprogramming mechanisms.

These results were based on a minimum colony size of 15,000 μm^2; however, the custom module for the high-throughput imaging analysis readily allows for changes in the colony size parameter. Figure D2 shows the resultant number of colonies for a smaller size cutoff (8,000 μm^2) or a larger size cutoff (25,000 μm^2). Within the 15,000 μm^2 analysis discussed above, 11 signal transduction factors significantly ($p<0.05$) altered the number of colonies. However, additional signaling factors were found to significantly modify reprogramming in both the 8,000 and 25,000 μm^2 cutoff analysis (13 and 12 genes, respectively). For instance, dominant-negative *Akt1* was found to increase reprogramming efficiency in both the 8,000 and 25,000 μm^2 analysis but was not statistically significant ($p<0.05$) in the 15,000 μm^2 analysis. Additionally, in the 25,000 μm^2 analysis, constitutively-active *Gsk3b* was found to be significantly ($p<0.01$) deleterious to reprogramming when considering larger colony sizes, which may act through similar mechanism as previously described[32].

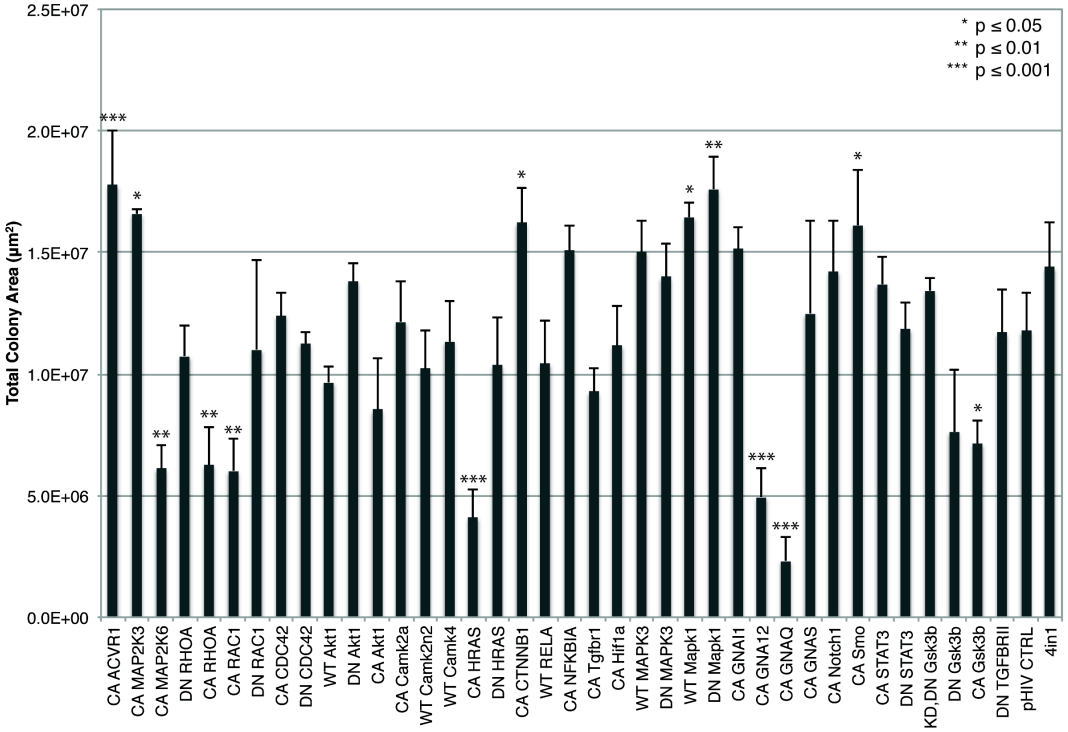

Figure 4. Total area of alkaline phosphatase positive colonies 9 days post-infection with a signal transduction gene and *Oct4*, *Sox2*, *Klf4*, and *c-Myc* as determined by high-content imaging and analysis. Statistical significance was measured using ANOVA with a post-hoc Dunnett test relative to the infection control, pHIV CTRL. The minimum colony size measured was 15,000 μm^2. Error bars represent standard deviation.

In addition to quantifying the resulting number of colonies after reprogramming, the custom module also measures the total area of all colonies (Fig. 4, or Fig. D3 for smaller 8,000 μm^2 or larger 25,000 μm^2 size cutoffs), which in the hypothetic event that individual colonies were difficult to define and segment could serve as a more effective metric for reprogramming. There were three important differences between the colony number and colony area analysis. First, unlike the colony number analysis, within the total area analysis, constitutively-active *Gsk3b*,

which decreased colony area, and constitutively-active *CTNNB1*, which increased colony area, were statistically significant and further highlighted the importance of the Wnt-β-catenin pathway in reprogramming. Second, both constitutively-active *RHOA* and *RAC1* significantly decreased colony area, which may further elucidate signaling mechanisms detrimental to reprogramming. Third, constitutively-active *ACVR1* caused a significant increase in colony area. ACVR1, an important protein in osteogenesis, reportedly yields alkaline phosphatase positive, bone-like cells[35] (Fig. D4). The observed cells – which are morphologically different from embryonic stem cells that in contrast have round, have a high nucleus to volume ratio, and form colonies – are thus readily distinguishable visually as false-positives. In summary, co-expression of signaling factors along with OSKM, coupled with high-content imaging analysis, enables rapid investigation of how numerous cellular signaling pathways impact pluripotency reprogramming.

Discussion

We have developed a medium-throughput system to investigate the likely complex interactions between signal transduction pathways and reprogramming mechanisms. In this system, we upregulated and/or downregulated numerous signaling pathways and analyzed their effects on reprogramming using high-content imaging and analysis. In particular, we inserted 38 signaling factors into individual lentiviral vectors, packaged small volumes of each virus, banked frozen viral supernatant, and used high-content imaging to titer lentiviruses and thereby normalize among different viral packaging efficiencies.

By utilizing a robust enzymatic stain with little-to-no background signal for the early reprogramming marker alkaline phosphatase, we generated a quantitative and high-throughput system to assay reprogramming colonies, which are otherwise often counted by hand. The software is capable of measuring numerous population metrics, including final colony number and total area of colonies, as well as individual colony area and a shape factor. These data may yield future insights into the uniformity and distribution of a population of colonies. For instance, a condition with larger colonies compared to the control may be a result of increased reprogramming kinetics or a growth advantage. Additionally, the shape factor may be an indicator of the stability or stochasticity of reprogramming.

By evaluating the factors that increased the number of alkaline phosphatase positive colonies, we found several pathways that were previously known to affect reprogramming. *MAPK1*, *Hif1a*, and *Smo* had a significant effect on colony number and reprogramming this study, consistent with prior work[31, 33, 34]. Furthermore, when we analyzed the total area of alkaline phosphatase positive colonies, Wnt-β-catenin pathway, which has been previously implied in mouse embryonic stem cell biology[36] and reprogramming[31], was found to alter the area of reprogramming. Specifically elevating β-catenin signaling with a constitutively-active *CTNNB1* resulted in increased colony area, and conversely decreasing the signaling, with a constitutively-active *Gsk3b*, decreased colony area and reprogramming efficiency.

However, we found that while activation of the AKT pathway did not alter reprogramming, a dominant-negative *Akt1* increased colony number. This result is contrary to previously published studies showing that AKT binds and positively regulates SOX2 to reprogram cells, and that an inhibitor of PTEN, an AKT pathway antagonist, improves reprogramming efficiency[37, 38]. However, a small molecule inhibitor of PI3K and thus of the AKT pathway has conversely been found to increase reprogramming efficiency[39].

Constitutively active versions of *MAP2K3*, *RAC1*, *HRAS*, *GNA12*, and *GNAQ*, which yielded fewer alkaline phosphatase positive colonies and were thus detrimental to reprogramming, have interesting implications for reprogramming biology. First, HRAS combined with KLF4 can induce oncogenic transformation of MEFs[40], which here could counteract pluripotency reprogramming; however, this possibility is unlikely since constitutively-active *HRAS* expression did not induce any apparent expansion of alkaline phosphatase negative colonies (Fig. D5). Alternatively, constitutively-active HRAS has been shown to induce premature senescence in mouse embryonic fibroblasts,[41] and *HRAS* may thus block reprogramming by initiating senescence[42]. Finally, constitutively-active RAS, with RAC1 as a possible effector, is important in epithelial to mesenchymal transition[43], which may run counter to the mesenchymal to epithelial transition that is a necessary early event in reprogramming[44].

In addition, *GNAQ* and *MAP2K3* may act though similar mechanisms to suppress reprogramming. GNAQ signals via MAP2K3 and MAP2K6, which ultimately activate MAPK14 (also known as p38 MAPK)[45]. GNAQ activation of MAP2K3 is independent of RHOA, and its activation of MAP2K6 occurs in a RHOA-dependent manner[45]. Constitutively-active GNAQ, RHOA, and MAP2K6, which each decreased reprogramming efficiency, may potentially thus act via the same pathway. Conversely, constitutively-active MAP2K3 increased the number of alkaline phosphatase colonies, which indicates MAP2K3 may be acting though an alternative mechanism to the GNAQ signaling pathway. Lastly, constitutively-active *GNA12* – which resulted in significantly fewer alkaline phosphatase colonies in our system – has been shown to upregulate expression of the tumor suppressor p53[46], shown to be a barrier to reprogramming[47, 48].

Ultimately, the results of this study may further our understanding of signaling and reprogramming. For instance, our screen has revealed that reprogramming is dramatically impacted by several GTPases, whose role in induced pluripotency has not previously been studied. Not only did we discover activating small GTPases (*HRAS*, *RHOA*, *RAC1*) reduced *Oct4*, *Sox2*, *Klf4*, and *c-Myc* mediated reprogramming, but activating alpha subunits of heterotrimeric GTPases (*GNAI1*, *GNA12*, *GNAQ*) also had significant impacts in reprogramming, wherein *GNA12* and *GNAQ* decreased reprogramming efficiency and *GNAI1* increased efficiency.

In summary, we have created a medium-throughput, quantitative system to modulate major signaling pathways and analyze effects on the reprogramming process. These findings can be further explored in future studies to elucidate the mechanistic roles of key canonical signaling pathways in induced pluripotency. In addition, this methodology could readily be implemented to determine whether these signaling pathways could substitute for individual Yamanaka factors. This would benefit reprogramming efforts, since *Klf4* and *c-Myc* are known oncogenes, and even *Oct4* expression has been linked with tumor dedifferentiation and progression to a cancer stem cell phenotype[49]. Therefore, replacing these genes with small molecule or growth factor modulators of signaling could enhance the safety of reprogramming. Finally, this lentiviral vector resource can be harnessed to study other aspects of mammalian cell and developmental biology, such as stem cell differentiation or lineage reprogramming from one differentiated cell state to another.

References

1. Takahashi, K. & Yamanaka, S. Induction of pluripotent stem cells from mouse embryonic and adult fibroblast cultures by defined factors. *Cell* **126**, 663-676 (2006).

2. Boeuf, H., Hauss, C., Graeve, F.D., Baran, N. & Kedinger, C. Leukemia inhibitory factor-dependent transcriptional activation in embryonic stem cells. *J Cell Biol* **138**, 1207-1217 (1997).
3. Cartwright, P. et al. LIF/STAT3 controls ES cell self-renewal and pluripotency by a Myc-dependent mechanism. *Development* **132**, 885-896 (2005).
4. Matsuda, T. et al. STAT3 activation is sufficient to maintain an undifferentiated state of mouse embryonic stem cells. *EMBO J* **18**, 4261-4269 (1999).
5. Niwa, H., Burdon, T., Chambers, I. & Smith, A. Self-renewal of pluripotent embryonic stem cells is mediated via activation of STAT3. *Genes Dev* **12**, 2048-2060 (1998).
6. Raz, R., Lee, C.K., Cannizzaro, L.A., d'Eustachio, P. & Levy, D.E. Essential role of STAT3 for embryonic stem cell pluripotency. *Proc Natl Acad Sci U S A* **96**, 2846-2851 (1999).
7. Ying, Q.L., Nichols, J., Chambers, I. & Smith, A. BMP induction of Id proteins suppresses differentiation and sustains embryonic stem cell self-renewal in collaboration with STAT3. *Cell* **115**, 281-292 (2003).
8. Samavarchi-Tehrani, P. et al. Functional genomics reveals a BMP-driven mesenchymal-to-epithelial transition in the initiation of somatic cell reprogramming. *Cell Stem Cell* **7**, 64-77 (2010).
9. Marson, A. et al. Wnt Signaling Promotes Reprogramming of Somatic Cells to Pluripotency. *Cell Stem Cell* **3**, 132-135 (2008).
10. McCurrach, M.E. & Lowe, S.W. Methods for studying pro- and antiapoptotic genes in nonimmortal cells. *Methods Cell Biol* **66**, 197-227 (2001).
11. Sommer, C.A. et al. Excision of reprogramming transgenes improves the differentiation potential of iPS cells generated with a single excisable vector. *Stem Cells* **28**, 64-74 (2010).
12. Welm, B.E., Dijkgraaf, G.J., Bledau, A.S., Welm, A.L. & Werb, Z. Lentiviral transduction of mammary stem cells for analysis of gene function during development and cancer. *Cell Stem Cell* **2**, 90-102 (2008).
13. Macias-Silva, M., Hoodless, P.A., Tang, S.J., Buchwald, M. & Wrana, J.L. Specific activation of Smad1 signaling pathways by the BMP7 type I receptor, ALK2. *J Biol Chem* **273**, 25628-25636 (1998).
14. Raingeaud, J., Whitmarsh, A.J., Barrett, T., Derijard, B. & Davis, R.J. MKK3- and MKK6-regulated gene expression is mediated by the p38 mitogen-activated protein kinase signal transduction pathway. *Mol Cell Biol* **16**, 1247-1255 (1996).
15. Keung, A.J., de Juan-Pardo, E.M., Schaffer, D.V. & Kumar, S. Rho GTPases mediate the mechanosensitive lineage commitment of neural stem cells. *Stem Cells* **29**, 1886-1897.
16. Lai, K., Kaspar, B.K., Gage, F.H. & Schaffer, D.V. Sonic hedgehog regulates adult neural progenitor proliferation in vitro and in vivo. *Nat Neurosci* **6**, 21-27 (2003).
17. Peltier, J., O'Neill, A. & Schaffer, D.V. PI3K/Akt and CREB regulate adult neural hippocampal progenitor proliferation and differentiation. *Developmental neurobiology* **67**, 1348-1361 (2007).
18. Miller-Jensen, K. et al. Chromatin accessibility at the HIV LTR promoter sets a threshold for NF-kappaB mediated viral gene expression. *Integrative biology : quantitative biosciences from nano to macro* **4**, 661-671 (2012).
19. Oh, I.H. & Eaves, C.J. Overexpression of a dominant negative form of STAT3 selectively impairs hematopoietic stem cell activity. *Oncogene* **21**, 4778-4787 (2002).

20. Kopan, R., Schroeter, E.H., Weintraub, H. & Nye, J.S. Signal transduction by activated mNotch: importance of proteolytic processing and its regulation by the extracellular domain. *Proc Natl Acad Sci U S A* **93**, 1683-1688 (1996).
21. Chang, B.H., Mukherji, S. & Soderling, T.R. Characterization of a calmodulin kinase II inhibitor protein in brain. *Proc Natl Acad Sci U S A* **95**, 10890-10895 (1998).
22. Wayman, G.A., Lee, Y.S., Tokumitsu, H., Silva, A.J. & Soderling, T.R. Calmodulin-kinases: modulators of neuronal development and plasticity. *Neuron* **59**, 914-931 (2008).
23. Reuter, J.A. & Khavari, P.A. Use of conditionally active ras fusion proteins to study epidermal growth, differentiation, and neoplasia. *Methods in enzymology* **407**, 691-702 (2006).
24. Choy, L. & Derynck, R. The type II transforming growth factor (TGF)-beta receptor-interacting protein TRIP-1 acts as a modulator of the TGF-beta response. *J Biol Chem* **273**, 31455-31462 (1998).
25. Mace, K.A., Yu, D.H., Paydar, K.Z., Boudreau, N. & Young, D.M. Sustained expression of Hif-1alpha in the diabetic environment promotes angiogenesis and cutaneous wound repair. *Wound Repair Regen* **15**, 636-645 (2007).
26. Robbins, D.J. et al. Regulation and properties of extracellular signal-regulated protein kinases 1 and 2 in vitro. *J Biol Chem* **268**, 5097-5106 (1993).
27. Yu, J.H. & Schaffer, D.V. Selection of novel vesicular stomatitis virus glycoprotein variants from a peptide insertion library for enhanced purification of retroviral and lentiviral vectors. *J Virol* **80**, 3285-3292 (2006).
28. Peltier, J. & Schaffer, D.V. Viral packaging and transduction of adult hippocampal neural progenitors. *Methods Mol Biol* **621**, 103-116.
29. Leonard, J.N., Shah, P.S., Burnett, J.C. & Schaffer, D.V. HIV evades RNA interference directed at TAR by an indirect compensatory mechanism. *Cell host & microbe* **4**, 484-494 (2008).
30. Brambrink, T. et al. Sequential expression of pluripotency markers during direct reprogramming of mouse somatic cells. *Cell Stem Cell* **2**, 151-159 (2008).
31. Silva, J. et al. Promotion of reprogramming to ground state pluripotency by signal inhibition. *PLoS Biol* **6**, e253 (2008).
32. Ying, Q.L. et al. The ground state of embryonic stem cell self-renewal. *Nature* **453**, 519-523 (2008).
33. Yoshida, Y., Takahashi, K., Okita, K., Ichisaka, T. & Yamanaka, S. Hypoxia enhances the generation of induced pluripotent stem cells. *Cell Stem Cell* **5**, 237-241 (2009).
34. Moon, J.H. et al. Reprogramming fibroblasts into induced pluripotent stem cells with Bmi1. *Cell Res* **21**, 1305-1315 (2011).
35. Aoki, H. et al. Synergistic effects of different bone morphogenetic protein type I receptors on alkaline phosphatase induction. *Journal of Cell Science* **114**, 1483-1489 (2001).
36. Hao, J., Li, T.-G., Qi, X., Zhao, D.-F. & Zhao, G.-Q. WNT/beta-catenin pathway up-regulates Stat3 and converges on LIF to prevent differentiation of mouse embryonic stem cells. *Dev Biol* **290**, 81-91 (2006).
37. Jeong, C.H. et al. Phosphorylation of Sox2 cooperates in reprogramming to pluripotent stem cells. *Stem Cells* **28**, 2141-2150 (2010).
38. Liao, J. et al. Inhibition of PTEN Tumor Suppressor Promotes the Generation of Induced Pluripotent Stem Cells. *Mol Ther* **21**, 1242-1250 (2013).

39. Chen, T. et al. Rapamycin and other longevity-promoting compounds enhance the generation of mouse induced pluripotent stem cells. *Aging cell* **10**, 908-911 (2011).
40. Rowland, B.D., Bernards, R. & Peeper, D.S. The KLF4 tumour suppressor is a transcriptional repressor of p53 that acts as a context-dependent oncogene. *Nat Cell Biol* **7**, 1074-1082 (2005).
41. Serrano, M., Lin, A.W., McCurrach, M.E., Beach, D. & Lowe, S.W. Oncogenic ras provokes premature cell senescence associated with accumulation of p53 and p16INK4a. *Cell* **88**, 593-602 (1997).
42. Ichida, J.K. et al. A small-molecule inhibitor of tgf-Beta signaling replaces sox2 in reprogramming by inducing nanog. *Cell Stem Cell* **5**, 491-503 (2009).
43. Edme, N., Downward, J., Thiery, J.P. & Boyer, B. Ras induces NBT-II epithelial cell scattering through the coordinate activities of Rac and MAPK pathways. *J Cell Sci* **115**, 2591-2601 (2002).
44. Li, R. et al. A mesenchymal-to-epithelial transition initiates and is required for the nuclear reprogramming of mouse fibroblasts. *Cell Stem Cell* **7**, 51-63 (2010).
45. Yamauchi, J., Tsujimoto, G., Kaziro, Y. & Itoh, H. Parallel regulation of mitogen-activated protein kinase kinase 3 (MKK3) and MKK6 in Gq-signaling cascade. *J Biol Chem* **276**, 23362-23372 (2001).
46. Kim, M.S. et al. G alpha 12/13 basally regulates p53 through Mdm4 expression. *Molecular cancer research : MCR* **5**, 473-484 (2007).
47. Hong, H. et al. Suppression of induced pluripotent stem cell generation by the p53-p21 pathway. *Nature* (2009).
48. Kawamura, T. et al. Linking the p53 tumour suppressor pathway to somatic cell reprogramming. *Nature* (2009).
49. Kumar, S.M. et al. Acquired cancer stem cell phenotypes through Oct4-mediated dedifferentiation. *Oncogene* **31**, 4898-4911 (2012).

CHAPTER 3

ANALYSIS OF SMOOTHENED, RAS, AND NOTCH SIGNAL TRANSDUCTION PATHWAYS DURING INDUCED PLURIPOTENT STEM CELL REPROGRAMMING

Abstract

Induced pluripotent stem cells exhibit the pluripotency and potential for regenerative medicine of embryonic stem cells. In our previous study, we utilized signaling factors to modulate reprogramming with the four transcription factors OCT4, SOX2, KLF4, and C-MYC. Here, we use the same signaling factors to see if we can replace the individual factors OCT4, SOX2, and KLF4. In preliminary experiments, we studied external modulation of the sonic hedgehog pathway during reprogramming. Second, we discovered two inhibitors were sufficient to switch on NANOG expression with constitutively-active *HRAS* in OCT4-negative reprogramming conditions. Lastly, we found constitutively-active *Notch1* was sufficient to produce cell lines expressing pluripotency markers in OCT4-negative conditions. However, upon *in vitro* differentiation, these cells were deficient in neuronal (ectodermal) differentiation. This screen also found constitutively-active *GNAS* to be sufficient to replace OCT4, which is covered in Chapter 4. These results further mechanistic understanding of the individual factors for inducing pluripotency.

Introduction

The ability to reprogram cells with four transcription factors was first discovered in 2006 by Kazutoshi Takahashi and Shinya Yamanaka[1]. However, two of the four factors, *Klf4* and *c-Myc* are known oncogenes, and even OCT4 expression has been linked with tumor dedifferentiation and progression to a cancer stem cell phenotype[2]. Thus, scientists have been working on new reprogramming methodologies to find new factors for reprogramming. Additionally, we gain mechanistic understanding of the role of each transcription factor by discovering replacement factors. For instance, OCT4-specific replacements are the transcription factor, NR5A2, the DNA hydroxylase, TET1, and the membrane protein, CDH1 (also known as E-cadherin)[3-5]. SOX2-specific replacements are the TGFβ inhibitors, SB-431542 and 616452 (also known as RepSox)[6, 7]. KLF4-specific replacements are BMP4 and the small molecule inhibitor, kenpaullone[8, 9]. These results do not include C-MYC, which was shown early on to be dispensable in reprogramming[10, 11].

Signaling pathways, rather than transcription factors, can be manipulated by small molecules and growth factors, which is advantageous for reprogramming. Small molecules can be added with temporal control and at variable concentrations, libraries of small molecules are readily available, and small molecules are relatively straightforward to use versus producing transgenic proteins or viral vectors. Small molecules have been previously used to improve reprogramming methodologies[12], and factor replacements have been discovered for SOX2[6, 7, 13, 14] and KLF4[8, 9, 15, 16]. To date, however, no small molecule replacement for OCT4 has been discovered.

Previously, we have shown the effects of signal transduction pathways on induced pluripotent stem cell reprogramming (Chapter 2). Here, we use a similar approach to determine if any signaling factors are sufficient to replace the reprogramming factors *Oct4*, *Sox2*, and *Klf4*.

Our initial screen resulted in few alkaline phosphatase positive colonies; however, their presence was sufficient to initiate studies on individual pathways. This chapter details the studies performed with the Sonic Hedgehog, Ras/MAPK, and Notch signaling pathways. An additional study with GNAS in OCT4 replacement is detailed in Chapter 4.

Methods

Cell Culture and Plasmid Construction

HEK293T cells were maintained in IMDM with 10% FBS and 1% penicillin/streptomycin. 129 MEF cells were a kind gift of Lin He (University of California, Berkeley) and isolated as previously described[17]. MEFs were maintained in DMEM (high glucose), 10% FBS, 1% GlutaMAX, and 1% penicillin/streptomycin (Invitrogen). Cells undergoing reprogramming were maintained in serum-containing, mouse embryonic stem cell (mESC-FBS) conditions: DMEM (high glucose), 15% FBS (Hyclone, SH3007003E), 0.5% penicillin/streptomycin, 1% GlutaMAX, 1% Sodium Pyruvate, 1% MEM NEAA, 0.1 mM 2-mercaptoethanol (Invitrogen), and 1000 U/mL LIF (Millipore, ESG1106). 15% KnockOut Serum Replacement (Invitrogen) was used in place of FBS in serum-free conditions (mESC-KSR). Differentiating embryoid bodies (EBs) were maintained in mESC-FBS media without LIF. Cells were maintained at 37°C with 5% CO_2.

STEMCCA-SKM loxP (SKM), STEMCCA-OKM loxP (OKM), and STEMCCA-OSM loxP (OSM) were constructed from the STEMCCA loxP vector[18]. Briefly, STEMCCA-SKM loxP was constructed by creating a NotI-Klf4-IRES-NdeI PCR fragment (NotI-Klf4 Forward: 5' - GTAATAT**GCGGCCGC**CATGGCTGTCAGCGACGCTCTG - 3', Nde-IRES Reverse: 5' - CCCCCCCCCC**CATATG**TGTGGCCATATTATCATCGTGTTTTTCAAAGGAAAACC - 3', restriction sites in bold). After enzymatic digestion, the PCR fragment was inserted into a NotI-NdeI digested STEMCCA loxP subsequently removing the *Oct4* gene. STEMCCA-OKM loxP was constructed by creating an NdeI-cMyc-ClaI PCR fragment (NdeI-cMyc Forward: 5' - GGATAG**CATATG**ATGCCCCTCAACGTGAACTTC - 3', ClaI-cMyc Reverse: 5' - CGATCT**ATCGAT**TTATGCACCAGAGTTTCGAAGCTGTTC - 3'). After enzymatic digestion, the PCR fragment was inserted into an NdeI-ClaI digested STEMCCA loxP subsequently removing the *Sox2* gene. STEMCCA-OSM loxP was constructed through overlap extension PCR. Two PCR fragments, NotI-Oct4-*STOP-IRES* and *Oct4*-IRES-NdeI, were created (NotI-Oct4-*STOP-IRES* Forward: 5' – GAATAA**GCGGCCGC**CATGGCTGGACACCTGGCT TCAGACTTCGCCTTCTCACC - 3', NotI-Oct4-*STOP-IRES* Reverse: 5' – GCCAGTAACGTT AGGGGGGGGGGAGTCAGTTTGAATGCATGGGAGAGCCCAGA - 3', *Oct4*-IRES-NdeI Forward: 5' – GGGCTCTCCCATGCATTCAAACTGACTCCCCCCCCCCTAACGTTACTGG CCGA - 3', *Oct4*-IRES-NdeI Reverse: 5' – GGGGGG**CATATG**TGTGGCCATATTATCATCG TGTTTTTCAAAGGAAAACCACGTCCCCGTGGTTCGGGGG - 3', sequences located in primer in italics). The two fragments were used in a subsequent PCR with the NotI-Oct4-*STOP-IRES* Forward and the *Oct4*-IRES-NdeI Reverse primers creating a NotI-Oct4-IRES-NdeI PCR fragment. After enzymatic digestion, the PCR fragment was inserted into a NotI-NdeI digested STEMCCA loxP subsequently removing the *Klf4* gene. DNA was prepared with QIAGEN Plasmid Maxi Kit per manufacturer's instructions. Plasmid sequences were verified by restriction enzyme digest and sequencing.

Viral Production and Titering

For the signal transduction vectors, lentiviral supernatant was produced by HEK293T cells in 6 well plates using calcium phosphate transfection as previously described (Chapter 2)[19]. Supernatant was collected 48 hours post transfection, aliquoted, and stored at -80°C. For the reprogramming cassettes, STEMCCA loxP, STEMCCA-SKM loxP, STEMCCA-OKM loxP, and STEMCCA-OSM loxP, the lentiviral transfection and centrifugation were performed as previously described[18, 19].

To quantify the amount of virus produced, 1,600 MEF cells were plated in black-walled 96 well plates (E+K Scientific) coated with gelatin. After the cells attached, virus was added to the media. Vector-mediated gene expression was analyzed 72 hours post post-infection. MEF cells were fixed in 4% paraformaldehyde for 15 minutes. The cells were blocked and permeabilized with 5% donkey serum with 0.3% Triton X-100 in PBS. The anti-GFP primary antibody (Invitrogen, A-11122, 1:500 dilution) was incubated overnight at 4°C. The secondary antibody (Invitrogen, A-21206, 1:250 dilution) was incubated for 2 hours at room temperature. DAPI (Invitrogen, 1:2000 dilution) was used as a nuclear stain. For *Oct4*-containing STEMCCA loxP cassette viruses, an anti-Oct4 antibody (Santa Cruz Biotechnology, sc-5279, 1:100 dilution) and a secondary antibody (Invitrogen, A-21235, 1:250 dilution) were used. For STEMCCA-SKM loxP, an anti-SOX2 antibody (Santa Cruz Biotechnology, sc-17320, 1:200) and a secondary antibody (Jackson ImmunoResearch, 705-165-147, 1:250) were used. GFP, SOX2, or OCT4 expression was imaged with the Molecular Devices ImageXpress Micro and analyzed with MetaXpress software. Infectious titers were calculated as previously described[19]. More information for the signal transduction titers on MEFs is found in Chapter 2.

iPS Cell Reprogramming – Factor Replacement

7,500 passage 3 MEF cells were plated into 48 well plates. The following day one signal transduction virus (24-650 μL) was added at an MOI of 1.0 (63% cells infected) and STEMCCA-loxP virus was added at an MOI of 0.3 (26% cells infected) to each condition. following day, the media were replaced with fresh MEF media. 48 hours post-infection, each 48 well was split into triplicate onto MEF feeder layers (GlobalStem, GSC-6101M) in mouse embryonic stem cell media. Media were changed every day. The 6-channel multichannel adjustable pipette (Rainin, LA6-1200XLS) was used to passage cells and change media.

9 days post-infection, cells were fixed with 4% paraformaldehyde for 15 minutes. Alkaline phosphatase expression was assayed using the ELF Phosphatase Detection Kit (ATCC, SCRR-3010) per manufacturer's instructions. (Note that ATCC kit has been discontinued, and we have found the ELF 97 Endogenous Phosphatase Detection Kit (Invitrogen, E-6601) to be an appropriate substitute). HCS NuclearMask Red stain (Invitrogen, H10326, 1:1000 dilution) was used to visualize nuclei.

The 24 well plates were imaged with a Molecular Devices ImageXpress Micro high-throughput imager. A custom filter cube (Semrock BrightLine filters, Excitation: FF01-377/50-25, Dichroic: FF409-Di03-25x36, Emission: FF01-536/40-25) was necessary to detect alkaline phosphatase expression. For image analysis, a custom journal was created in the MetaXpress software to merge the images and identify colonies/regions of alkaline phosphatase expression.

Sonic Hedgehog Reprogramming

Hyaluronic-acid-SHH conjugates and recombinant SHH were kind gifts of Randolph Ashton. Reprogramming was performed as previously described. After passage to feeder layers,

the HyA-SHH construct was added at 200 ng/mL, and the HyA-EMCH backbone control was added at the same volume as the HyA-SHH construct. The small molecule SAG was added (100 nM, Calbiochem, 566660) after passage. Media was changed daily. Cells were fixed 8 days after infection and stained for NANOG expression (Abcam, ab70482, 1:250 and Jackson ImmunoResearch, 711-605-152, 1:500). Colonies were analyzed as previously described.

NANOG Analysis

Cells were reprogrammed as previously described. Briefly, 9000 passage 3 MEFs were plated in 48 well plates. The following day the cells were infected the respective STEMCCA virus and signaling factor. 24 hours later, the medium was replaced with MEF media. The following day, the cells were passaged into 12 well plates with mitomycin-c treated feeder layers in mouse embryonic stem cell medium. In conditions with CHIR99021 and PD0325901, small molecules were added five days post-infection, unless otherwise noted, in serum-free mouse embryonic stem cell medium. Once colony formation was apparent, cells were fixed and stained against NANOG (Abcam, ab70482, 1:250 and Jackson ImmunoResearch, 711-605-152, 1:500). Various small molecules were used during reprogramming: CHIR99021 (3 μM, Cayman Chemical, 13122), PD 0325901 (1 μM, Cayman Chemical, 13034), SC1 (300 nM, Cayman Chemical, 10009557), FGF (10 ng/μL, Peprotech, 100-18B), and EGF (10 ng/μL, Peprotech, 315-09).

Cell Line Isolation and Pluripotency Immunostaining

Cells were reprogrammed as previously described. Twelve or more days post-infection, cells were manually selected under a microscope (EVOS xl core, AMG), trypsinized, and added to separate wells in a 48 well plate with mitomycin-c treated MEF feeder layers in serum-containing mouse embryonic stem cell media. Cells were passaged upon confluency. To probe for expression of pluripotency proteins, confluent cells were fixed and stained with the following antibodies: SSEA1, OCT4, and NANOG (previously described). For SSEA1, the primary antibody (Millipore, MAB4301, 1:200) and secondary antibody (Invitrogen, A-21045, 1:1000) were used. As SSEA1 is cell surface marker, no Triton-X100 was used to permeabilize the cells. The staining was imaged on the ImageXpress Micro (Molecular Devices).

Embryoid Body Differentiation

iPS cell lines were trypsinized and incubated on 0.1% gelatin-coated tissue culture plates in EB medium for 1 hour at 37°C with 5% CO_2 to separate the MEF feeder layers from the iPS cells. The unattached cells were collected and diluted to $2.25x10^4$ cells/mL. 20 μL drops were pipetted onto a 15 cm lid. 10 mL PBS buffer was added to the plate and the lid was gently placed on top of the plate. The hanging drops were incubated at 37°C with 5% CO_2 for two days. The drops were collected and the embryoid body suspension was added to a bacterial-grade sterile 10 cm dish. The embryoid bodies were incubated for three or more days before pipetting individual embryoid bodies into the wells of a 24 well plate coated with gelatin. The following day, the media was partially changed. The media was changed every other day or every day upon confluency. The embryoid bodies were fixed when the EBs had attached, cells had migrated and appeared differentiated (12-20 days after hanging drop). The cardiomyocyte videos were captured using a Nikon Eclipse TE2000-E microscope.

To visualize the expression of differentiation markers, the wells were fixed and stained with one the following antibodies: for mesoderm, anti-α-smooth muscle actin (Sigma Aldrich,

A2547, 1:500) and the secondary (Invitrogen, A-11003, 1:1000); for endoderm, anti-HNF3β (also known as FOXA2) (Millipore, 07-633, 1:500); and for ectoderm, anti-β3-tubulin (Covance, MRB-435P, 1:500). The secondary antibody (Invitrogen, A11-012, 1:1000) was used for HNF3β and β3-tubulin staining. The staining was imaged on the ImageXpress Micro (Molecular Devices).

Results

Screening for OCT4, KLF4, or SOX2 Replacements Results in Minimal Reprogramming

After studying the ability of signaling pathways to modulate induced pluripotent stem cell reprogramming (Chapter 2), we subsequently asked if any signaling pathways were able to replace the reprogramming factors OCT4, SOX2, or KLF4. The STEMCCA loxP cassette[18] was modified to create the 3-factor vectors: STEMCCA-SKM loxP (SKM), STEMCCA-OKM loxP (OKM), and STEMCCA-OSM loxP (OSM), which removed *Oct4*, *Sox2*, and *Klf4* from the viral transgene, respectively (Figure E1). Viral titers were calculated as in Chapter 2.

To assay whether any signaling pathways could substitute for OCT4, SOX2, or KLF4 during reprogramming, passage 3 MEFs were plated and infected with STEMCCA loxP vectors (MOI of 0.3 viruses/cell resulting in ~26% of cells infected) and lentiviruses encoding constitutively-active, dominant-negative, or wild-type signal transduction genes (MOI of 1.0 resulting in ~63% of cells infected). The construction of the library and the methodology for the reprogramming screen is detailed in Chapter 2. Briefly, cells were passaged into mouse embryonic stem cell conditions 2 days post-infection. Once colony morphology was apparent, the cells were fixed and stained for alkaline phosphatase expression, an early reprogramming marker: 10 days post-infection for OSM (*Klf4*-negative), 16 days post-infection for OKM (*Sox2*-negative), and 13 days post-infection for SKM (*Oct4*-negative). High-content imaging and analysis (Chapter 2) was used to quantify the number of alkaline phosphatase positive colonies. The results of the screen are shown in Table I.

Table I. Reprogramming factor replacement

Replacing Factor	Gene Symbol	Number of Alkaline Phosphatase+ Colonies
KLF4	CA *HRAS*	24 ± 2
KLF4	CA *Smo*	0.3 ± 0.6
KLF4	DN *STAT3*	0.3 ± 0.6
SOX2	DN *RHOA*	0.3 ± 0.6
SOX2	WT *Camk4*	0.3 ± 0.6
SOX2	CA *Notch1*	0.7 ± 0.6
SOX2	CA *Smo*	0.3 ± 0.6
OCT4	CA *RHOA*	0.3 ± 0.6
OCT4	DN *RAC1*	0.3 ± 0.6
OCT4	CA *CDC42*	0.7 ± 1.1
OCT4	WT *Akt1*	0.3 ± 0.6
OCT4	CA *HRAS*	0.3 ± 0.6
OCT4	CA *NFKBIA*	0.3 ± 0.6
OCT4	CA *Tgfbr1*	0.3 ± 0.6

OCT4	CA *Hif1a*	0.3 ± 0.6
OCT4	WT *Mapk1*	0.3 ± 0.6
OCT4	CA *GNAS*	0.7 ± 1.1
OCT4	CA *Notch1*	0.7 ± 0.6
OCT4	CA *Smo*	0.7 ± 0.6
OCT4	CA *STAT3*	0.3 ± 0.6
OCT4	DN *Gsk3b*	0.3 ± 0.6
OCT4	DN *TGFBR2*	0.3 ± 0.6
OCT4	pHIV CTRL	0.3 ± 0.6

Colony formation was a rare event, with only 1-2 colonies maximally appearing per condition, with the sole exception of constitutively-active *HRAS* during KLF4 replacement (Table I). As the cells were infected an MOI of 0.3 for the STEMCCA loxP viruses and 1.0 for the signaling viruses, ~410 cells per well were infected with both viruses, as estimated by the viral titer and a Poisson distribution. Since reprogramming is a rare process[20], it is likely that too few cells were infected to determine how well the signaling factors were at replacing each reprogramming factor. However, as OCT4, SOX2, and KLF4 are necessary for the reprogramming of mouse embryonic fibroblasts[1, 6, 7, 9], alkaline phosphatase positive colony formation is a promising indicator of the potential to replace a respective factor. Example colonies from the *Klf4*-negative condition are shown in Figure 1.

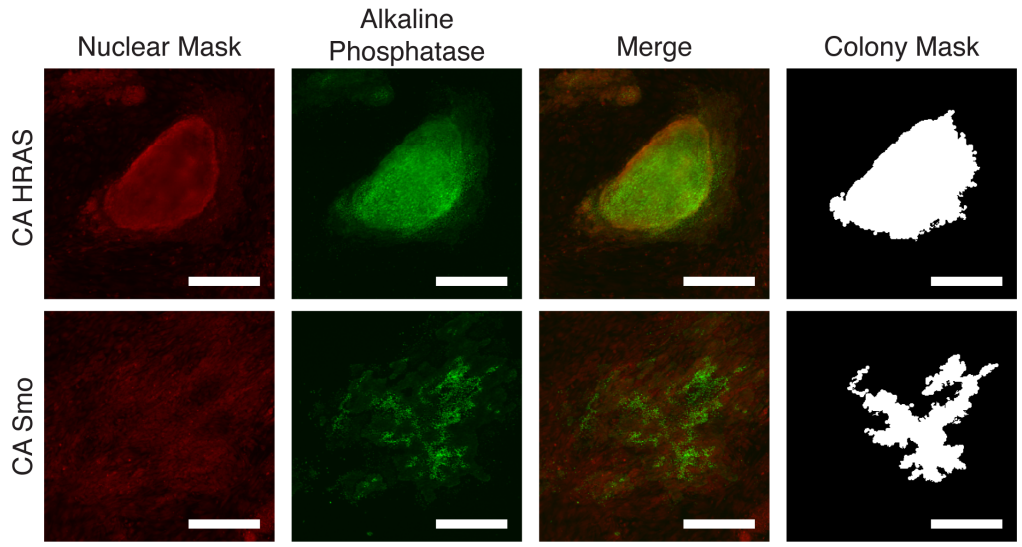

Figure 1. Signaling pathways can induce alkaline phosphatase colonies in the absence of KLF4. Colonies were infected with OSM and the virus containing each signaling factor. 10 days post-infection, cells were fixed and stained for alkaline phosphatase expression. Cells were analyzed by high-content imaging and analysis, which resulted in a colony mask to define individual colonies. Minimum colony size measured was 31,200 μm^2. Scale bars are 300 µm.

Constitutively-active *HRAS*, an activator of MAPK signaling, was able to replace KLF4 to form alkaline phosphatase positive colonies morphologically similar to mouse embryonic stem cell colonies. However, in comparison, constitutively-active *Smo*, the cell surface receptor

Smoothened, only resulted in one alkaline phosphatase positive region which did not readily form into colony shape (Fig. 1), which indicates that *Smo* may or may not be able to replace some of KLF4's function. Similarly, constitutively-active *Smo* also resulted in alkaline phosphatase positive regions for SOX2 replacement albeit without colony morphology (Fig. 2). This induction of alkaline phosphatase without KLF4 or SOX2 expression may indicate that *Smo* is a general factor that may be able to improve reprogramming via mechanisms not specific to one reprogramming factor.

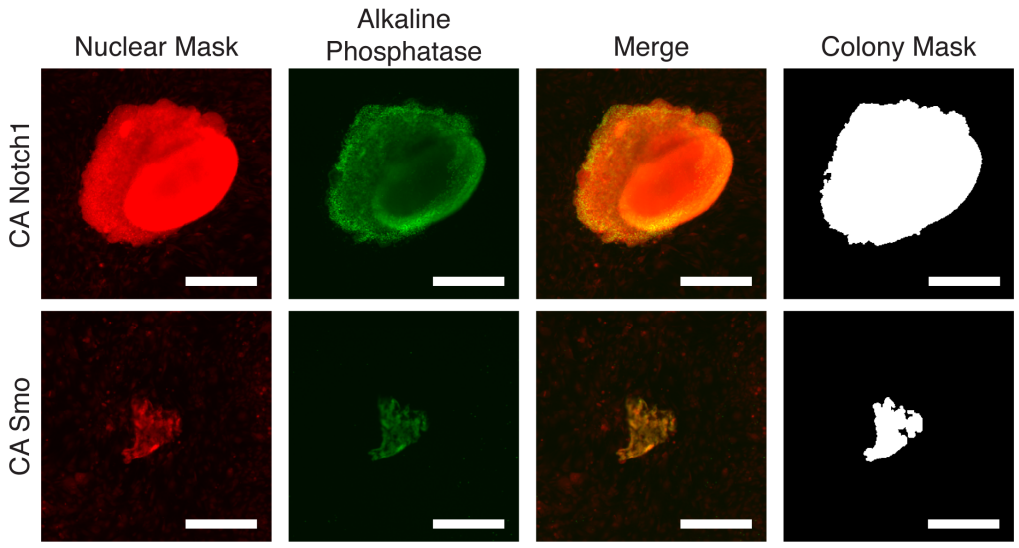

Figure 2. Signaling pathways can induce alkaline phosphatase colonies in the absence of SOX2. Colonies were infected with OKM and the virus containing each signaling factor. 16 days post-infection, cells were fixed and stained for alkaline phosphatase expression. Cells were analyzed by high-content imaging and analysis, which resulted in a colony mask to define individual colonies. Minimum colony size measured was 31,200 μm^2. Scale bars are 300 μm.

Additionally, a constitutively-active *Notch1*, a cell surface receptor, was able to generate alkaline phosphatase positive colonies in the absence of SOX2 (Figure 2). Interestingly, constitutively-active *Notch1* and *Smo* also generated alkaline-phosphatase positive colonies in the absence of OCT4 (Figure 3). The SKM screen resulted in the most hits for factor replacement. For example, even the pHIV CTRL infection control resulted in one region of alkaline phosphatase expression (Figure 2), however, the expression was not uniform and no colonies were present, indicating that the cells would be unlikely to reprogram completely to the iPS cell state. Constitutively-active *GNAS*, a cell surface receptor, was able to generate alkaline phosphatase positive colonies and is discussed further in Chapter 4 (Figure 2).

Even though HRAS signaling was indicated in the KLF4-negative screen, constitutively-active *HRAS* was unable to generate alkaline phosphatase colonies without the *Oct4* transgene. However, several areas of proliferation and colony morphology were both apparent in the SKM *HRAS* condition (Figure E2). One colony did have non-uniform alkaline phosphatase expression (Figure 2) indicating that it may be possible to generate colonies in the absence of OCT4 by activation of the MAPK pathway.

Ultimately, these results led us to perform preliminary experiments on three signaling pathways: sonic hedgehog (CA *Smo*), MAPK (CA *HRAS*), and notch (CA *Notch1*) pathways.

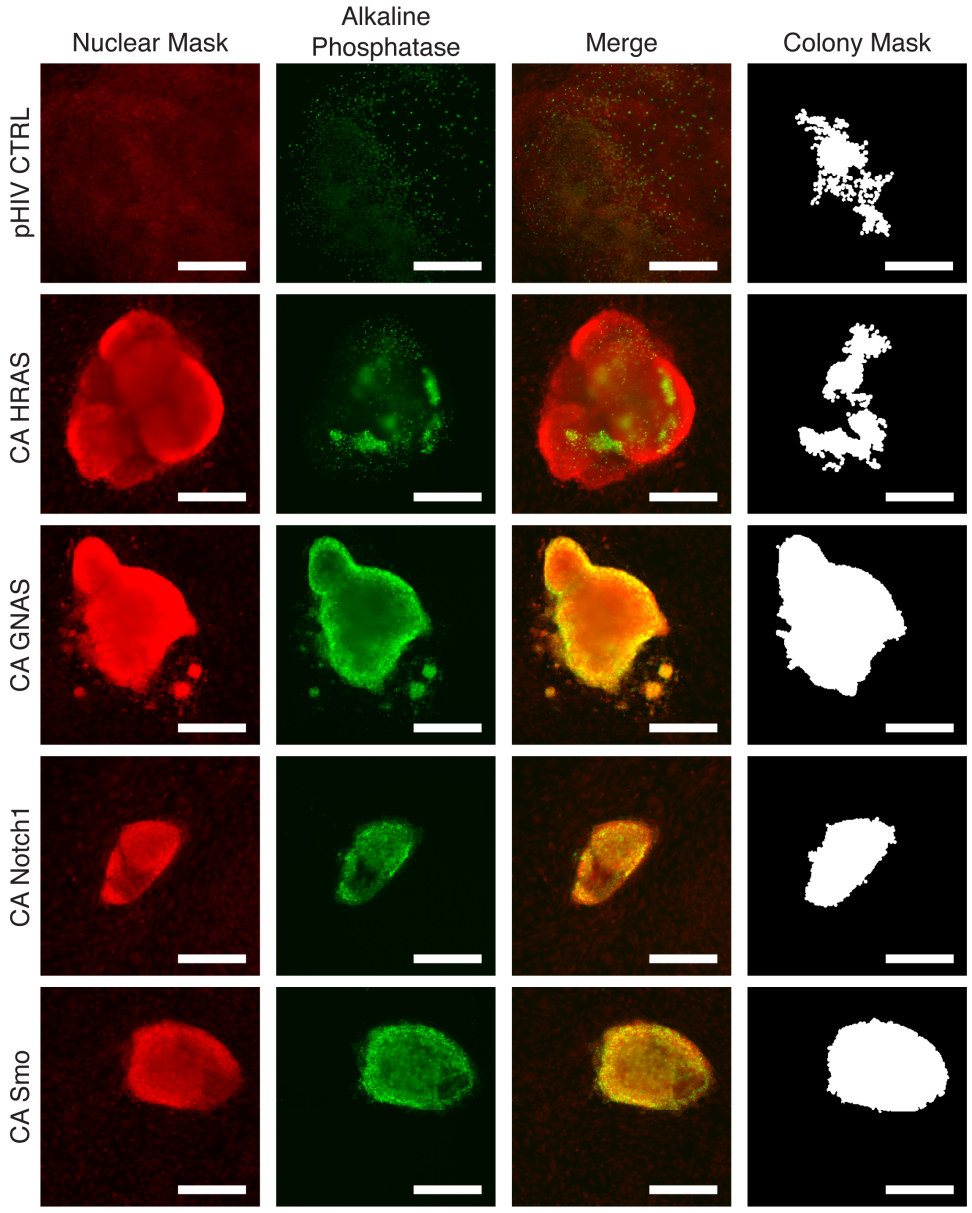

Figure 3. Signaling pathways can induce alkaline phosphatase colonies in the absence of OCT4. Colonies were infected with SKM and the virus containing each signaling factor. 13 days post-infection, cells were fixed and stained for alkaline phosphatase expression. Cells were analyzed by high-content imaging and analysis, which resulted in a colony mask to define individual colonies. Minimum colony size measured was 31,200 μm^2. Scale bars are 300 μm.

External Activation of the Sonic Hedgehog Pathway Minimally Improves Reprogramming

As constitutively-active *Smo* was able to generate an alkaline phosphatase positive colony without OCT4 and alkaline phosphatase regions in KLF4- and SOX2-negative conditions, we wanted to see if activation of the sonic hedgehog pathway could improve reprogramming. Additionally, as previously discussed, constitutively-active *Smo* was able to significantly increase the number of alkaline phosphatase colonies in OSKM reprogramming ($p < 0.05$,

Chapter 2). During reprogramming, we added recombinant SHH and the small molecule agonist against Smoothened, SAG. Neither the protein nor the small molecule resulted in a significant increase in the number of NANOG positive colonies (Figure 4a). In contrast, when a multivalent form of SHH was added to reprogramming cultures, the number of reprogrammed colonies and reprogramming efficiency was significantly increased ($p < 0.05$, Figure 4b). Due to the small increase reprogramming, however, we decided not to pursue further studies with the sonic hedgehog pathway.

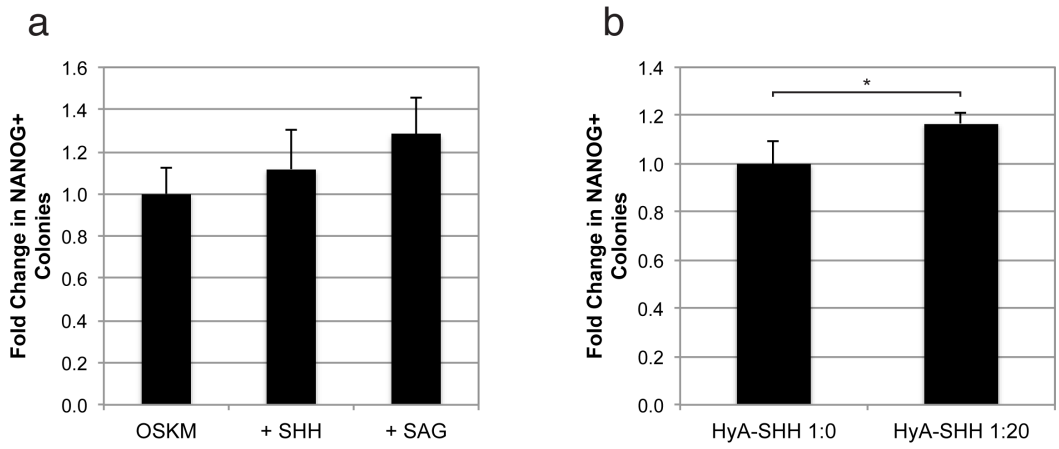

Figure 4. External modulation of the sonic hedgehog signaling pathway does not strongly affect OSKM reprogramming. (a) OSKM reprogrammed cells (MOI of 0.1) were treated with recombinant SHH or the small molecule agonist, SAG. Colony number is normalized to the OSKM condition. (b) OSKM reprogrammed cells were treated with a hyaluronic acid-SHH conjugate. Colony number is normalized to the SHH negative condition. Colonies were fixed 8 days post infection and analyzed by high-content imaging and analysis. The minimum colony size is 10,000 μm^2. Statistical significance was measured using a Student's t-Test (two-tailed, homoscedastic) with * $p < 0.05$. Error bars represent standard deviation.

Activation of the MAPK Pathway Can Replace KLF4 or OCT4 to Result in NANOG Positive Colonies

We wanted to further study the effect of *HRAS* in OCT4-negative conditions. As some alkaline phosphatase expression was present, we hypothesized that the addition of the 2 small molecule inhibitors (2i), CHIR99021 and PD 0325901, that have the potential to stabilize partially reprogrammed cells[21], might be enough to turn on pluripotency genes. As shown in Figure 5, MEFs infected with SKM and constitutively-active (CA) *HRAS* express NANOG, a later stage reprogramming marker, when the 2i inhibitors are added after 5 days post-infection in serum-free medium. Compared to the OSM and CA *HRAS* infected cells, the colonies have smooth borders, are densely packed with cells, and strongly express NANOG (Figure 5, E3).

We further wanted to test the necessity of both inhibitors on the CA *HRAS* replacement of OCT4. Preliminary experiments indicate that both inhibitors can produce NANOG positive colonies individually (Figure E4a), which is surprising as the target of the PD 0325901 inhibitor in downstream in the MAPK pathway. An additional preliminary experiment also showed that earlier addition of the 2i small molecules might further improve reprogramming (Figure E4b).

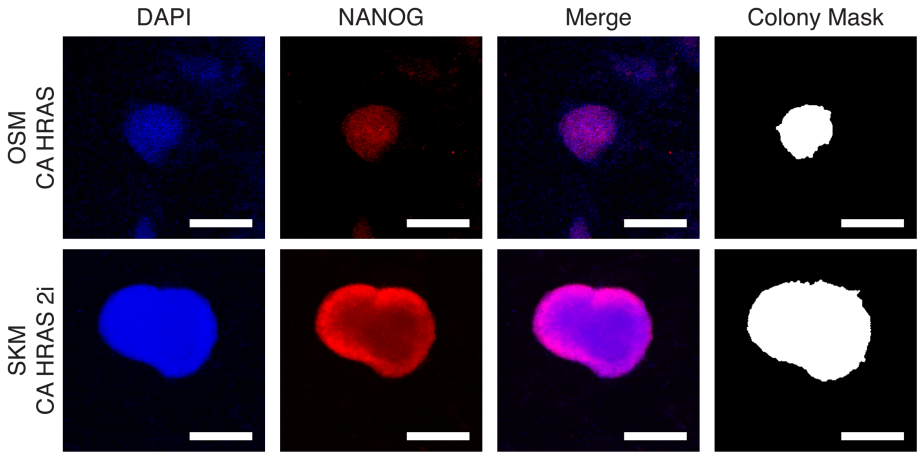

Figure 5. Constitutively-active HRAS can induce NANOG expression without the *Klf4* or *Oct4* transgene. Passage 3 MEFs were reprogrammed with OSM and constitutively-HRAS and stained for NANOG expression 8 days post-infection. Passage 3 MEFs were also reprogrammed with SKM and constitively-active HRAS with the 2i inhibitors (CHIR99021 and PD 0325901) added in serum-free conditions 5 days post-infection. Cells were analyzed for NANOG expression 14 days post-infection. Cells were analyzed by high-content imaging and analysis. Minimum colony size measured was 15,000 μm^2. The images were post-processed differently as SKM CA HRAS 2i and OSM CA HRAS had dissimilar colony morphology and expression. Scale bars are 300 μm.

As PD 0325901 with CA *HRAS* and SKM was able to generate NANOG positive colonies, we wanted to test if the small molecule SC1 could also generate colonies in the absence of OCT4. SC1 is a small molecule that activates Ras/MAPK signaling but inhibits the downstream effector of MAPK signaling, ERK1[22]; This is mechanism is similar to PD 0325901 inhibiting the downstream effector, MEK, during activation of *HRAS*. SC1 added during OCT4-reprogramming resulted in NANOG positive colonies (Figure 6).

Additionally, as activation of MAPK signaling may have been necessary for SC1 addition, we added the growth factors EGF or FGF in addition to SC1 in preliminary experiments. As shown in Figure E5, the addition of FGF increased colony formation by 2.4-fold. To further test the pluripotency of the SC1 SKM FGF cells, we selected 4 colonies for cell line expansion. However, all 4 colonies failed to form cell lines, indicating the colonies may not have fully reached pluripotency, and we did not further study the effect of the *HRAS* signaling pathway in OCT4-replacement.

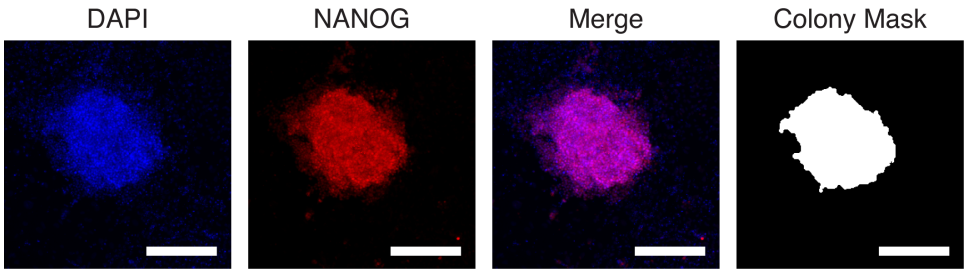

Figure 6. The small molecule, SC1, can induce NANOG expression without the *Oct4* transgene. Passage 3 MEFs were reprogrammed with SKM and SC1 was added 3 days post-infection. 5 days post-infection CHIR99021 was added in serum-free media. Medium and small molecules were changed every other day.

Cells were analyzed for NANOG expression 9 days post-infection. Cells were analyzed by high-content imaging and analysis. Minimum colony size measured was 15,000 μm^2. Scale bars are 300 μm.

Notch1 Activates Pluripotency Markers in the Absence of OCT4 but Fails to Induce Ectoderm Differentiation

Constitutively-active *Notch1* appeared in both the SOX2- and OCT4-negative screens. Further studies indicated that SOX2 replacement was highly inefficient, as when more cells were infected, only a few colonies were generated (data not shown). We further studied *Notch1*'s ability to replace OCT4. CA *Notch1* and SKM reprogrammed colonies were further isolated and propagated to form cell lines. As shown in Figure 7, the cell lines, such as SKM Notch-01, expressed the pluripotency markers, SSEA1, OCT4, and NANOG.

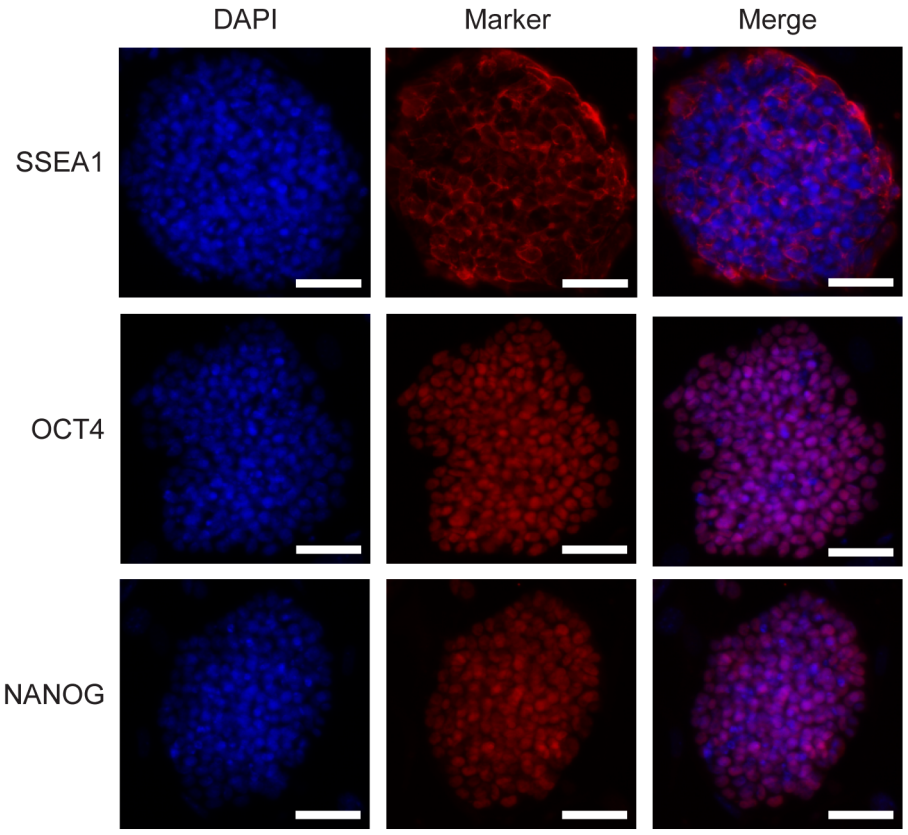

Figure 7. Activating *Notch1* expression activates endogenous pluripotency genes. The cell line, SKM Notch-01, was stained for pluripotency markers, SSEA1, OCT4, and NANOG. The cell line was imaged seven passages after isolation. Scale bars are 50 μm.

To further test the pluripotency of the *Notch* cell lines, we performed *in vitro* embryoid body differentiation experiments. While cells staining positive for mesoderm and endoderm markers were readily apparent in the differentiated outgrowths (Figure 8), the cultures failed to produce bIII-tubulin positive, ectodermal cells, indicating that the *Notch1* replacement of OCT4 did not fully result in pluripotency.

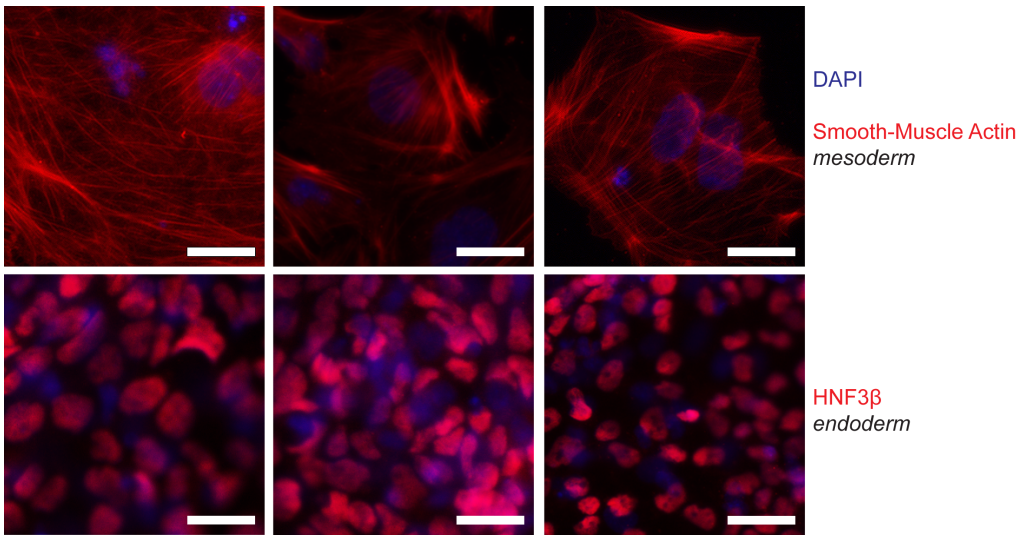

Figure 8. Constitutively-active *Notch1* cell lines form embryoid bodies and produce two germ layers *in vitro*. SKM Notch-01 differentiates into two of the three germ layers: images are of different regions expressing smooth-muscle actin or HNF3β, respectively, in embryoid body outgrowth. No βIII-tubulin cells were identified. Scale bars are 25 μm.

Discussion

The induction of pluripotent stem cells from adult cells has the potential to impact personalized and regenerative medicine. However, *Klf4*, *c-Myc*, and possibly *Oct4* are considered oncogenes, and ongoing research is determining new ways to reprogram to find safer, more efficient methodologies. Here, we describe screening methodology to replace OCT4, SOX2, and KLF4 through modulating signaling pathways by utilizing 38 signaling genes in combination with three of the four reprogramming factors (using SKM, OKM, OSM vectors, respectively).

During the screening for an OCT4 replacement, more signaling factors resulted in alkaline phosphatase expression than in SOX2- and KLF4-negative screens. The SKM vector was modified from the STEMCCA loxP plasmid[18], in which the F2A sequence was later determined to be ineffective for processing of OCT4 and KLF4 proteins[23]. However, in the creation of the SKM vector, the F2A sequence is removed, theoretically resulting in higher expression of KLF4. As the three factors, SOX2, KLF4, and C-MYC, are co-expressed and we used the permissive 129 mouse strain and embryonic fibroblasts to reprogram[21], we minimized the barriers to reprogramming and found a robust system to find substitutions for *Oct4* in reprogramming. Additionally, the F2A sequence remaining in the OKM vector may be one reason for which SOX2 replacements were hard to discover in this screen.

Within the OCT4-negative conditions, we initially analyzed three signaling pathways: sonic hedgehog, Ras/MAPK, and notch pathway. The sonic hedgehog pathway, as mentioned in Chapter 2, has already been implicated for reprogramming. BMI1, activated downstream of the sonic hedgehog, is a transcription factor capable of transdifferentiating cells to a neural stem cell like-state and in combination with OCT4, results in induced pluripotent stem cells[24]. As constitutively-active *Smo* was able to generate alkaline phosphatase expression in SOX2- and KLF4-negative conditions as well as an alkaline phosphatase colony in the absence of OCT4 we wanted to test if external activation of the pathway could aid in reprogramming. While we only

saw a few colonies when a multivalent SHH construct was added in SKM conditions (data not shown), we were able to generate significantly more NANOG positive colonies in OSKM conditions. These initial experiments may indicate that manipulation of the sonic hedgehog pathway may be useful for improving reprogramming or even replacing OCT4; however, further studies need to be performed.

Subsequently, we studied the ability of constitutively-active *HRAS* to replace KLF4 and OCT4. HRAS has been shown to activate KLF5[25], and KLF5 has been shown to partially recover KLF4-negative reprogramming conditions[10]. This mechanism is perhaps why constitutively-active *HRAS* can generate alkaline phosphatase positive colonies in KLF4-negative reprogramming conditions. Interestingly, *HRAS* is also able to form colony-like morphology in OCT4-negative conditions. These colonies were not pluripotent by alkaline phosphatase expression, but upon the addition of the 2i small molecule inhibitors[21], NANOG expression was readily apparent. The inhibitor, PD 0325901, is an agonist for MAPK signaling, the pathway that HRAS activates. This led us to test the small molecule SC1, which has been shown to activate RAS signaling while inhibiting MAPK signaling[22]. In SKM and FGF reprogramming conditions, SC1 was able to generate NANOG positive colonies; however, the colonies were unsuccessful in forming stable pluripotent cell lines. Future work could further our understanding of the MAPK signaling pathway during reprogramming. For example, ERAS is a Ras-like protein found in mouse embryonic stem cells that does not activate the MAPK pathway[26], and it would be of interest to see if ERAS could also replace OCT4 during reprogramming. However, one concern when activating RAS is a risk of oncogenesis[27], especially as we saw highly dense, proliferative colonies with SKM, *HRAS* and 2i, and any cell lines created with modification of the Ras pathway should be scrutinized for tumorigenic properties.

In analysis of the *Notch1* replacement of OCT4, we discovered we were able to generate cell lines with iPS cell-like morphologically and with expression of SSEA1, OCT4, and NANOG. However, after *in vitro* differentiation of these cell lines, no neuronal cells were found in the differentiated outgrowth. Previous studies have indicated that persistent expression of Notch signaling can hinder neuronal differentiation[28-30]. The lack of differentiation to the neural lineage may be the first indication that the cells have prolonged expression of *Notch1* in the induced pluripotent state and that the lentiviral transgene may not be silenced or may become reactivated during differentiation[31, 32]. In future studies, it may be possible to activate *Notch1* transiently or without the use of viral vectors for the hypothesis that *Notch1* may be necessary only during reprogramming but harmful once pluripotency is established.

In addition to the individual factor replacement, we additionally studied if the signaling factors that were indicated in the OSKM screen or the factor replacement screens would be able to replace all four reprogramming factors. Unfortunately, different combinations of the signaling genes were not able to result in colony like formation (detailed in Table EI, EII). While complete replacement was unsuccessful and we only delved briefly into studying three signaling pathways, this screen did lead to a successful OCT4 replacement that is presented in detail in Chapter 4.

References

1. Takahashi, K. & Yamanaka, S. Induction of pluripotent stem cells from mouse embryonic and adult fibroblast cultures by defined factors. *Cell* **126**, 663-676 (2006).

2. Kumar, S.M. et al. Acquired cancer stem cell phenotypes through Oct4-mediated dedifferentiation. *Oncogene* **31**, 4898-4911 (2012).
3. Gao, Y. et al. Replacement of Oct4 by Tet1 during iPSC induction reveals an important role of DNA methylation and hydroxymethylation in reprogramming. *Cell Stem Cell* **12**, 453-469 (2013).
4. Heng, J.-C.D. et al. The Nuclear Receptor Nr5a2 Can Replace Oct4 in the Reprogramming of Murine Somatic Cells to Pluripotent Cells. *Cell Stem Cell* **6**, 167-174 (2010).
5. Redmer, T. et al. E-cadherin is crucial for embryonic stem cell pluripotency and can replace OCT4 during somatic cell reprogramming. *EMBO Rep* **12**, 720-726 (2011).
6. Ichida, J.K. et al. A small-molecule inhibitor of tgf-Beta signaling replaces sox2 in reprogramming by inducing nanog. *Cell Stem Cell* **5**, 491-503 (2009).
7. Maherali, N. & Hochedlinger, K. Tgfbeta signal inhibition cooperates in the induction of iPSCs and replaces Sox2 and cMyc. *Curr Biol* **19**, 1718-1723 (2009).
8. Chen, J. et al. BMPs functionally replace Klf4 and support efficient reprogramming of mouse fibroblasts by Oct4 alone. *Cell Res* (2010).
9. Lyssiotis, C.A. et al. Reprogramming of murine fibroblasts to induced pluripotent stem cells with chemical complementation of Klf4. *Proc Natl Acad Sci U S A* (2009).
10. Nakagawa, M. et al. Generation of induced pluripotent stem cells without Myc from mouse and human fibroblasts. *Nat Biotechnol* **26**, 101-106 (2008).
11. Wernig, M., Meissner, A., Cassady, J.P. & Jaenisch, R. c-Myc is dispensable for direct reprogramming of mouse fibroblasts. *Cell Stem Cell* **2**, 10-12 (2008).
12. Li, W. & Ding, S. Small molecules that modulate embryonic stem cell fate and somatic cell reprogramming. *Trends Pharmacol Sci* **31**, 36-45 (2010).
13. Li, W. et al. Generation of Human Induced Pluripotent Stem Cells in the Absence of Exogenous Sox2. *Stem Cells* (2009).
14. Shi, Y. et al. Induction of pluripotent stem cells from mouse embryonic fibroblasts by Oct4 and Klf4 with small-molecule compounds. *Cell Stem Cell* **3**, 568-574 (2008).
15. Huangfu, D. et al. Induction of pluripotent stem cells from primary human fibroblasts with only Oct4 and Sox2. *Nat Biotechnol* **26**, 1269-1275 (2008).
16. Li, Y. et al. Generation of iPSCs from mouse fibroblasts with a single gene, Oct4, and small molecules. *Cell Res* **21**, 196-204 (2011).
17. McCurrach, M.E. & Lowe, S.W. Methods for studying pro- and antiapoptotic genes in nonimmortal cells. *Methods Cell Biol* **66**, 197-227 (2001).
18. Sommer, C.A. et al. Excision of reprogramming transgenes improves the differentiation potential of iPS cells generated with a single excisable vector. *Stem Cells* **28**, 64-74 (2010).
19. Peltier, J. & Schaffer, D.V. Viral packaging and transduction of adult hippocampal neural progenitors. *Methods Mol Biol* **621**, 103-116.
20. Kiskinis, E. & Eggan, K. Progress toward the clinical application of patient-specific pluripotent stem cells. *J Clin Invest* **120**, 51-59 (2010).
21. Silva, J. et al. Promotion of reprogramming to ground state pluripotency by signal inhibition. *PLoS Biol* **6**, e253 (2008).
22. Chen, S. et al. Self-renewal of embryonic stem cells by a small molecule. *Proc Natl Acad Sci U S A* **103**, 17266-17271 (2006).

23. Carey, B.W. et al. Reprogramming factor stoichiometry influences the epigenetic state and biological properties of induced pluripotent stem cells. *Cell Stem Cell* **9**, 588-598 (2011).
24. Moon, J.H. et al. Reprogramming fibroblasts into induced pluripotent stem cells with Bmi1. *Cell Res* **21**, 1305-1315 (2011).
25. Nandan, M.O. et al. Kruppel-like factor 5 mediates the transforming activity of oncogenic H-Ras. *Oncogene* **23**, 3404-3413 (2004).
26. Takahashi, K., Mitsui, K. & Yamanaka, S. Role of ERas in promoting tumour-like properties in mouse embryonic stem cells. *Nature* **423**, 541-545 (2003).
27. Giehl, K. Oncogenic Ras in tumour progression and metastasis. *Biological chemistry* **386**, 193-205 (2005).
28. Baek, J.H., Hatakeyama, J., Sakamoto, S., Ohtsuka, T. & Kageyama, R. Persistent and high levels of Hes1 expression regulate boundary formation in the developing central nervous system. *Development* **133**, 2467-2476 (2006).
29. Castella, P., Sawai, S., Nakao, K., Wagner, J.A. & Caudy, M. HES-1 repression of differentiation and proliferation in PC12 cells: role for the helix 3-helix 4 domain in transcription repression. *Mol Cell Biol* **20**, 6170-6183 (2000).
30. Shimojo, H., Ohtsuka, T. & Kageyama, R. Oscillations in notch signaling regulate maintenance of neural progenitors. *Neuron* **58**, 52-64 (2008).
31. Okita, K., Ichisaka, T. & Yamanaka, S. Generation of germline-competent induced pluripotent stem cells. *Nature* **448**, 313-317 (2007).
32. Pfeifer, A., Ikawa, M., Dayn, Y. & Verma, I.M. Transgenesis by lentiviral vectors: lack of gene silencing in mammalian embryonic stem cells and preimplantation embryos. *Proc Natl Acad Sci U S A* **99**, 2140-2145 (2002).

CHAPTER 4

CAMP AND EPAC SIGNALING CAN FUNCTIONALLY REPLACE OCT4 DURING INDUCED PLURIPOTENT STEM CELL REPROGRAMMING

Abstract

The advent of induced pluripotent stem cells – via the ectopic overexpression of reprogramming factors such as OCT4, SOX2, KLF4, and C-MYC (OSKM) in a differentiated cell type – has enabled groundbreaking research efforts in regenerative medicine, disease modeling, and drug discovery. While initial studies have focused on the effect of nuclear factors, increasing evidence highlights the role of signal transduction during reprogramming. By utilizing a quantitative, medium-throughput screen to systematically upregulate or downregulate several major signaling pathways for transcription factor replacement, we discovered that cAMP signal activation enables reprogramming in the absence of OCT4. Constitutively-active GNAS (G-alpha s subunit) and forskolin, which both activate cAMP signaling, reactivate endogenous OCT4 expression during reprogramming. Additionally, we have determined that the downstream EPAC signaling pathway, and not the PKA pathway, is necessary and sufficient to induce colony formation. Ultimately, cAMP signaling increases epithelial gene expression, decreases mesenchymal gene expression, and increases cell proliferation decreasing the barriers to reprogramming.

Introduction

The induction of pluripotent stem cells from adult cells has powerful clinical applications for drug discovery and personalized medicine. In 2006, it was discovered that overexpression of four transcription factors – OCT4, SOX2, KLF4, and C-MYC – was sufficient to revert mouse embryonic fibroblasts to a pluripotent, embryonic stem cell-like state capable of self-renewal[1]. These induced cells have the ability to differentiate into virtually any adult cell type creating possibilities for cell-replacement therapies and *in vitro* drug discovery and screening. Furthering the mechanistic understanding of cellular reprogramming and finding alternate reprogramming factors will allow for improved methodologies for downstream applications.

Signal transduction pathways, which consist of a series of protein-protein interactions to transduce an extracellular signal to the nucleus, have been shown to regulate embryonic stem cell biology. For instance, activation of the WNT-β-Catenin, or inhibition of the antagonist GSK3β, has been shown to positively effect embryonic stem cell self-renewal through the downstream effector STAT3[2-4]. To date, several signaling pathways have also been implicated in reprogramming. Similarly, the WNT signaling pathway has also been shown to affect reprogramming: WNT3A can improve reprogramming in the absence of C-MYC[5] and a GSK3β inhibitor was initially shown to stabilize partially reprogrammed cells[6]. As signaling pathways have the potential to be modified by external growth factors or small molecules, there is potential for discovering novel reprogramming methodologies.

Here, to further mechanistic understanding of the reprogramming factors, we have systematically screened major cellular signaling pathways for their ability to replace individual reprogramming factors. Subsequently, we discovered that the activation of cyclic AMP via the adenylyl cyclase signaling pathway is sufficient to generate OCT4 positive colonies in the

absence of the *Oct4* transgene, consistent with a previous report[7]. We verify that activating cAMP with forskolin, and adding the 2i (CHIR99021 and PD 0325901) inhibitors, was able to replace OCT4 at relatively high efficiency (0.72% versus 1.1% with or without *Oct4*, respectively) and resulted in pluripotency. We further explore the mechanism of forskolin-mediated OCT4 replacement: by studying the downstream cAMP signaling effectors, we show EPAC is sufficient for replacement, and the downstream effector RAP1 is necessary during reprogramming and OCT4 replacement. Forskolin additionally reduces the barriers for reprogramming by regulating mesenchymal-to-epithelial transition genes, particularly by upregulation of EPCAM and downregulation of mesenchymal markers, and promoting cellular proliferation.

Materials and Methods

Cell Culture

HEK293T cells were maintained in IMDM with 10% FBS and 1% penicillin/streptomycin. 129 MEF cells were a kind gift of Lin He (University of California, Berkeley) and isolated as previously described[8]. MEFs were maintained in DMEM (high glucose), 10% FBS, 1% GlutaMAX, and 1% penicillin/streptomycin (Invitrogen). Cells undergoing reprogramming were maintained in serum-containing, mouse embryonic stem cell (mESC-FBS) conditions: DMEM (high glucose), 15% FBS (Hyclone, SH3007003E), 0.5% penicillin/streptomycin, 1% GlutaMAX, 1% Sodium Pyruvate, 1% MEM NEAA, 0.1 mM 2-mercaptoethanol (Invitrogen), and 1000 U/mL LIF (Millipore, ESG1106). Feeder-free cell lines were maintained with GMEM (Sigma Aldrich) instead of DMEM. 15% KnockOut Serum Replacement (Invitrogen) was used in place of FBS in serum-free conditions (mESC-KSR). Differentiating embryoid bodies (EBs) were maintained in mESC-FBS media without LIF. Cells were maintained at 37°C with 5% CO_2.

Viral Production and Titer

Constitutively-active *GNAS* lentivirus was produced by HEK293T cells using calcium phosphate transfection and concentrated as previously described without a sucrose layer[9]. For the reprogramming cassette, STEMCCA loxP (OSKM), and STEMCCA-SKM loxP (SKM), the lentiviral transfection and centrifugation were performed as previously described[10, 11]. The STEMCCA loxP viruses are second-generation lentiviruses, and CLPIT Tat-mCherry[12] was thus added during transfection to promote viral genomic mRNA expression. 0.45 μm bottle top filters (Thermo Scientific, 09-740-28D) were used to filter the virus, and no sucrose layer was used in ultracentrifugation. The concentrated virus was aliquoted and stored at -80°C. Aliquots were only thawed once.

To quantify the amount of lentivirus, 1,600 MEFs were plated in 0.1% gelatin-coated (Millipore, ES-006-B) black-walled 96 well plates (E+K Scientific). After cell attachment, varying volumes of virus were added to the media. 72 hours post-infection, viral transgene expression was analyzed. After fixation with 4% paraformaldehyde, antibodies were used to amplify the protein expression: for STEMCCA loxP virus, an anti-OCT4 antibody (Santa Cruz Biotechnology, sc-5279, 1:100 dilution) and a secondary antibody (Invitrogen, A-21235, 1:250) were used; for STEMCCA-SKM loxP, an anti-SOX2 antibody (Santa Cruz Biotechnology, sc-17320, 1:200) and a secondary antibody (Jackson ImmunoResearch, 705-165-147, 1:250) were used; for constitutively-active *GNAS*, an anti-GFP primary antibody (Abcam, ab13970, 1:250) and a secondary antibody (Jackson Immunoresearch, 703-545-155, 1:250) were used. DAPI

(Invitrogen, 1:2000) was used as a nuclear stain. OCT4, SOX2, or GFP expression was imaged with the Molecular Devices ImageXpress Micro and analyzed with MetaXpress software. Infectious titers were calculated as previously described[10].

iPS Cell Reprogramming and Efficiency Calculations

4,000 passage 3 mouse embryonic fibroblasts were plated per sample and combined into four wells for infection: SKM, OSKM, SKM and CA GNAS, or SKM and pHIV CTRL, with cell densities between 9,473-12,631 cells/cm^2. Approximately 12 hours after passage, the wells were infected with SKM or OSKM at an MOI of 0.47 infectious particles/cell. Additionally, virus expressing constitutively-active *GNAS* or the infection control, pHIV CTRL, was added to their respective wells at an MOI of 1.2. 24 hours after infection, the media was replaced with MEF media. 48 hours after infection, cells were passed to 24 well plates with mitomycin-c treated MEF feeder layers (GlobalStem, GSC-6101M) with mESC-FBS media with or without forskolin (10 μM, Enzo Life Sciences, BML-CN100-0010). Media and small molecules were changed daily. At five days post-infection, the small molecules CHIR99021 (3 μM, Cayman Chemical, 13122) and PD 0325901 (1 μM, Cayman Chemical, 13034) were added to the appropriate wells. All conditions containing CHIR99021 and/or PD 0325901 were cultured in serum-free (mESC-KSR) media upon small molecule addition. The small molecules and media were changed daily. After passage, all wells were maintained in 0.22% DMSO. The wells were fixed nine days post-infection.

To account for differences in cell division between the four viral infections, three wells per viral infection were also plated on a 24 well plate with feeder layers in mESC-FBS medium with 0.22% DMSO during the passage. Eight hours later the cells were fixed with 4% paraformaldehyde. The wells were stained for SOX2 or SOX2 and GFP expression with an anti-Sox2 antibody and an anti-GFP antibody (antibodies previously described). The wells were imaged with the Molecular Devices ImageXpress Micro and analyzed with MetaXpress software. By normalizing between the numbers of cells infected per condition, the number of resulting OCT4 colonies are comparable. Reprogramming efficiency was calculated as the number of OCT4 colonies (divided by the ratio of cells infected in the condition to cells infected in the SKM condition) divided by the number of cells infected in the SKM condition.

The fixed reprogrammed cells were stained for OCT4 and NANOG expression: an anti-OCT4 antibody (Santa Cruz Biotechnology, sc-5279, 1:100) and an anti-NANOG antibody (Abcam, ab70482, 1:250) were incubated for 1 hour at room temperature. The secondary antibodies (Jackson ImmunoResearch, 715-585-150 and 711-605-152, 1:500) were incubated for two hours at room temperature. For image analysis, a custom journal was created in the MetaXpress software to merge the images and identify colonies/regions of OCT4 or NANOG expression (Chapter 2). The colony numbers were normalized to the SKM condition. Significance was measured using a Student's t-Test (two-tailed, homoscedastic).

Cell Line Isolation and Pluripotency Immunostaining

Cells were reprogrammed as previously described. Twelve or more days post-infection, cells were manually selected under a microscope (EVOS xl core, AMG), trypsinized, and added to separate wells in a 48 well plate with mitomycin-c treated MEF feeder layers. The SKM FK 2i cell lines were maintained in mESC-KSR media with forskolin, CHIR99021, and PD 0325901 for 1-3 passages and then transferred to mESC-FBS media without small molecules. The cells were passed every 2-3 days in mESC-FBS media on feeder layers.

To transfer the cells to feeder-free conditions, the cells were plated into gelatin-coated plates with GMEM-based mESC media that had been conditioned with mitomycin-c treated MEF feeder layers, harvested, and supplemented with LIF (GMEM-CM). 48 hours later, the cells were incubated with 50% GMEM-CM and 50% GMEM mESC media. The following day the cells were passaged. 48 hours after passage, the cells were maintained in 100% GMEM mESC media.

To probe for expression of pluripotency proteins, confluent cells were fixed and stained with the following antibodies: SSEA1, OCT4, and NANOG (previously described). For SSEA1, the primary antibody (Millipore, MAB4301, 1:200) and secondary antibody (Invitrogen, A-21045, 1:1000) were used. As SSEA1 is cell surface marker, no Triton-X100 was used to permeabilize the cells. The staining was imaged on the ImageXpress Micro (Molecular Devices).

Embryoid Body Differentiation

iPS cell lines were trypsinized and incubated on 0.1% gelatin-coated tissue culture plates in EB medium for 1 hour at 37°C with 5% CO_2 to separate the MEF feeder layers from the iPS cells. The unattached cells were collected and diluted to $2.25x10^4$ cells/mL. 20 μL drops were pipetted onto a 15 cm lid. 10 mL PBS buffer was added to the plate and the lid was gently placed on top of the plate. The hanging drops were incubated at 37°C with 5% CO_2 for two days. The drops were collected and the embryoid body suspension was added to a bacterial-grade sterile 10 cm dish. The embryoid bodies were incubated for three or more days before pipetting individual embryoid bodies into the wells of a 24 well plate coated with gelatin. The following day, the media was partially changed. The media was changed every other day or every day upon confluency. The embryoid bodies were fixed when the EBs had attached, cells had migrated and appeared differentiated (12-20 days after hanging drop). The cardiomyocyte videos were captured using a Nikon Eclipse TE2000-E microscope.

To improve neural differentiation in cultures, retinoic acid (5 μM, Enzo Life Sciences, BML-GR100-0500) was added during the transfer of the hanging drops to the suspension culture. Every other day, 50% of the media was changed with retinoic acid. The retinoic acid treatment was stopped when the EBs were transferred for attachment.

To visualize the expression of differentiation markers, the wells were fixed and stained with one the following antibodies: for mesoderm, anti-α-smooth muscle actin (Sigma Aldrich, A2547, 1:500) and the secondary (Invitrogen, A-11003, 1:1000); for endoderm, anti-HNF3β (also known as FOXA2) (Millipore, 07-633, 1:500); and for ectoderm, anti-β3-tubulin (Covance, MRB-435P, 1:500). The secondary antibody (Invitrogen, A11-012, 1:1000) was used for HNF3β and β3-tubulin staining. The staining was imaged on the ImageXpress Micro (Molecular Devices).

Small Molecule Reprogramming Assay

Cells were reprogrammed, stained, and analyzed as previously described. Small molecules were added two days post-infection: 476485 (Millipore, 476485), GGTI-298 (Santa Cruz Biotech, sc-221673), and 8-pCPT-2′-O-Me-cAMP (Sigma Aldrich, C8988). The small molecules and media were changed daily. After passage, all wells were maintained in 0.22% DMSO. The wells were fixed nine days post-infection.

Proliferation Assay

Cells were reprogrammed as previously described. Three, four, or five days post-infection, the cells were incubated with 10 μM EdU (Invitrogen, E10187) for 1 hour. The cells were washed, fixed, and subsequently stained for SOX2 expression (antibody previously described) with a secondary antibody (Jackson ImmunoResearch, 705-545-147, 1:500). The cells were then stained with the Click-iT EdU Alexa Fluor 594 Imaging Kit (Invitrogen, C10339). Nuclei were visualized with DAPI (1:2000). The SOX2 and EdU staining was imaged with the Molecular Devices ImageXpress Micro and analyzed with MetaXpress software.

Quantitative RT-PCR

Cells were reprogrammed as previously described. Briefly, 6,000 passage 3 MEFs per sample were combined for SKM or OSKM infection. The following day, the cells were infected at an MOI of 0.3 infectious particles/cell. The passage and media changes remained the same as the previous protocol. All conditions were maintained in 0.1% DMSO after passage. Three, five, or seven days post-infection, RNA was isolated using the RNeasy Micro Kit (Qiagen, 74004) per manufacturer's instructions. RNA was quantified, normalized, and reverse-transcribed using the ThermoScript RT-PCR for First-Strand cDNA Synthesis (Invitrogen, 11146) per manufacturer's instructions. The samples were analyzed for gene expression on the BioRad iQ5 with standard curves, water samples, and melt curve controls. qPCR primers are listed in Table FI.

Results

Adenylyl Cyclase Activators Produce OCT4 Positive Colonies in the Absence of the Oct4 Transgene

To determine if any signaling factors could replace OCT4 in induced pluripotent stem cell reprogramming, we infected mouse embryonic fibroblasts (MEFs) with 38 individual viruses encoding signaling factors and the STEMCCA-SKM loxP (SKM) virus (Chapter 3). This initial screen indicated that constitutively-active (CA) *GNAS* could result in OCT4 positive colonies. To further quantify this OCT4 replacement, we infected more MEFs with virus encoding CA *GNAS* and SKM virus (both at higher MOIs). Additionally, as GNAS activates adenylyl cyclase and cAMP signaling, we added the small molecule agonist, forskolin, in our reprogramming experiments. Nine days post-infection, colonies expressing OCT4 were present in both the CA *GNAS* and the forskolin conditions (Fig. 1a), and by using high-content imaging and analysis, we quantified the number of OCT4 positive colonies (Fig. 1b, F1).

To accurately calculate reprogramming efficiency, we normalized for differences in cell division rates between infection and passage into mouse embryonic stem cell conditions (Fig. S6). For example, cells infected with SKM and GNAS or SKM and the lentiviral control had different proliferation rates, which effects the efficiency calculations ($p<0.05$, Fig. F2). Efficiencies for various conditions, including controls, are included in Table I.

The activation of cAMP signaling via CA *GNAS* or forskolin with SKM significantly increased the number of OCT4 positive colonies ($p<0.05$) compared to the negative control (Fig. 1c). However, forskolin resulted in a greater increase (2.2-fold) in colony number compared to CA *GNAS*, which may be due to differences in mechanistic activation of cAMP activation. As CA *GNAS* and forskolin resulted significantly fewer colonies than with OCT4 reprogramming ($p<0.005$, 12-fold and 6-fold reduction, respectively) (Fig. 1d), we next asked if we could increase the number of colonies to reach similar efficiencies of OSKM reprogramming. As the 2i inhibitors (CHIR99021 and PD 0325901) have been shown to aid in reprogramming[6], we

added them with the cAMP activators during reprogramming. 2i inhibition resulted in an ~4-fold increase in the number of OCT4 positive colonies both conditions (Fig. 1c).

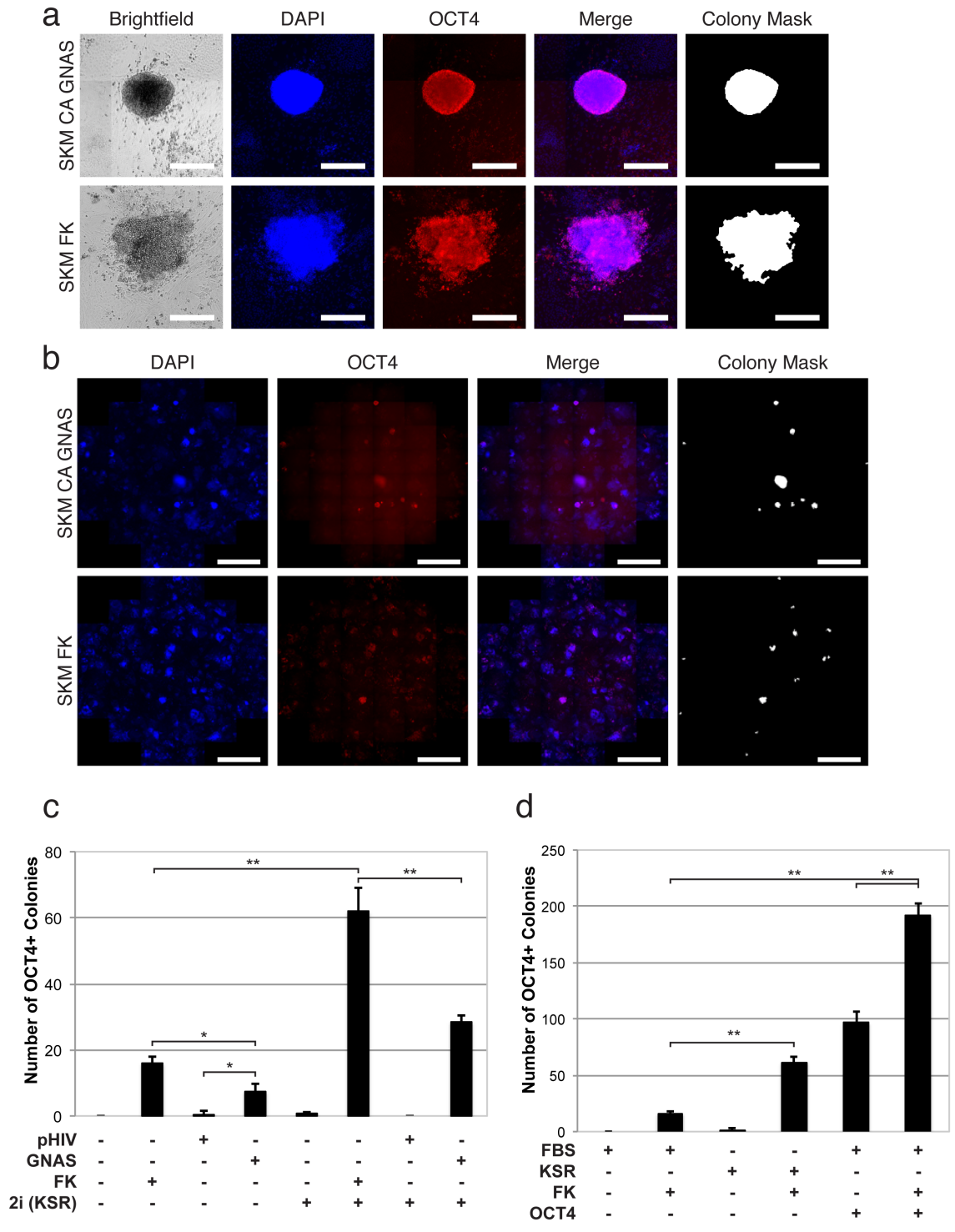

Figure 1. The cAMP activators, constitutively-active *GNAS* and forskolin, induce OCT4 positive colonies in the absence of the *Oct4* transgene. (a) Example colony images from the *Sox2*, *Klf4*, *c-Myc*, and constitutively-active *GNAS* condition and the *Sox2*, *Klf4*, *c-Myc*, and forskolin (FSKM) condition are

shown. Scale bars are 300 μm. (b) Example images of the entire 24 wells are shown. The minimum colony size measured in the colony mask was 15,000 μm^2. Scale bars are 3 mm. (c) The number of OCT4 positive colonies measured from high-throughput analysis for constitutively-active *GNAS*, the infection control, pHIV CTRL, and forskolin with SKM. Conditions with and without 2i small molecule inhibitors in serum-free media are shown. (d) The number of OCT4 positive colonies with forskolin, DMSO, and *Oct4* conditions. The *Oct4* conditions were normalized to the SKM conditions due to variability of infection. Statistical significance was measured using a Student's t-Test (two-tailed, homoscedastic) with * $p < 0.05$ and ** $p < 0.005$. Negative controls are $p < 0.005$. The minimum colony size was 15,000 μm^2. Error bars represent s.d. (n=3). All conditions were cultured in 0.22% DMSO and fixed with paraformaldehyde nine days post-infection.

We wanted to further quantify the necessity each of the 2i inhibitors in addition to the effects of the serum-free media that used when we added the inhibitors. When the SKM and forskolin condition (FSKM) was cultured in serum-free media, the 3.9-fold increase was replicated, indicating that the medium is sufficient for the increase in colony number rather than the 2i inhibitors (Fig. 1d). Additionally, when added alone, PD 0325901 could also significantly increase the number of OCT4 positive colonies compared to the 2i condition, giving us insight into the mechanism of replacement (Fig. F3).

As additional controls, we also varied the colony cut-off size in the analysis as well as measuring NANOG expression (Fig. F4, F5). However, NANOG staining was not as robust and not ideal for the automated analysis, although the trends for forskolin remain (Fig. F5a).

Table I. Normalized reprogramming efficiencies

Condition	Reprogramming Efficiency (%) ± Standard Deviation
OSKM FK	2.22 ± 0.12
OKSM	1.12 ± 0.11
SKM FK PD 0325901	0.98 ± 0.08
SKM FK 2i	0.72 ± 0.08
SKM FK (KSR)	0.71 ± 0.06
SKM FK CHIR99021	0.68 ± 0.06
SKM CA GNAS 2i	0.33 ± 0.02
SKM FK (FBS)	0.19 ± 0.02
SKM CA GNAS	0.09 ± 0.03
SKM (KSR)	0.02 ± 0.02
SKM CHIR99021	0.02 ± 0.00
SKM PD 0325901	0.01 ± 0.01
SKM 2i	0.01 ± 0.01
SKM pHIV CTRL	0.01 ± 0.01

cAMP Activation with 2i Inhibition Results in Pluripotency without the Oct4 Transgene

During our reprogramming studies, we noticed the addition of forskolin induces early morphological changes in MEFs compared to the positive and negative controls (Fig. 2a) For instance, colonies were visible five days post-infection in with forskolin; SKM and OSKM also form colonies although they are less distinctive from surrounding cells than forskolin-induced colonies. By seven days post-infection, SKM colonies are no longer apparent, and OSKM and FSKM both exhibit colony formation, a first indication of pluripotency.

Next, to determine if the resultant cells were pluripotent, MEFs were reprogrammed with SKM, forskolin, and the 2i inhibitors. The inhibitors were added as they had the potential to stabilize the pluripotent state[6] and were not detrimental to reprogramming. Colonies were isolated and passaged to form cell lines. iPS lines, such as SKM FK 2i-02, were stained for pluripotent markers, SSEA1, OCT4, and NANOG (Fig. 2b, F6). SSEA1 expression was present, but not uniform in all colonies (Fig. F6). However, cAMP activation reactivated endogenous OCT4 and NANOG expression (Fig. 2b, F6). For ease of culture, the iPS cell lines could also be transitioned to feeder-free conditions, and pluripotency marker expression remained (Fig. F7). Cell lines maintained colony morphology in culture for at least 19 passages (Fig. F8).

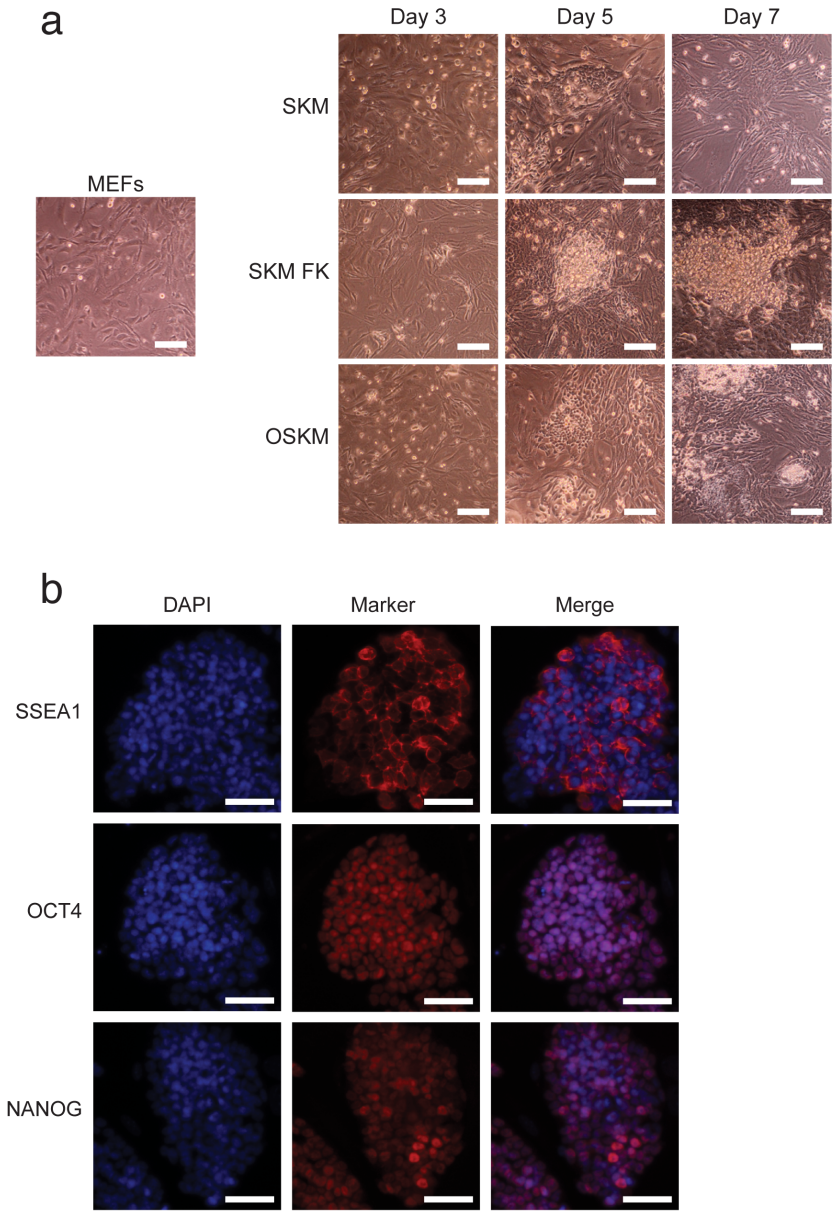

Figure 2. cAMP signaling induces morphological changes and activates pluripotent gene expression with 2i and without the *Oct4* transgene. (a) Brightfield images show the change in morphology of mouse embryonic fibroblasts 3, 5, and 7 days post-infection with SKM, FSKM, and OSKM, respectively.

Conditions contain 0.1% DMSO. Scale bars are 40 µm. (b) The cell line, SKM FK 2i-02, was stained for pluripotency markers, SSEA1, OCT4, and NANOG. The cell line was imaged seven passages after isolation and four passages in serum containing media without 2i and FK. Scale bars are 50 µm.

To test the ability for the cell lines to differentiate into the three germ layers, the iPS cell lines were induced to differentiate in hanging drops in the absence of LIF. The embryoid bodies were cultured in suspension and then attached for cells to migrate and differentiate (Fig. 3a). The resulting cultures were stained for the mesodermal marker, smooth-muscle actin; the ectodermal marker, β-III tubulin; and the endoderm marker, HNF3β (Fig. 3b, F9). To improve the neuronal differentiation, retinoic acid was added to embryoid-body suspension culture, and mesodermal and endodermal markers were still apparent in the cultures with retinoic acid (Fig. 3b). Additionally, one cell line, SKM FK 2i-01, readily formed cardiomyocytes during embryoid-body differentiation (four AVI files, available upon request).

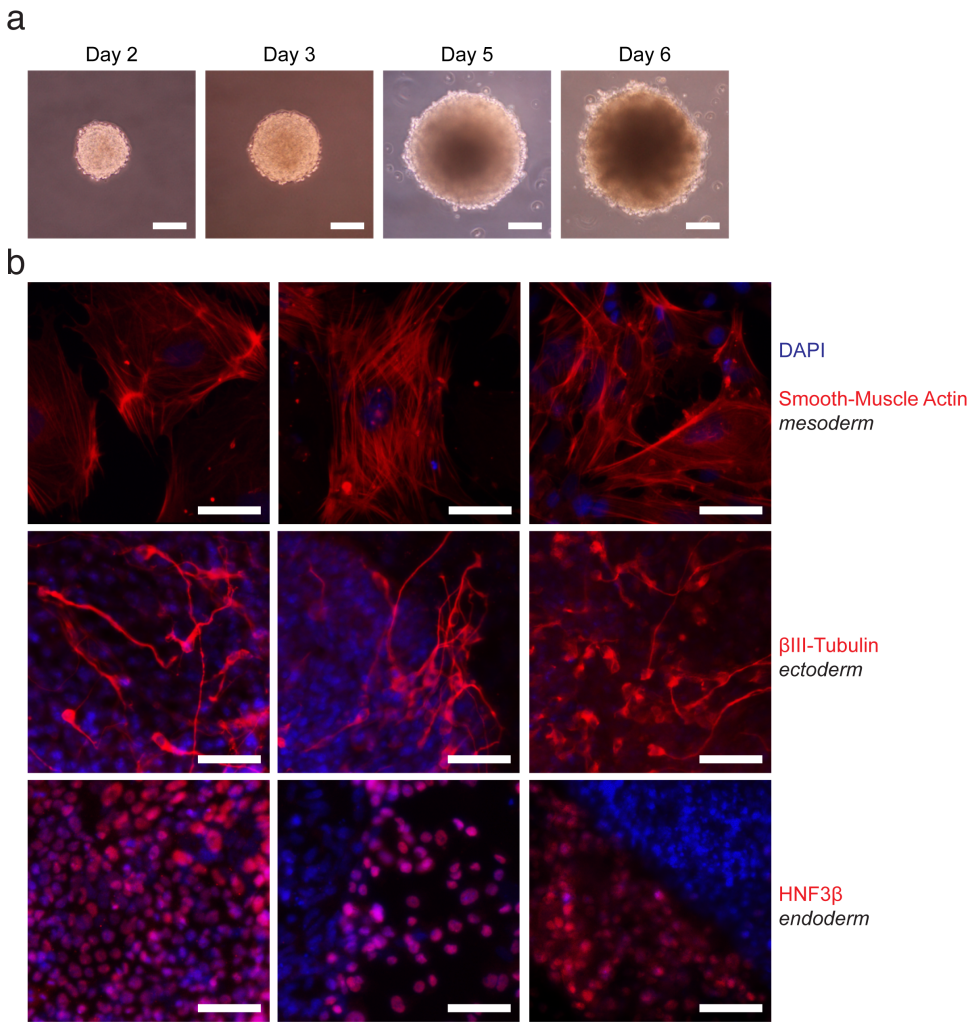

Figure 3. Forskolin 2i cell lines form embryoid bodies and produce three germ layers *in vitro*. (a) SKM FK 2i-06 forms embryoid bodies after initial culture for two days in hanging drops. Pictures are shown two, three, five, and six days in differentiation conditions. Scale bars are 40 µm. (b) SKM FK 2i-06 differentiates into three germ layers. Images are of different regions expressing smooth-muscle actin,

βIII-tubulin, or HNF3β, respectively, in embryoid body outgrowth. Retinoic acid (5 μm) was added to the differentiation media during embryoid body suspension culture. Scale bars are 25 μm.

cAMP Acts Through the EPAC-RAP1 Pathway to Induce Reprogramming

We had determined that the activation of adenylyl cyclase/cAMP signaling was sufficient to replace OCT4 during reprogramming; however, we were uncertain as which effectors were necessary for reprogramming. Adenylyl cyclases, which are expressed throughout many organ systems[13], catalyze the reaction of ATP to 3', 5'-cyclic AMP (cAMP). cAMP subsequently signals through two main effectors, PKA and EPAC[14, 15]. We next modulated the downstream PKA and EPAC pathways to determine their importance in OCT4 replacement and reprogramming (Fig. 4).

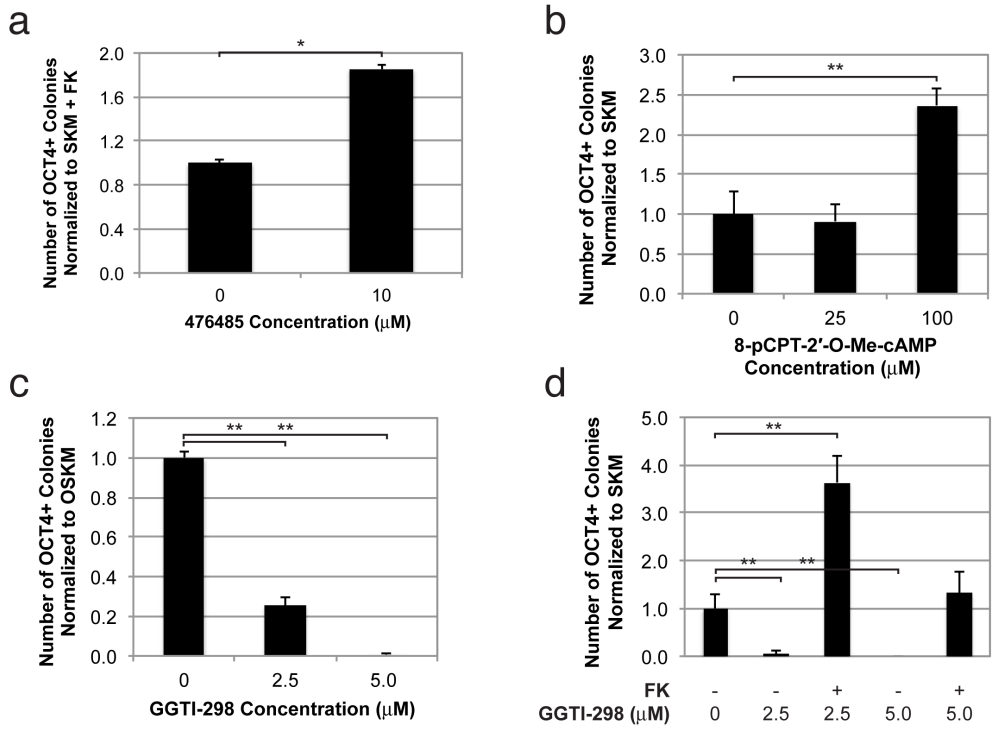

Figure 4. The EPAC-RAP1 pathway is necessary for replacement of OCT4. (a) The PKA inhibitor, 476485, increases the number of OCT4 positive colonies in forskolin induced reprogramming. (b) Adding the EPAC analog, 8-pCPT-2'-O-Me-cAMP at higher concentrations increases the number of OCT4 positive colonies compared to a SKM control. (c) The RAP1 inhibitor, GGTI-298, decreases the number of reprogrammed colonies in OSKM reprogramming. (d) The RAP1 inhibitor, GGTI-298, decreases the number of OCT4 positive colonies in forskolin reprogramming at increased concentrations. Statistical significance was measured using a Student's t-Test (two-tailed, homoscedastic) with * $p < 0.05$ and ** $p < 0.005$. The minimum colony size was 15,000 μm^2. Error bars represent s.d. (n=3). All conditions were cultured in 0.22% DMSO and fixed with paraformaldehyde nine days post-infection.

First, to understand whether the PKA pathway is necessary to replace OCT4, the PKA inhibitor, 476485, was added during FSKM reprogramming. Inhibiting PKA signaling caused a significant increase ($p<0.05$) in the number of OCT4 positive colonies (Fig. 4a), which indicates cAMP signaling is not acting through PKA to replace OCT4.

Next, we wanted to determine if the other major effector of cAMP signaling, EPAC, was sufficient to replace OCT4. The EPAC-specific cAMP analog, 8-pCPT-2'-O-Me-cAMP[16], was added to SKM during reprogramming. The addition of the cAMP analog resulted in a significant increase ($p<0.005$) in the number of OCT4 positive colonies compared to the negative control (Fig. 4b), which indicates that EPAC pathway activation is sufficient to replace OCT4.

Last, to determine if the EPAC pathway is necessary during reprogramming, we inhibited an effector of EPAC, RAP[14]. The RAP1 inhibitor, GGTI-298, was titrated on MEFs to determine toxic concentrations; concentrations higher than 5 μM decreased MEF viability (Fig. S14a). Adding 2.5 μM GGTI-298 to OSKM reprogramming caused a significant decrease in colony number ($p<0.005$), and adding 5 μM drastically decreased OSKM reprogramming (158-fold decrease) (Fig. 4c). Similarly, increasing the concentration of GGTI-298 in FSKM reprogramming reduced the levels compared to the negative control (Fig. 4d), which indicates that the EPAC signaling pathway is necessary for reprogramming and OCT4 replacement.

cAMP Signaling Increases Cellular Division Rates and Regulates Genes Involved in the Mesenchymal to Epithelial Transition to Replace OCT4

After determining the role of the cAMP effectors, we next asked what role cAMP signaling may have in reprogramming. Due to the early presence of colonies in the reprogramming, we wanted to determine if cell proliferation was augmented, especially as cell division is a barrier to reprogramming[17-19]. Cells were treated with EdU and assayed for EdU incorporation and viral transgene expression using an antibody against SOX2. The addition of the cAMP signaling agonist, forskolin, to SKM increases the percentage of dividing cells 24 hours after addition (24% versus 17% of the cells dividing with or without forskolin, respectively) (Fig. 5a). The cell division remains higher 48 and 72 hours after forskolin addition (Fig. 5a), which may decrease the barriers to reprogramming.

Additionally, due to the early changes in cell morphology, we wanted to study whether activating cAMP signaling altered the expression of the mesenchymal and epithelial genes, particularly as the mesenchymal to epithelial transition is an early barrier to reprogramming[20, 21]. Quantitative RT-PCR was used to analyze genes three, five, or seven days post-infection. The cAMP signaling agonist, forskolin, increased the expression of epithelial genes, *Cdh1* and *Epcam* (Fig. 5e, f), and decreased the expression of mesenchymal genes, *Cdh2* and *Slug* (Fig. 5g, h) compared to the SKM negative control. The expression for *Epcam*, *Cdh2*, and *Slug* differed from the OSKM expression levels, indicating that cAMP signaling differs in function from OCT4 by decreasing mesenchymal gene expression and increasing *Epcam* expression.

As cAMP signaling was sufficient to replace OCT4, we also studied the pathway's effects on pluripotency genes. Activating cAMP with forskolin resulted in an increase in *Oct4* expression but failed to upregulate *Nanog* at seven days post-infection compared to OSKM (2-fold, 14-fold, 348-fold increase for *Nanog* with SKM, FKSM, and OSKM, respectively) (Fig. 5b, d). Interestingly, forskolin decreased the expression of *Klf4* during the timeframe studied (Fig. 5c) even though previous studies had indicated *Klf4* was downstream of forksolin activation[22, 23]. Thus, activated cAMP acts in a *Klf4*-independent manner but is capable of upregulating *Oct4* during reprogramming.

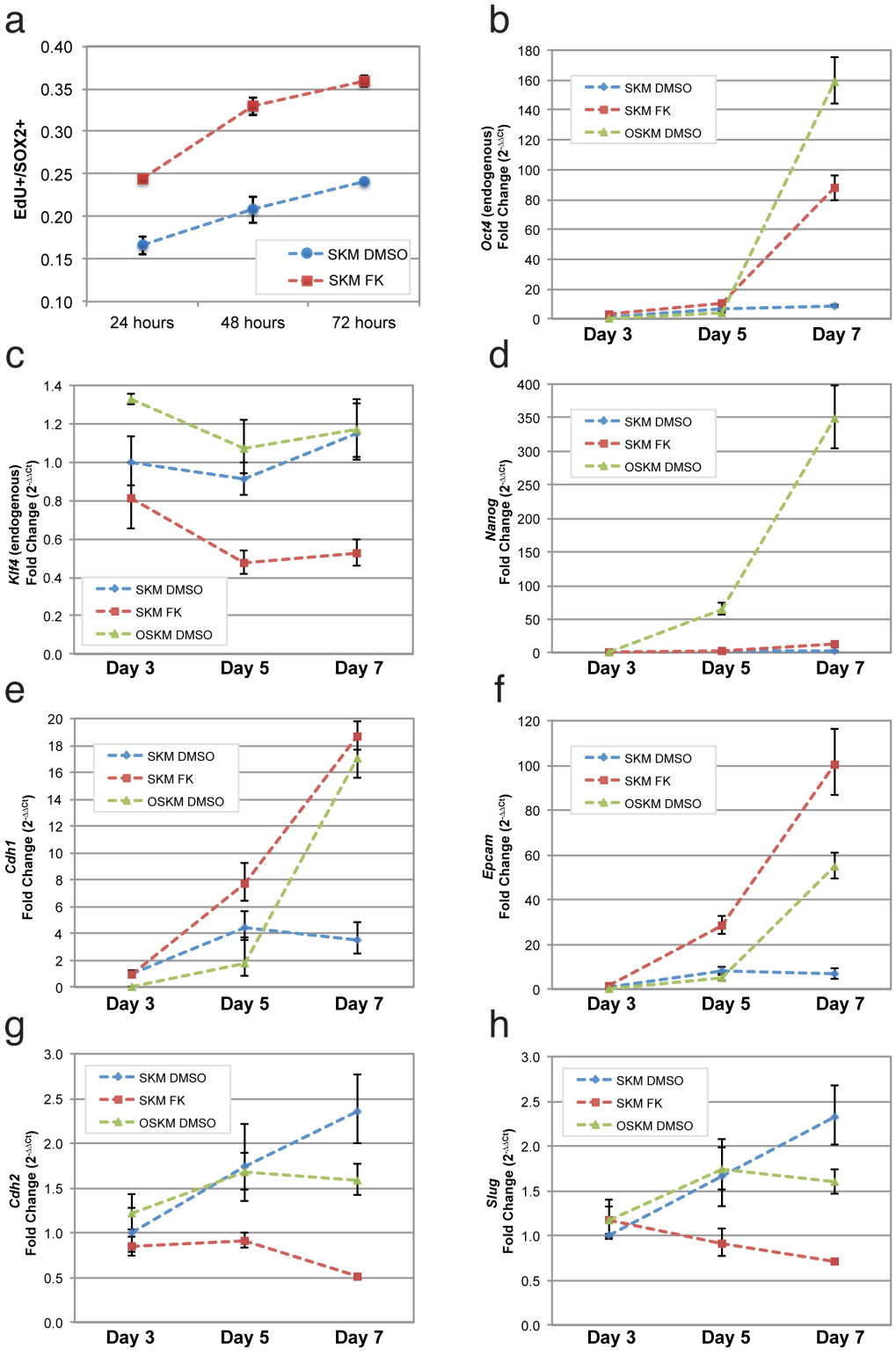

Figure 5. cAMP activation induces cell division changes and gene expression changes to lower the barrier to reprogramming. (a) Forskolin causes an increase in cell division rate hours after addition. Mouse embryonic fibroblasts were infected with SKM. Two days post-infection, cells were split in mouse embryonic stem cell conditions with forskolin or DMSO. EdU was incubated for 1 hour and the

cells were fixed. To account for non-infected cells, the cells were costained against SOX2, which is present in the viral transgene. Error bars represent s.d. (n=3). (b-h) mRNA levels of pluripotency genes (b-d), epithelial genes (e-f), and mesenchymal genes (g-h) were analyzed at early time points in reprogramming. Each gene expression was normalized to the internal control gene, *Hprt*. Each condition was subsequently normalized to the SKM day 3 control condition. Error bars represent s.d. (n=2, technical).

Discussion

Inducing pluripotent stem cells from adult cells has immense potential for the regenerative medicine field and improving reprogramming methodologies will lead to greater accessibility for research and mechanistic understanding. Small molecule libraries, which have been used successfully for transcription factor replacement, can be disadvantageous to study signaling pathways due to an abundance of inhibitors rather than activators, variable target specificity, and cellular toxicity. Here, we present a methodology to screen the upregulation and downregulation of major cellular signaling pathways with distinct protein targets and low cellular toxicity, which we have applied to discover novel replacements and mechanisms for reprogramming factor replacement. By discovering a constitutively-active GNAS in a screen to replace OCT4, we have elucidated the adenylyl cyclase/cAMP signaling pathway as a target to further study in the reprogramming context. We additionally found that the small molecule agonist, forskolin, was also able to replace OCT4 in reprogramming, which was also elucidated in a previous report[7].

A first indication of reprogramming mechanism was when we found that the addition of the MEK inhibitor, PD 0325901, alone with cAMP activation increased the reprogramming efficiency to 0.98%, due to the inhibition of the MAPK pathway. Forskolin activates PKA, which has been shown to activate the MAPK pathway for neuronal differentiation[24-26]; in contrast PKA has been shown to be inhibitory to the MAPK pathway in fibroblasts[27-29]. As forskolin is added in combination with other reprogramming factors (SOX2, KLF4, and C-MYC), the signaling state within the reprogramming MEFs is different than that in wild-type fibroblasts. Therefore, in our system, PD 0325901 inhibiting MAPK signaling may be preventing PKA-mediated differentiation during reprogramming resulting in an increase in the number of OCT4 positive colonies and reprogramming efficiency. Additionally, we found switching the media from serum to serum-free at five days post-infection had similar reprogramming efficiencies with or without 2i inhibition, which indicated that serum-free conditions enhance reprogramming efficiency. This difference may be due to differences in the concentration of growth factors between the Knockout Serum Replacement (Invitrogen) and fetal bovine serum, which ultimately activate the MAPK pathway. Mechanistically, the inhibition or reduction of the MAPK signaling pathway leading to improved reprogramming is the first indication that cAMP signaling pathway may be working via activating the EPAC pathway rather than the PKA pathway.

Subsequently, we further studied the role of cAMP's effectors, EPAC and PKA. When we inhibited PKA during forskolin, SOX2, KLF4, and C-MYC (FSKM) reprogramming, the reprogramming efficiency increased 1.9-fold, indicating that PKA is not necessary for cAMP-mediated OCT4 replacement. Conversely, if the downstream effector of the EPAC pathway, RAP1, was inhibited with the inhibitor, GGTI-298, OSKM reprogramming was hindered up to 158-fold at 5 μM concentrations. Additionally, if GGTI-298 was added to FSKM reprogramming, the number of OCT4 colonies returned to SKM baseline levels. Unsurprisingly, RAP1 inhibition has also been found to be detrimental to human embryonic stem cells[30]. Our

results indicate that RAP1, and possibly EPAC, is essential and necessary for OSKM and FKSM reprogramming.

To determine if EPAC signaling alone is sufficient for SKM reprogramming, the EPAC-specific cAMP analog, 8-pCPT-2'-O-Me-cAMP[16], was added during SKM reprogramming. 8-pCPT-2'-O-Me-cAMP was able to generate 2.5-fold more colonies than SKM baseline, indicating that EPAC is able to generate OCT4 colonies, although less robustly than forskolin. Thus, activating the EPAC signaling pathway is sufficient but does not fully recapitulate the effects of forskolin. However, it would be interesting to see if the potent, cell-permeable analog, 8-pCPT-2'-O-Me-cAMP-AM[31], would fully replace cAMP signaling in the absence of OCT4.

To study the downstream effects of cAMP signaling during reprogramming with SKM, we used quantitative RT-PCR to measure various genes. We studied the expression of reprogramming genes: *Oct4*, *Nanog*, and *Klf4*. At seven days post-infection, the cAMP agonist, forskolin, increased endogenous *Oct4* expression, but not as much as OSKM reprogramming, which is unsurprising as exogenous OCT4 can modulate *Oct4* expression[32, 33]. Surprisingly, forskolin resulted in a decrease in *Klf4* expression, which was contrary to previous studies that had shown *Klf4* is a downstream of forskolin[22, 23], indicating forskolin is acting in a *Klf4*-independent manner. Additionally, *Nanog* expression slightly increased with forskolin but drastically increased with OSKM reprogramming. As OCT4 and SOX2 are exogenously expressed in OSKM reprogramming and bind to the promoter region of *Nanog*[32, 34-36], it is unsurprising that *Nanog* expression is higher in conditions with OCT4 (and SOX2).

As cAMP signaling had an early effect on the reprogramming cultures' morphology, we also studied mesenchymal and epithelial genes at various time points; the mesenchymal to epithelial transition is an important morphological transition during early reprogramming[20, 21]. In particular, cAMP activation caused a 2.0-fold decrease in the expression of the mesenchymal gene, *Cdh2* (compared to an increase in OSKM reprogramming) at seven days post-infection. Similarly, *Slug* expression decreased post-cAMP activation (compared to a 1.6 fold-increase for OSKM). The decrease in the expression of mesenchymal genes, *Cdh2* and *Slug*, compared to the increase in expression with OSKM reprogramming indicates that the cAMP signaling pathway may act differently than OCT4 by diminishing mesenchymal gene expression, a barrier to reprogramming.

Conversely, cAMP activation increased the expression of the epithelial marker, *Epcam* 100-fold (compared to 55-fold in OSKM reprogramming). *Epcam* has been shown to be important to mouse embryonic stem cell renewal[37] and a pluripotency marker for human embryonic stem cells[38], and may be aiding in reprogramming in the absence of OCT4. Additionally, cAMP signaling also increased *Cdh1* expression 19-fold similar to OSKM (17-fold). CDH1 (also known as E-cadherin) has been previously shown to be able to replace *Oct4* in reprogramming[39]. RAP1 has been shown to interact with CDH1 in human embryonic stem cells to maintain self-renewal[30], which suggests cAMP could be activating RAP1 and CDH1 to replace OCT4.

Additionally, we wanted to determine if cAMP activation was inducing cell cycle changes, as previous studies have indicated cell division to be a barrier to reprogramming and necessary for embryonic stem cell maintenance[17-19]. cAMP activation increased the number of cells undergoing cell division 24-72 hours after addition. Thus, cAMP may be aiding reprogramming by increasing the cell division rate.

In order to verify the OCT4 positive colonies were pluripotent, we isolated cell lines and characterized the pluripotent protein expression. While the resulting cells expressed the three

pluripotent markers, SSEA1, OCT4, and NANOG, the SSEA1 expression appeared to be the most variable. Interestingly, when human embryonic stem cells are cultured to a naïve, mouse embryonic stem cell-like state with LIF, CHIR99021, PD 0325901, and forskolin, the cells maintain expression of the hESC marker, SSEA4, and do not express SSEA1[22]. Therefore, the addition of forskolin with the 2i inhibitors may lead to abnormal SSEA1 expression, even though the cell lines robustly express OCT4 and NANOG and are able to differentiate into the three germ layers *in vitro*. It would be interesting to determine in the future if there is a fluctuation in SSEA1 expression in the population throughout long-term culture and to determine if the SSEA1 positive or negative population is more susceptible to differentiation.

While cAMP signaling and the underlying mechanism for replacement hold promise for reprogramming technologies, we were unsuccessful in isolating iPS cell lines from adult mouse ear fibroblasts reprogrammed with FSKM. However, we were able to increase the number of OCT4 positive cells by the addition of small molecules (Fig. F11), which indicates conditions may exist to generate iPS cell lines in other conditions. In our studies, we used 129 mouse embryonic fibroblasts, a strain more permissive to reprogramming[6]. Future studies can determine how universal forskolin is in the replacement of *Oct4* for differing cell types. Additionally, we wanted to determine if we could reprogram using only small molecules (combinations shown in Table FII) that have been used to replace other reprogramming factors[6, 40-44]. None of these conditions resulted in reprogrammed colonies. Due to the nature of the crosstalk and feedback within the pluripotency network, it may be necessary to have strong expression of at least one pluripotent gene[32-36], which may prove to be difficult with small molecules. Therefore, initial studies for small molecule reprogramming may best be suited in cell types that already express one or more of the reprogramming factors.

To date, few studies have been done regarding cAMP signaling in embryonic stem cells and reprogramming. For examples, a study has reported the cAMP-analog, 8-Br-cAMP, can increase human fibroblast reprogramming 2-fold[45]. Additionally, forskolin in combination with the 2i inhibitors, CHIR99021 and PD 0325901[6], and LIF is sufficient to transform human embryonic stem cells to a naïve, mouse embryonic-like state[22]. Ultimately, this work furthers the understanding of the cAMP signaling pathway in reprogramming and in the replacement of OCT4. Furthermore, the screening methodology presented here may be useful to study the importance of signaling pathways in mammalian cell biology.

References

1. Takahashi, K. & Yamanaka, S. Induction of pluripotent stem cells from mouse embryonic and adult fibroblast cultures by defined factors. *Cell* **126**, 663-676 (2006).
2. Hao, J., Li, T.G., Qi, X., Zhao, D.F. & Zhao, G.Q. WNT/beta-catenin pathway up-regulates Stat3 and converges on LIF to prevent differentiation of mouse embryonic stem cells. *Dev Biol* **290**, 81-91 (2006).
3. Sato, N., Meijer, L., Skaltsounis, L., Greengard, P. & Brivanlou, A.H. Maintenance of pluripotency in human and mouse embryonic stem cells through activation of Wnt signaling by a pharmacological GSK-3-specific inhibitor. *Nature medicine* **10**, 55-63 (2004).
4. Ying, Q.L. et al. The ground state of embryonic stem cell self-renewal. *Nature* **453**, 519-523 (2008).
5. Marson, A. et al. Wnt Signaling Promotes Reprogramming of Somatic Cells to Pluripotency. *Cell Stem Cell* **3**, 132-135 (2008).

6. Silva, J. et al. Promotion of reprogramming to ground state pluripotency by signal inhibition. *PLoS Biol* **6**, e253 (2008).
7. Hou, P. et al. Pluripotent Stem Cells Induced from Mouse Somatic Cells by Small-Molecule Compounds. *Science* (2013).
8. McCurrach, M.E. & Lowe, S.W. Methods for studying pro- and antiapoptotic genes in nonimmortal cells. *Methods Cell Biol* **66**, 197-227 (2001).
9. Yu, J.H. & Schaffer, D.V. Selection of novel vesicular stomatitis virus glycoprotein variants from a peptide insertion library for enhanced purification of retroviral and lentiviral vectors. *J Virol* **80**, 3285-3292 (2006).
10. Peltier, J. & Schaffer, D.V. Viral packaging and transduction of adult hippocampal neural progenitors. *Methods Mol Biol* **621**, 103-116.
11. Sommer, C.A. et al. Excision of reprogramming transgenes improves the differentiation potential of iPS cells generated with a single excisable vector. *Stem Cells* **28**, 64-74 (2010).
12. Leonard, J.N., Shah, P.S., Burnett, J.C. & Schaffer, D.V. HIV evades RNA interference directed at TAR by an indirect compensatory mechanism. *Cell host & microbe* **4**, 484-494 (2008).
13. Defer, N., Best-Belpomme, M. & Hanoune, J. Tissue specificity and physiological relevance of various isoforms of adenylyl cyclase. *American journal of physiology. Renal physiology* **279**, F400-416 (2000).
14. Cheng, X., Ji, Z., Tsalkova, T. & Mei, F. Epac and PKA: a tale of two intracellular cAMP receptors. *Acta biochimica et biophysica Sinica* **40**, 651-662 (2008).
15. Insel, P.A. & Ostrom, R.S. Forskolin as a tool for examining adenylyl cyclase expression, regulation, and G protein signaling. *Cell Mol Neurobiol* **23**, 305-314 (2003).
16. Enserink, J.M. et al. A novel Epac-specific cAMP analogue demonstrates independent regulation of Rap1 and ERK. *Nat Cell Biol* **4**, 901-906 (2002).
17. Hanna, J. et al. Direct cell reprogramming is a stochastic process amenable to acceleration. *Nature* **462**, 595-601 (2009).
18. Ghule, P.N. et al. Reprogramming the pluripotent cell cycle: restoration of an abbreviated G1 phase in human induced pluripotent stem (iPS) cells. *J Cell Physiol* **226**, 1149-1156 (2011).
19. Ruiz, S. et al. A high proliferation rate is required for cell reprogramming and maintenance of human embryonic stem cell identity. *Curr Biol* **21**, 45-52 (2011).
20. Samavarchi-Tehrani, P. et al. Functional genomics reveals a BMP-driven mesenchymal-to-epithelial transition in the initiation of somatic cell reprogramming. *Cell Stem Cell* **7**, 64-77 (2010).
21. Li, R. et al. A mesenchymal-to-epithelial transition initiates and is required for the nuclear reprogramming of mouse fibroblasts. *Cell Stem Cell* **7**, 51-63 (2010).
22. Hanna, J. et al. Human embryonic stem cells with biological and epigenetic characteristics similar to those of mouse ESCs. *Proc Natl Acad Sci U S A* **107**, 9222-9227.
23. Godmann, M., Kosan, C. & Behr, R. Kruppel-like factor 4 is widely expressed in the mouse male and female reproductive tract and responds as an immediate early gene to activation of the protein kinase A in TM4 Sertoli cells. *Reproduction* **139**, 771-782.
24. Yao, H., York, R.D., Misra-Press, A., Carr, D.W. & Stork, P.J. The cyclic adenosine monophosphate-dependent protein kinase (PKA) is required for the sustained activation

of mitogen-activated kinases and gene expression by nerve growth factor. *J Biol Chem* **273**, 8240-8247 (1998).
25. Yao, H. et al. Cyclic adenosine monophosphate can convert epidermal growth factor into a differentiating factor in neuronal cells. *J Biol Chem* **270**, 20748-20753 (1995).
26. Kim, S.S. et al. cAMP induces neuronal differentiation of mesenchymal stem cells via activation of extracellular signal-regulated kinase/MAPK. *Neuroreport* **16**, 1357-1361 (2005).
27. Wu, J. et al. Inhibition of the EGF-activated MAP kinase signaling pathway by adenosine 3',5'-monophosphate. *Science* **262**, 1065-1069 (1993).
28. Cook, S.J. & McCormick, F. Inhibition by cAMP of Ras-dependent activation of Raf. *Science* **262**, 1069-1072 (1993).
29. Burgering, B.M., Pronk, G.J., van Weeren, P.C., Chardin, P. & Bos, J.L. cAMP antagonizes p21ras-directed activation of extracellular signal-regulated kinase 2 and phosphorylation of mSos nucleotide exchange factor. *EMBO J* **12**, 4211-4220 (1993).
30. Li, L. et al. A unique interplay between Rap1 and E-cadherin in the endocytic pathway regulates self-renewal of human embryonic stem cells. *Stem Cells* **28**, 247-257 (2010).
31. Vliem, M.J. et al. 8-pCPT-2'-O-Me-cAMP-AM: an improved Epac-selective cAMP analogue. *Chembiochem* **9**, 2052-2054 (2008).
32. Boyer, L.A. et al. Core transcriptional regulatory circuitry in human embryonic stem cells. *Cell* **122**, 947-956 (2005).
33. Okumura-Nakanishi, S., Saito, M., Niwa, H. & Ishikawa, F. Oct-3/4 and Sox2 regulate Oct-3/4 gene in embryonic stem cells. *J Biol Chem* **280**, 5307-5317 (2005).
34. Kuroda, T. et al. Octamer and Sox elements are required for transcriptional cis regulation of Nanog gene expression. *Mol Cell Biol* **25**, 2475-2485 (2005).
35. Rodda, D.J. et al. Transcriptional regulation of nanog by OCT4 and SOX2. *J Biol Chem* **280**, 24731-24737 (2005).
36. Loh, Y.H. et al. The Oct4 and Nanog transcription network regulates pluripotency in mouse embryonic stem cells. *Nat Genet* **38**, 431-440 (2006).
37. Gonzalez, B., Denzel, S., Mack, B., Conrad, M. & Gires, O. EpCAM is involved in maintenance of the murine embryonic stem cell phenotype. *Stem Cells* **27**, 1782-1791 (2009).
38. Ng, V.Y., Ang, S.N., Chan, J.X. & Choo, A.B.H. Characterization of epithelial cell adhesion molecule as a surface marker on undifferentiated human embryonic stem cells. *Stem Cells* **28**, 29-35 (2010).
39. Redmer, T. et al. E-cadherin is crucial for embryonic stem cell pluripotency and can replace OCT4 during somatic cell reprogramming. *EMBO Rep* **12**, 720-726 (2011).
40. Shi, Y. et al. Induction of pluripotent stem cells from mouse embryonic fibroblasts by Oct4 and Klf4 with small-molecule compounds. *Cell Stem Cell* **3**, 568-574 (2008).
41. Li, Y. et al. Generation of iPSCs from mouse fibroblasts with a single gene, Oct4, and small molecules. *Cell Res* **21**, 196-204 (2011).
42. Huangfu, D. et al. Induction of pluripotent stem cells by defined factors is greatly improved by small-molecule compounds. *Nat Biotechnol* **26**, 795-797 (2008).
43. Lyssiotis, C.A. et al. Reprogramming of murine fibroblasts to induced pluripotent stem cells with chemical complementation of Klf4. *Proc Natl Acad Sci U S A* (2009).
44. Ichida, J.K. et al. A small-molecule inhibitor of tgf-Beta signaling replaces sox2 in reprogramming by inducing nanog. *Cell Stem Cell* **5**, 491-503 (2009).

45. Wang, Y. & Adjaye, J. A cyclic AMP analog, 8-Br-cAMP, enhances the induction of pluripotency in human fibroblast cells. *Stem Cell Rev* **7**, 331-341 (2011).

APPENDIX A. GENE INFORMATION

Table AI. Plasmid information, retroviral library

No.	Gene		Original Name of Plasmid	Final Plasmid
P1	CA	*ACVR1*	pCMV5 ALK-2 Q207D	CLGPIT ALK2 Q207D
P2	CA	*MAP2K3*	pRC/RSV Flag MKK3(glu)	CLGPIT Flag MKK3(glu)
P3	CA	*MAP2K6*	pCDNA3-Flag MKK6(glu)	CLGPIT Flag MKK6(glu)
P4	DN	*RHOA*	CLGPIT myc DN RhoA T19N	CLGPIT myc DN RhoA T19N
P5	CA	*RHOA*	CLGPIT myc CA RhoA Q63L	CLGPIT myc CA RhoA Q63L
P6	CA	*RAC1*	CLGPIT CA Rac1(Q61L)	CLGPIT CA Rac1(Q61L)
P7	DN	*RAC1*	CLGPIT DN Rac1(T17N)	CLGPIT DN Rac1(T17N)
P8	CA	*CDC42*	CLGPIT CA Cdc42(Q61L)	CLGPIT CA Cdc42(Q61L)
P9	DN	*CDC42*	CLGPIT DN Cdc42(T17N)	CLGPIT DN Cdc42(T17N)
P10	WT	*Akt1*	CLGPIT Akt1	CLGPIT Akt1
P11	DN	*Akt1*	CLGPIT Akt AAA	CLGPIT Akt AAA
P12	CA	*Akt1*	CLGPIT Akt DD	CLGPIT Akt DD
P14	CA	*Camk2a*	CLGPIT CaMKII T286D	CLGPIT CaMKII T286D
P15	WT	*Camk2n2*	CLGPIT CaMKIIN	CLGPIT CaMKIIN
P16	WT	*Camk4*	CLGPIT CaMKIV	CLGPIT CaMKIV
P17	CA	*HRAS*	CLGPIT HRas G12V	CLGPIT HRas G12V
P18	DN	*HRAS*	CLGPIT HRas S17N	CLGPIT HRas S17N
P19	CA	*CTNNB1*	CLPIT CTNNB1 S33Y	CLGPIT CTNNB1 S33Y 2xFLAG
P20	WT	*RELA*	pEN RelA	CLGPIT RelA
P21	CA	*NFKBIA*	pEN IkBa	CLGPIT IkBa S32A S36A
P22	CA	*Tgfbr1*	pRK5F FLAG TbRI T202D (or RK5 R4TD202 FLAG)	CLGPIT FLAG TbRI T202D

P23	CA	*Hif1a*	pCDNA3.1+ HIF ΔODD	CLGPIT HIF ΔODD
P24	WT	*MAPK3*	pCEP4 ERK1	CLGPIT ERK1 HA TAG
P25	DN	*MAPK3*	pCEP4 ERK1 K71R	CLGPIT ERK1 K71R HA TAG
P26	WT	*Mapk1*	3XFLAG-CMV7 ERK2	CLGPIT ERK2
P27	DN	*Mapk1*	3XFLAG-CMV7 ERK2 K52R	CLGPIT ERK2 K52R
P28	CA	*GNAI1*	pCDNA3.1+ Ga i1 Q204L	CLGPIT Gai1 Q204L
P29	CA	*GNA12*	pCDNA3.1+ Ga 12 Q231L	CLGPIT Ga12 Q231L
P30	CA	*GNAQ*	pCDNA3.1+ Ga q Q209L	CLGPIT Gaq Q209L
P31	CA	*GNAS*	pCDNA3.1+ Ga s Q227L	CLGPIT Gas Q227L
P32	CA	*Notch1*	CLPIT mNICD	CLGPIT mNICD
P33	CA	*Smo*	pBS SK SP Smo	CLGPIT Smo W539L
P34	CA	*STAT3*	MIG STAT3	CLGPIT STAT3 A662C, N664C
P35	DN	*STAT3*	MIG DN STAT3	CLGPIT DN STAT3
P36	KD,DN	*Gsk3b*	CLPIT GSK3b K85R	CLGPIT Gsk3b K85R
P37	DN	*Gsk3b*	CLPIT GSK3b R96A	CLGPIT Gsk3b R96A
P38	CA	*Gsk3b*	CLPIT GSK3b S9A	CLGPIT Gsk3b S9A
P39	DN	*TGFBR2*	CLPC DNRI	CLGPIT DN TGFBRII

Table AII. Database and cloning information

No.	Accession	Full Title (NCBI: www.ncbi.nlm.nih.gov)	Sequence Deviations and *Cloning* Information
P1	NP_001096	activin A type I receptor precursor [Homo sapiens]	Q207D
P2	NP_002747	mitogen-activated protein kinase kinase 3 isoform A [Homo sapiens]	S189E, T193E, FLAG N-term (E312K mutation, +)
P3	NP_002749	mitogen-activated protein kinase kinase 6 [Homo sapiens]	S207E, T211E, FLAG N-term
P4	NP_001655	ras homolog gene family, member A [Homo sapiens]	T19N, myc N-term
P5	NP_001655	ras homolog gene family, member A [Homo sapiens]	Q63L, myc N-term
P6	NP_008839	ras-related C3 botulinum toxin substrate 1 isoform Rac1 [Homo sapiens]	Q61L
P7	NP_008839	ras-related C3 botulinum toxin substrate 1 isoform Rac1 [Homo sapiens]	T17N
P8	NP_001782	cell division cycle 42 isoform 1 [Homo sapiens]	Q61L
P9	NP_001782	cell division cycle 42 isoform 1 [Homo sapiens]	T17N
P10	NP_033782	Akt1 thymoma viral proto-oncogene 1 [Mus musculus]	
P11	NP_033782	Akt1 thymoma viral proto-oncogene 1 [Mus musculus]	T308A, S473A, K179A
P12	NP_033782	Akt1 thymoma viral proto-oncogene 1 [Mus musculus]	T308D, S473D
P14	NP_037052	Camk2a calcium/calmodulin-dependent protein kinase II alpha [Rattus norvegicus]	T286D
P15	NP_067710	Camk2n2 calcium/calmodulin-dependent protein kinase II inhibitor 2 [Rattus norvegicus]	
P16	NP_036859	Camk4 calcium/calmodulin-dependent protein kinase IV [Rattus norvegicus]	
P17	NP_005334	v-Ha-ras Harvey rat sarcoma viral oncogene homolog isoform 1 [Homo sapiens]	G12V
P18	NP_005334	v-Ha-ras Harvey rat sarcoma viral oncogene homolog isoform 1 [Homo sapiens]	S17N, *recloned backbone*
P19	NP_001895	catenin (cadherin-associated protein), beta 1, 88kDa [Homo sapiens]	*QC to S33Y, QC to remove S374G,* 2xFLAG C-term
P20	NP_068810	v-rel reticuloendotheliosis viral oncogene homolog A [Homo sapiens]	P180S, S is correct
P21	NP_065390	nuclear factor of kappa light polypeptide gene enhancer in B-cells inhibitor, alpha [Homo sapiens]	*S32A, S36A*
P22	P80204	TGF-beta receptor type-1	GSM after N148, T202D, FLAG N-term, *PCR out*

P23	Q61221	Hypoxia-inducible factor 1 alpha	M1-L400, Q614-STOP(837) (oxygen detecting domain removed), *QC in STOP codon*
P24	NP_002737	mitogen-activated protein kinase 3 isoform 1 [Homo sapiens]	HA tag N-term
P25	NP_002737	mitogen-activated protein kinase 3 isoform 1 [Homo sapiens]	K71R, HA tag N-term
P26	NP_446294	mitogen activated protein kinase 1 [Rattus norvegicus]	5 alanines instead of six from A2-A7, ok from lab
P27	NP_446294	mitogen activated protein kinase 1 [Rattus norvegicus]	5 alanines instead of six from A2-A7, ok from lab, K52R
P28	NP_002060	guanine nucleotide binding protein (G protein), alpha inhibiting activity polypeptide 1 [Homo sapiens]	Q204L
P29	NP_031379	guanine nucleotide binding protein (G protein) alpha 12 [Homo sapiens]	Q231L, *PCR into CaMKIV*
P30	NP_002063	guanine nucleotide binding protein (G protein), q polypeptide [Homo sapiens]	Q209L, *PCR into CaMKIV*
P31	NP_000507	GNAS complex locus isoform a [Homo sapiens]	Q227L
P32	EDL08321	Notch gene homolog 1 (Drosophila) [Mus musculus]	V1744-S2184, 6 C-terminus myc epitopes
P33	NP_036939	smoothened homolog [Rattus norvegicus]	*QC in W539L, removed extra start codon by recloning into pBS KS PS*
P34	NP_003141	signal transducer and activator of transcription 3 isoform 2 [Homo sapiens]	*PCR STAT3 into CLGPIT, QC in A662C, N664C, (used NotI instead of PmeI destroyed in cloning)*
P35	NP_644805	signal transducer and activator of transcription 3 isoform 1 [Homo sapiens]	M1-K685, *PCR DN STAT3 into CLGPIT*
P36	NP_114469	glycogen synthase kinase 3 beta [Rattus norvegicus]	K85R, *QC to remove R144STOP*
P37	NP_114469	glycogen synthase kinase 3 beta [Rattus norvegicus]	R96A
P38	NP_114469	glycogen synthase kinase 3 beta [Rattus norvegicus]	S9A, *QC to remove N370S*
P39	NP_003233	transforming growth factor, beta receptor II isoform B precursor [Homo sapiens]	M1-I219 (of 567) with S122I point mutation (note P37173 in UniProt)

Table AIII. Gene size and homology

No.	Protein Size (AA)	Gene Size (kilobases)	Homology (of wildtype gene) to mouse (**Homologene:** www.ncbi.nlm.nih.gov/homologene)
P1	509	1.53	Score = 1038 bits (2683), Expect = 0.0, Identities = 501/509 (98%), Positives = 506/509 (99%), Gaps = 0/509 (0%)
P2	318	0.96	Score = 681 bits (1756), Expect = 0.0, Identities = 335/347 (96%), Positives = 343/347 (98%), Gaps = 0/347 (0%)
P3	343	1.03	Score = 663 bits (1710), Expect = 0.0, Identities = 327/334 (97%), Positives = 331/334 (99%), Gaps = 0/334 (0%)
P4	193	0.58	Score = 395 bits (1015), Expect = 1e-108, Identities = 192/193 (99%), Positives = 193/193 (100%), Gaps = 0/193 (0%)
P5	193	0.58	Score = 395 bits (1015), Expect = 1e-108, Identities = 192/193 (99%), Positives = 193/193 (100%), Gaps = 0/193 (0%)
P6	192	0.58	Score = 384 bits (987), Expect = 3e-105, Identities = 192/211 (90%), Positives = 192/211 (90%), Gaps = 19/211 (9%)
P7	192	0.58	Score = 384 bits (987), Expect = 3e-105, Identities = 192/211 (90%), Positives = 192/211 (90%), Gaps = 19/211 (9%)
P8	191	0.58	Score = 390 bits (1001), Expect = 6e-107, Identities = 191/191 (100%), Positives = 191/191 (100%), Gaps = 0/191 (0%)
P9	191	0.58	Score = 390 bits (1001), Expect = 6e-107, Identities = 191/191 (100%), Positives = 191/191 (100%), Gaps = 0/191 (0%)
P10	480	1.44	NA
P11	480	1.44	NA
P12	480	1.44	NA
P14	478	1.44	Score = 981 bits (2536), Expect = 0.0, Identities = 478/478 (100%), Positives = 478/478 (100%), Gaps = 0/478 (0%)
P15	79	0.24	Score = 164 bits (414), Expect = 3e-39, Identities = 79/79 (100%), Positives = 79/79 (100%), Gaps = 0/79 (0%)
P16	474	1.43	Score = 830 bits (2145), Expect = 0.0, Identities = 425/478 (88%), Positives = 436/478 (91%), Gaps = 13/478 (2%)
P17	189	0.57	Score = 381 bits (978), Expect = 2e-104, Identities = 188/189 (99%), Positives = 188/189 (99%), Gaps = 0/189 (0%)
P18	189	0.57	Score = 381 bits (978), Expect = 2e-104, Identities = 188/189 (99%), Positives = 188/189 (99%), Gaps = 0/189 (0%)
P19	781	2.35	Score = 1548 bits (4008), Expect = 0.0, Identities = 780/781 (99%), Positives = 780/781 (99%), Gaps = 0/781 (0%)
P20	551	1.66	Score = 979 bits (2531), Expect = 0.0, Identities = 487/553 (88%), Positives = 509/553 (92%), Gaps = 6/553 (1%)
P21	317	0.95	Score = 585 bits (1508), Expect = 3e-165, Identities = 288/317 (90%), Positives = 297/317 (93%), Gaps = 3/317 (0%)
P22	501	1.51	Score = 994 bits (2569), Expect = 0.0, Identities = 493/503 (98%), Positives = 494/503 (98%), Gaps = 6/503 (1%)

P23	623	1.87	NA
P24	379	1.14	Score = 743 bits (1919), Expect = 0.0, Identities = 367/378 (97%), Positives = 368/378 (97%), Gaps = 0/378 (0%)
P25	379	1.14	Score = 743 bits (1919), Expect = 0.0, Identities = 367/378 (97%), Positives = 368/378 (97%), Gaps = 0/378 (0%)
P26	357	1.07	Score = 736 bits (1899), Expect = 0.0, Identities = 358/358 (100%), Positives = 358/358 (100%), Gaps = 0/358 (0%)
P27	357	1.07	Score = 736 bits (1899), Expect = 0.0, Identities = 358/358 (100%), Positives = 358/358 (100%), Gaps = 0/358 (0%)
P28	354	1.07	Score = 712 bits (1837), Expect = 0.0, Identities = 354/354 (100%), Positives = 354/354 (100%), Gaps = 0/354 (0%)
P29	381	1.15	Score = 733 bits (1891), Expect = 0.0, Identities = 374/381 (98%), Positives = 379/381 (99%), Gaps = 2/381 (0%)
P30	359	1.08	Score = 718 bits (1854), Expect = 0.0, Identities = 358/359 (99%), Positives = 359/359 (100%), Gaps = 0/359 (0%)
P31	394	1.19	Score = 800 bits (2065), Expect = 0.0, Identities = 393/394 (99%), Positives = 394/394 (100%), Gaps = 0/394 (0%)
P32	441	1.33	NA
P33	793	2.38	Score = 1619 bits (4193), Expect = 0.0, Identities = 781/793 (98%), Positives = 786/793 (99%), Gaps = 0/793 (0%)
P34	769	2.31	Score = 1552 bits (4018), Expect = 0.0, Identities = 768/769 (99%), Positives = 769/769 (100%), Gaps = 0/769 (0%)
P35	685	2.06	Score = 1552 bits (4018), Expect = 0.0, Identities = 768/769 (99%), Positives = 769/769 (100%), Gaps = 0/769 (0%)
P36	420	1.26	Score = 850 bits (2195), Expect = 0.0, Identities = 420/420 (100%), Positives = 420/420 (100%), Gaps = 0/420 (0%)
P37	420	1.26	Score = 850 bits (2195), Expect = 0.0, Identities = 420/420 (100%), Positives = 420/420 (100%), Gaps = 0/420 (0%)
P38	420	1.26	Score = 850 bits (2195), Expect = 0.0, Identities = 420/420 (100%), Positives = 420/420 (100%), Gaps = 0/420 (0%)
P39	261	0.79	Score = 1139 bits (2947), Expect = 0.0, Identities = 541/592 (91%), Positives = 568/592 (95%), Gaps = 0/592 (0%)

APPENDIX B. CLONING PRIMER INFORMATION

Table BI. Quikchange and cloning primers

Primer Name	Primer Sequence	Reason
Smo QC Forward	5'-GCCATGAGCACCTTGGTCTGGACCAAG GCCACCCTG-3'	W539L
Smo QC Reverse	5'-CAGGGTGGCCTTGGTCCAGACCAAGGTG CTCATGGC-3'	W539L
IkBa QC Forward	5'-CGCCACGACGCTGGCCTGGACGCCATGAA AGACGAGG-3'	S32A, S36A
IkBa QC Reverse	5'-CCTCGTCTTTCATGGCGTCCAGGCCAGCG TCGTGGCG-3'	S32A, S36A
STAT3 QC Forward	5'-GATCATGGATTGTACCTGTATCCTGGTGT CTCCACTGGTC-3'	A662C, N664C
STAT3 QC Reverse	5'-GACCAGTGGAGACACCAGGATACAGGTA CAATCCATGATC-3'	A662C, N664C
Gq QC Forward	5'-GCTGACTCGAGATGACTCTGGAGTCCAT CAT-3'	Create Restriction Site
Gq QC Reverse	5'-GCCATCGTTTAAACTTAGACCAGATTGTA CTCCTTCAGG-3'	Create Restriction Site
G12 QC Forward	5'-GCTGACTCGAGATGTCCGGGGTGGTGCG GAC-3'	Create Restriction Site
G12 QC Reverse	5'-GCCATCGTTTAAACTCACTGCAGCATGA TGTCCTTCAGG-3'	Create Restriction Site
GSK3b K85R QC Forward	5'-TACAGAGTCGCCAGACACTATA-3'	Remove Mutation
GSK3b K85R QC Reverse	5'-TATAGTGTCTGGCGACTCTGTA-3'	Remove Mutation
GSK3b S9A QC Forward	5'-CTGTCAAGTAACCCACCTCTGG-3'	Remove Mutation
GSK3b S9A QC Reverse	5'-CCAGAGGTGGGTTACTTGACAG-3'	Remove Mutation
CTNNB1 S33Y QC Forward	5'-TCTTACCTGGACTATGGAATCCATTCT-3'	S33Y
CTNNB1 S33Y QC Reverse	5'-AGAATGGATTCCATAGTCCAGGTAAGA-3'	S33Y
CTNNB1 MSMut QC Forward	5'-CACCTGACAGATCCAAGTCAACGTCTT GTTC-3'	Remove Mutation
CTNNB1 MSMut QC Reverse	5'-GAACAAGACGTTGACTTGGATCTGTCAG GTG-3'	Remove Mutation
DN STAT3 PCR Reverse	5'-CCCCGTTTAAACCTACTTTCCAAATGCCT CCT-3'	PCR out
STAT3 PCR Forward	5'-GGCGGGCCGCCTGGGCCAAATGGCTCAG TGGAACCAGCTGC-3'	PCR out
STAT3 PCR Reverse	5'-CCCCGTTTAAACTCACATGGGGGAGGTA GCACACT-3'	PCR out
CA TbRI Forward	5'-GAGAGGGGCCACCTGGGCCAAATGGAGG CGGCGTCGGCTG-3'	PCR out
CA TbRI Reverse	5'-CGCATACCCGTTTAAACTTACATTTTGATG CCTTCCTGTTG-3'	PCR out
HIFdelODD Forward	5'-GCTTTGGATCAAGTTAACTAACTCGAGTT TAAACGCGGT-3'	Add Stop codon
HIFdelODD Reverse	5'-ACCGCGTTTAAACTCGAGTTAGTTAACTT GATCCAAAGC-3'	Add Stop codon
STAT3 A662C N664C	5'-CATCATGGGCTATAAGATCATGGATTGCA	A662C, N664C

Forward	CCTGCATCCTGGTGTCTCCACTTGTCTAC-3'	
STAT3 A662C N664C Reverse	5'-GTAGACAAGTGGAGACACCAGGATGCAG GTGCAATCCATGATCTTATAGCCCATGATG-3'	A662C, N664C
TbRI PCR Reverse	5'-CCCCCCCGTTTAAACCCCTCACTTGTCGTC GTCGTCCTTGTAG-3'	PCR out
TbRI PCR Forward	5'-GAAAAAGGCCACCTAGGCCATGGAGGCAG CATCGGCT-3'	PCR out

Table BII. Sequencing primers

Primer Name	**Primer Sequence**
CLPIT VSVG 5' Seq	5'-AGACGCCATCCAACGCTGTTT-3'
CLPIT VSVG 3' Seq	5'-AGAGCCTGGACCACTGATATCCTGTCT-3'
delSTAT3 3' Fwd Seq01 AF	5'-ATCCTGGTGTCTCCACTTGT-3'
delSTAT3 5' Rev Seq01 AF	5'-TGGGGAAGCTGTCGCTGTAC-3'
delSTAT3 3' Fwd Seq02 AF	5'-TCATGGATGCGACCAACATC-3'
delSTAT3 5' Rev Seq02 AF	5'-ATGTGACTCTTTGCTGGCTG-3'
mNICD Mid1 Seq AF	5'-TGTCTTCCAGATCCTGCTCC-3'
Smo Mid1 Seq	5'-GTGAGGACAGACAACCCCAA-3'
Smo Mid2 Seq	5'-CCCAATTGGCCTGGTGCTTA-3'
CTNNB1 Mid Seq1	5'-TACGACAGACTGCCTTCAAA-3'
CTNNB1 Mid Seq2	5'-GTGGTGGTTAATAAGGCTGC-3'
CaMKII Mid Seq	5'-GGGAGCAGCAGGCATGGTTT-3'
MIG Seq Fwd	5'-CTGGAGTCAGCGCAGGCCGG-3'
MIG Seq Rev	5'-TCAAGAAGACAGGGCCAGGT-3'
STAT3 Mid1 Seq	5'-AATGGAAACAACCAGTCTGT-3'
STAT3 Mid2 Seq	5'-ATGTTGCTGCCCTCAGAGGGTCTC-3'
HifdODD Mid Seq	5'-AGTTGATGGGTTATGAGCCG-3'

Table BIII. Cloning oligos used in pHIV IG loxP cloning

lox66 forward	5'-CTAGATAACTTCGTATAGCATACATTATACGAACGGTAGAGGGCCGCCT GGGCCCCTCGAGTT-3'
lox66 reverse	5'-CTAGAACTCGAGGGGCCCAGGCGGCCCTCTACCGTTCGTATAATGTATG CTATACGAAGTTAT-3'
MCS forward	5'-GATCCAACCGAATTCAACCATTTAAATAACCGGCGCGCCAACCGTTTAAA CG-3'
MCS reverse	5'-GATCCGTTTAAACGGTTGGCGCGCCGGTTATTTAAATGGTTGAATTCGGT TG-3'
lox71 forward	5'-CGATCTATTTGTCATCATCGTCCTTATAGTCCATGGTGGCTTAATTTATT GAAGCATATTACATACGATATGCTTGCCATAT-3'
lox71 reverse	5'-CGATATGGCAAGCATATCGTATGTAATATGCTTCAATAAATTAAGCCACC ATGGACTATAAGGACGATGATGACAAATAGAT-3'

APPENDIX C. COLONY COUNTING CODE

Colony Counting Setup

Written with Paula Gedraitis, Molecular Devices
MetaXpress Software MX3, MX5 compatible

This particular code is named "ColonyCounting24wellAF_setup"
This should be used for a particular imaging pattern in 24 well plates. Otherwise, the "Montage set up" section should be modified.

Alkaline Phosphatase is imaged in the DAPI channel with the Alkaline Phosphatase Cube (Chapter 2). HCS NuclearMask Red is with the Cy5 cube/channel.

(I) indicates interactive sections of the code (user prompts)

Image settings: this is originally designed for alkaline phosphatase staining, however any marker can be used in place of the "AP image"

```
(I) 1: Select Image("Select nuclear image (do NOT select HTS image)")
NuclearImage = Image.Name
(I) 2: Select Image("Select AP image (do NOT select HTS image)")
APImage = Image.Name
3: Show Message and Wait("Please set the…", NO TIMEOUT)
```

Threshold settings – nuclear image: this will interactively allow the user to select the minimum and maximum thresholds for including colonies

```
4: Select Image("%Nuclear Image%")
IF Image.ThreshState=0 THEN
        Image.ThreshMin = 300
        Image.ThreshState = 1
ELSE
END IF
Image.ThreshMax = 4095
(I)5: Threshold Image("%NuclearImage%", 100, 4095, Inclusive)
NuclearThresholdMin = Image.ThreshMin
NuclearThresholdMax = Image.ThreshMax
```

Threshold settings – AP image: this will interactively allow the user to select the minimum and maximum thresholds for including colonies

```
6: Select Image("%APImage%")
IF Image.ThreshState=0, THEN
        Image.ThreshMin = 300
        Image.ThreshState = 1
ELSE
END IF
Image.ThreshMax = 4095
```

(I)5: Threshold Image("%APImage%", 100, 4095, Inclusive)
APThresholdMin = Image.ThreshMin
APThresholdMax = Image.ThreshMax

Get IMA settings from user: this is the setting for the minimum colony area, each analysis the IMA file is resaved, only the minimum colony area should be modified in the IMA. ColonyCounting_AP must be present in the folder with the journal. This is the initial IMA that is modified.
8: Integrated Morphometry – Load State("ColonyCounting_AP")
9: Show Message and Wait("In the next dialo…", NO TIMEOUT)
(I)10: Integrated Morphometry – Measure("%APImage%")
Define IMA Name
APSettings = Prompt User(String)
APSettingsFile = "C:\assay\ColonyCounting24wellAF\" + APSettings + ".IMA"
Ashley – 4000 is from previous analysis, this will update to the newest APSettingsFile
11: Integrated Morphometry – Save State("Ashley – 4000")
    State File = APSettingsFile

Binning set up: images can be binned during image acquisition or before image analysis. Binning images decreases the amount of memory and speeds up processing time; however, if the binning is modified before analysis, the blank site size must be adjusted
ImageWidth = Image.Width
ImageHeight =Image.Height
12: Select Image("APStack")
ImageXCal = Image.XCalibration
ImageYCal = Image.YCalibration
Binning = VAL(MID(Image.Annotation, INSTR(Image.Annotation, "Binning")+LEN("Binning: ")))
IF Binning = 1 THEN
    BinImages = Prompt User(YesNo)
    IF BinImages="Y" THEN
        ImageXCal = ImageXCal*2
        ImageYCal = ImageYCal*2
    ELSE
    END IF
ELSE
    BinImage = "N"
END IF

Montage set up: this inserts blank images where the edges of the well were not imaged. A montage should be used to ensure no colonies are counted multiple times (e.g. when a colony spans multiple images). A montage image is similar to stitching. This will give an image of the entire well.
MontageRows = 8
MontageColumns = 6
TotalSiteNumber = 36

```
MontageZoom = 100
If ImageExists("BlankSite") THEN
        13: Close("BlankSite"
ELSE
END IF
IF BinImages = "Y" THEN
        14: BlankSite = New(16, 0)
        Width = ImageWidth/2
        Height = ImageHeight/2
ELSE
        15: BlankSite = New(16,0)
        Width = ImageWidth
        Height = ImageHeight
END IF
16: Minimized Image Window("BlankSite")
```

Image saving set up: the user has the option of saving the montages (nuclear stain, alkaline phosphatase, and mask). Additionally, the summary log (Excel file) contains the thresholds and the name of the IMA file used for minimum colony area.

```
SaveMontages = Prompt User(YesNo)
IF SaveMontages = "Y" THEN
        FileDirectory = Prompt User(String)
        IF RIGHT(FileDirectory,1) <> "\" THEN
                FileDirectory = FileDirectory + "\"
        ELSE
        END IF
        FileBaseName =MID(Image.Annotation, LEN("Experiment base name:")+1,
        (INSTR(Image.Annotation,"Experiment set:")-LEN("Experiment base name:")-3))
ELSE
END IF
17: Open Summary Log(OPENDDE and OVERWRITEMODE, "")
18: Open Object Log(OPENDDE and OVERWRITEMODE, "")
19: Annotate Log File(SUMMARY, "Threshold Settings")
20: Annotate Log File(SUMMARY, "Nuclear Minimum Threshold, Nuclear Maximum
        Threshold, AP Minimum Threshold, AP Maximum Threshold, AP Settings Filename)
22: Log Variable(NuclearThresholdMin, NEWLINE, NO HEADER)
23: Log Variable(NuclearThresholdMax, NONEWLINE, NO HEADER)
24: Log Variable(APThresholdMin, NONEWLINE, NO HEADER)
25: Log Variable(APThresholdMax, NONEWLINE, NO HEADER)
26: Log Variable(APSettings, NONEWLINE, NO HEADER)
27: Log Variable(FileBaseName, NEWLINE, NO HEADER)
28: Annotate Log File(SUMMARY, "Minimum colony size(um2) based on IMA (manual
        entry)")
29: Show Message and Wait("Analysis setup is…", NO TIMEOUT)
```

Colony Counting Journal

This particular code is named "ColonyCounting24wellAF"

Determine current well, site: for automation through plate

```
1: Select Image("%APImage%")
CurrentWell = LEFT(Image.StageLabel, 3)
CurrentSiteValue = VAL(RIGHT(Image.StageLabel, LEN(Image.StageLabel) –
        INSTR(Image.StageLabel, "Site")-4))
Trace (CurrentSiteValue)
```

Add in extra blanks as needed: must be modified for non-24 well plates or different imaging patterns

```
IF (CurrentSiteValue = 1) THEN
        PreSiteBlanks = 2
ELSE
        IF (CurrentSiteValue = 3) OR (CurrentSiteValue = 35) THEN
                PreSiteBlanks = 3
        ELSE
                IF (CurrentSiteValue = 7) OR (CurrentSiteValue = 31) THEN
                        PreSiteBlanks = 1
                ELSE
                        PreSiteBlanks = 0
                END IF
        END IF
END IF

IF PreSiteBlanks > 0 THEN
        FOR NumberOfBlanks = 1 TO PreSiteBlanks STEP 1
                2: Add Plane("BlankSite", "APStack", NOCLOSESOURCE)
                3: Add Plane("BlankSite", "NuclearStack", NOCLOSESOURCE)
        NEXT
ELSE
END IF
```

Add actual site images (binning first as needed)

```
IF BinImages="Y" THEN
        4: Set Image Zoom("%APImage%", 50)
        5: Image/Plane with Zoom("%APImage%)
        BinnedAPImage = "Zoomed Copy of " + APImage
        6: Add Plane("%BinnedAPImage%", "APStack", NOCLOSESOURCE)
        7: Close("%BinnedAPImage%"
        8: Set Image Zoom ("%NuclearImage%", 50)
        9: Image/Plane with Zoom("%NuclearImage%")
        BinnedNuclearImage = "Zoomed Copy of " + NuclearImage
        10: Add Plane("%BinnedNuclearImage%", "NuclearStack", NOCLOSESOURCE)
```

```
        11: Close("%BinnedNuclearImage%")
ELSE
        12: Add Plane("%APImage%", "APStack", NOCLOSESOURCE)
        13: Add Plane("%NuclearImage%", "NuclearStack", NOCLOSESOURCE)
END IF

If this is the final site
IF CurrentSiteValue = TotalSiteNumber THEN
Write out well position: on summary log
14: Log Variable(CurrentWell, NEWLINE, NO HEADER)
15: Log Variable(CurrentWell, NEWLINE, NO HEADER)

Add final blank sites
FOR NumberOfBlanks = 1 TO 2 STEP 1
        16: Add Plane("BlankSite", "APStack", NOCLOSESOURCE)
        17: Add Plane("BlankSite", "NuclearStack", NOCLOSESOURCE)
NEXT

Create AP montage image and close stack
18: Overwrite "APMontage" = Montage("APStack", HORIZONTAL, 100)
        Rows = MontageRows
        Columns = MontageColumns
19: Close("APStack"
20: Select Image("APMontage")
Image.ScaleAutoScale = 1
IF ImageXCal = 1.6125 THEN
        21: Calibrate Distances(SPECIFICIMAGE, "APMontage", 1.6125, 1.6125, "um")
ELSE
        IF ImageXCal = 3.225 THEN
                22: Calibrate Distances(SPECIFICIMAGE, "APMontage", 3.225, 3.225, "um")
        ELSE
        END IF
END IF

Create nuclear montage image and close stack
18: Overwrite "NuclearMontage" = Montage("NuclearStack", HORIZONTAL, 100)
        Rows = MontageRows
        Columns = MontageColumns
19: Close("NuclearStack"
20: Select Image("NuclearMontage")
Image.ScaleAutoScale = 1
IF ImageXCal = 1.6125 THEN
        21: Calibrate Distances(SPECIFICIMAGE, "NuclearMontage", 1.6125, 1.6125, "um")
ELSE
        IF ImageXCal = 3.225 THEN
```

```
            22: Calibrate Distances(SPECIFICIMAGE, "NuclearMontage", 3.225, 3.225,
            "um")
        ELSE
        END IF
END IF

Begin analysis on montage images: dilates the AP image to 5 um to help segment colony
29: Overwrite "APDilated" = Morphological Open-Close("APMontage", Circle, Diameter=5,
Use Reconstruction = False, Use Sequential Filtering = False)

Use threshold to define colonies
31: Select Image("APDilated")
Image.ThreshState = 1
Image.ThreshMin = APThresholdMin
Image.ThreshMax = APThresholdMax

Load colony state to filter based on minimum colony size: determined in setup.  Apply
morphometry to alkaline phosphatase (dilated) montage
32: Integrated Morphometry – Load State("Ashley – 4000")
        State File = APSettingsFile
33: Integrated Morphometry – Measure("APDilated)

Create mask based on alkaline phosphatase and apply to nuclear montage
IF ImageExists("IMA Objects Mask") THEN
        34: Close("IMA Objects Mask")
ELSE
END IF
35: Integrated Morphometry – Create Objects Mask()
36: Close("APDilated")
37: Overwrite "NuclearMeasured" = "NuclearMontage" AND "IMA Objects Mask"

Threshold resulting nuclear image
38: Select Image([37: Arithmetic])
Image.ThreshState = 1
Image.ThreshMin = NuclearThresholdMin
Image.ThreshMax = NuclearThresholdMax

Load colony state for nuclear detection
39: Integrated Morphometry – Load State("Ashley – 4000")
        State File = APSettingsFile
41: Integrated Morphometry – Measure ("NuclearMeasured")

Create mask to be used on AP montage: without dilation
IF ImageExists ("IMA Objects Mask") THEN
        42: Close("IMA Objects Mask")
ELSE
```

```
END IF
43: Integrated Morphometry – Create Objects Mask()
44: Close ([37: Arithmetic])

Save and close nuclear montage
45: Select Image("NuclearMontage")
IF SaveMontages = "Y" THEN
        Image.FilePath = FileDirectory + FileBaseName + "_" + CurrentWell + "_" +
        NuclearImage + ".tif"
        46: Save([Last Result])
ELSE
END IF
47: Close([Last Result])

Apply mask to AP and record measurements on summary log
48: Overwrite "Measured" = "APMontage" AND "IMA Objects Mask"
49: Threshold Image("Measured", 5, 4095, Inclusive)
51: Integrated Morphometry – Load State("Ashley – 4000")
        State File = APSettingsFile
52: Integrated Morphometry – Measure("Measured")
53: Integrated Morphometry – Log Data("Measured", SUMMARY, CURRENTDATA, 1, 2)
54: Integrated Morphometry – Log Data("Measured", OBJECTS, CURRENTDATA, 1, 2)

Create final mask
IF ImageExists("IMA Objects Mask") THEN
        56: Close("IMA Objects Mask")
ELSE
END IF
57: Integrated Morphometry – Create Objects Mask ()
58: Close("Measured")

Save and close AP montage
59: Select Image("APMontage")
IF SaveMontages = "Y" THEN
        Image.FilePath = FileDirectory + FileBaseName + "_" + CurrentWell + "_" + APImage
        + ".tif"
        60: Save([Last Result])
ELSE
END IF
61: Close([Last Result])

Save and close mask
62: Select Image("IMA Objects Mask")
IF SaveMontages = "Y" THEN
        Image.FilePath = FileDirectory + FileBaseName + "_" + CurrentWell + "_Mask" + ".tif"
        63: Save([Last Result])
```

```
ELSE
END IF
64: Close([Last Result])
ELSE
END IF
```

APPENDIX D: SUPPLEMENTAL FIGURES FOR CHAPTER 2

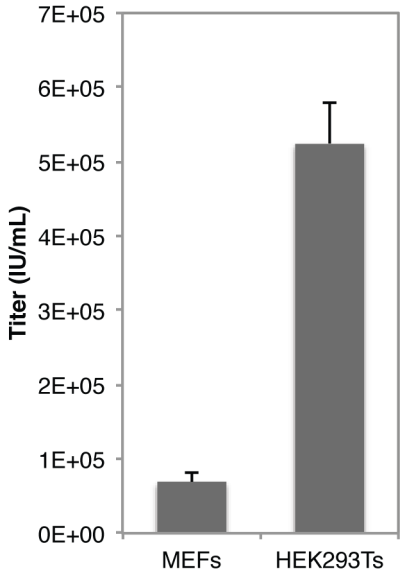

Figure D1. Lentiviral titers from the cassette virus, STEMCCA loxP, which expresses *Oct4*, *Sox2*, *Klf4*, and *c-Myc*. MEF or HEK293T cells were infected with varying amounts of lentivirus. 72 hours post infection, cells were assayed for OCT4 expression by immunocytochemistry. High-throughput imaging and analysis were used to determine viral titer (Infectious Units/mL). The same batch of virus was used, but the cell types were analyzed at differing time points. Error bars represent 95% confidence interval.

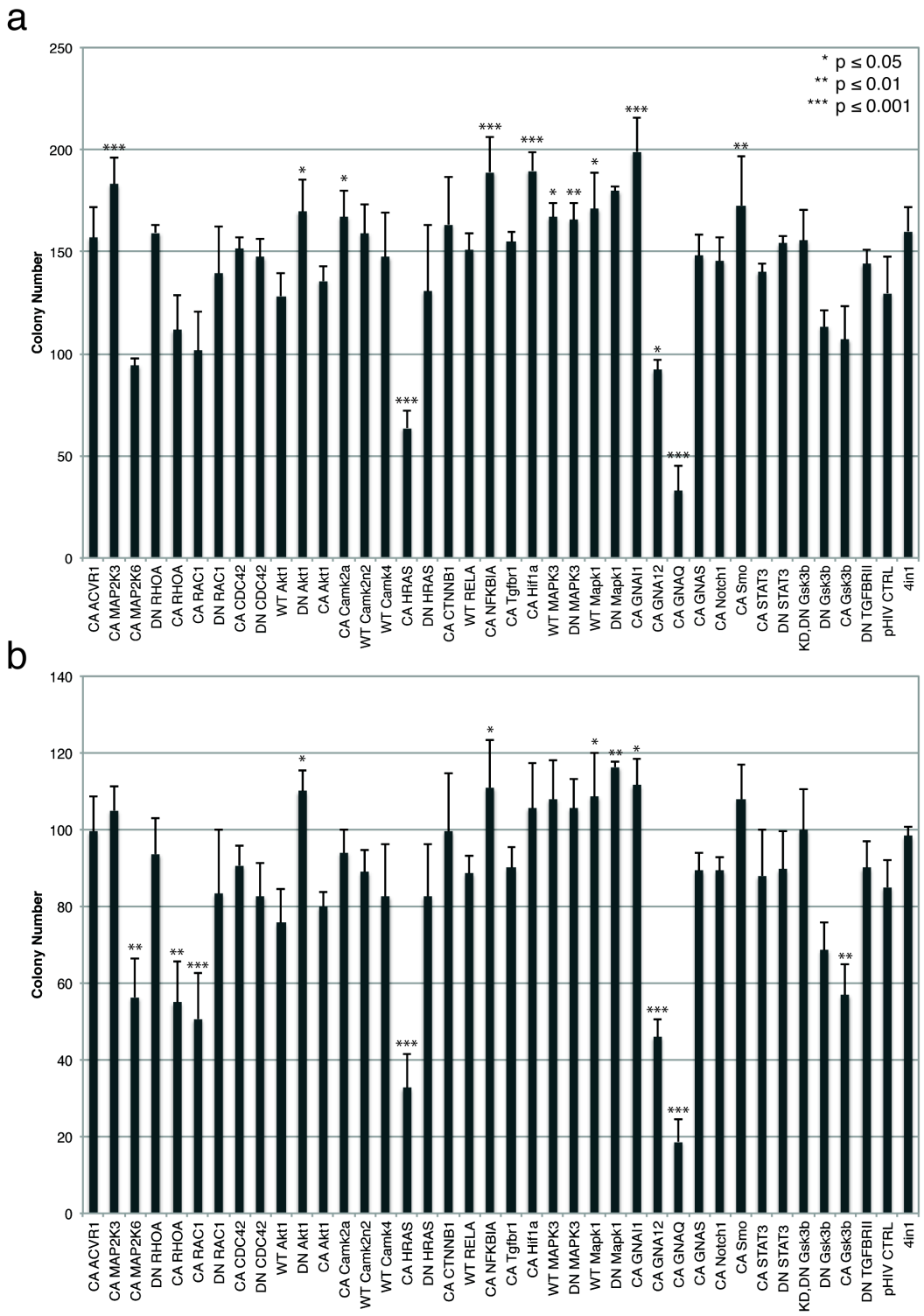

Figure D2. Number of alkaline phosphatase positive colonies 9 days post-infection with cDNA encoding a signal transduction factor, as well as *Oct4*, *Sox2*, *Klf4*, and *c-Myc*, as determined by high-throughput imaging and analysis. The minimum colony size measured was (a) 8,000 μm^2 or (b) 25,000 μm^2. Statistical significance was measured using ANOVA with a post-hoc Dunnett test relative to the infection control, pHIV CTRL. Error bars represent standard deviation.

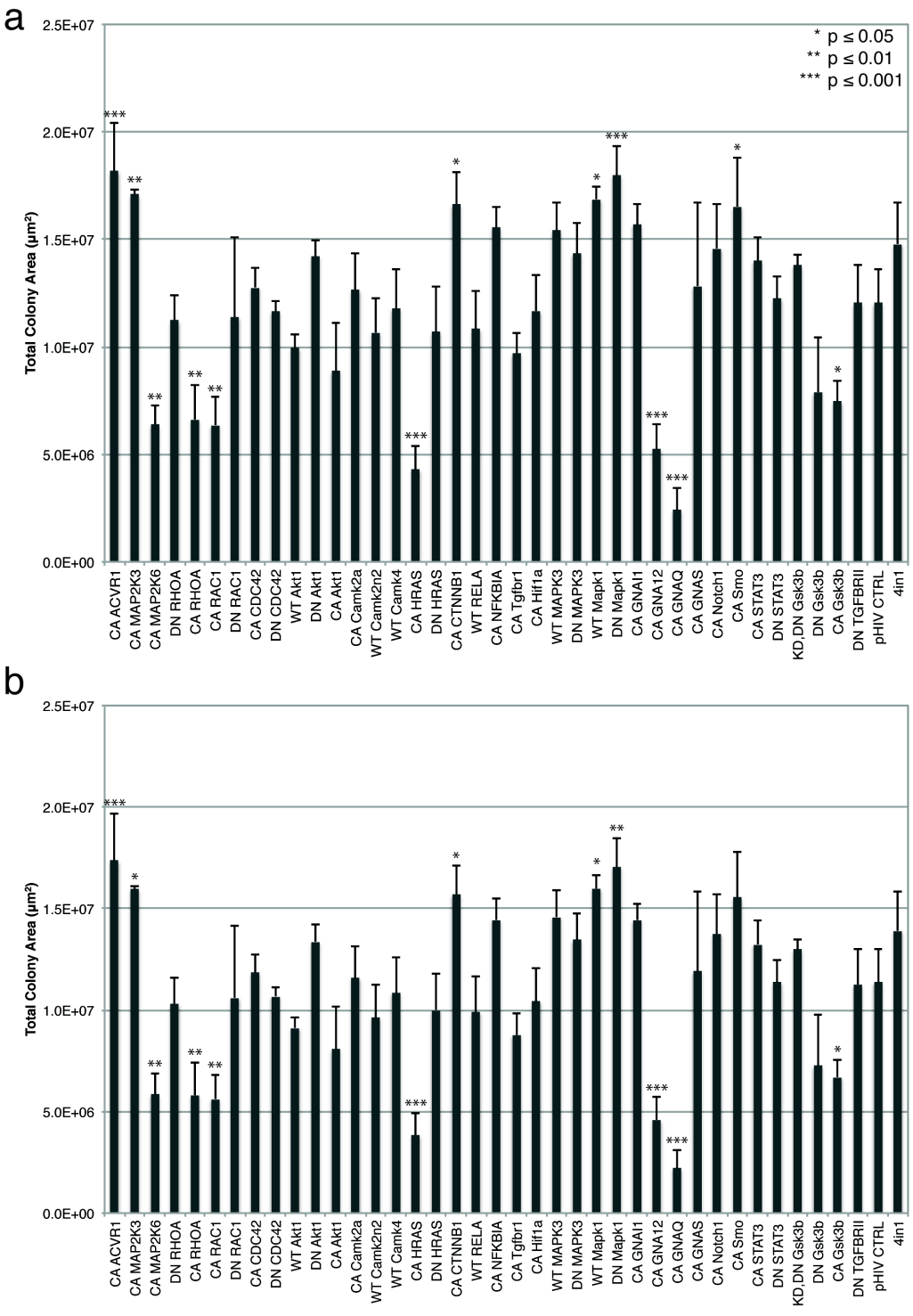

Figure D3. Total area of alkaline phosphatase positive colonies 9 days post-infection with cDNA encoding a signal transduction factor, as well as *Oct4*, *Sox2*, *Klf4*, and *c-Myc*, as determined by high-throughput imaging and analysis. The minimum colony size measured was (a) 8,000 μm^2 or (b) 25,000 μm^2. Statistical significance was measured using ANOVA with a post-hoc Dunnett test relative to the infection control, pHIV CTRL. Error bars represent standard deviation.

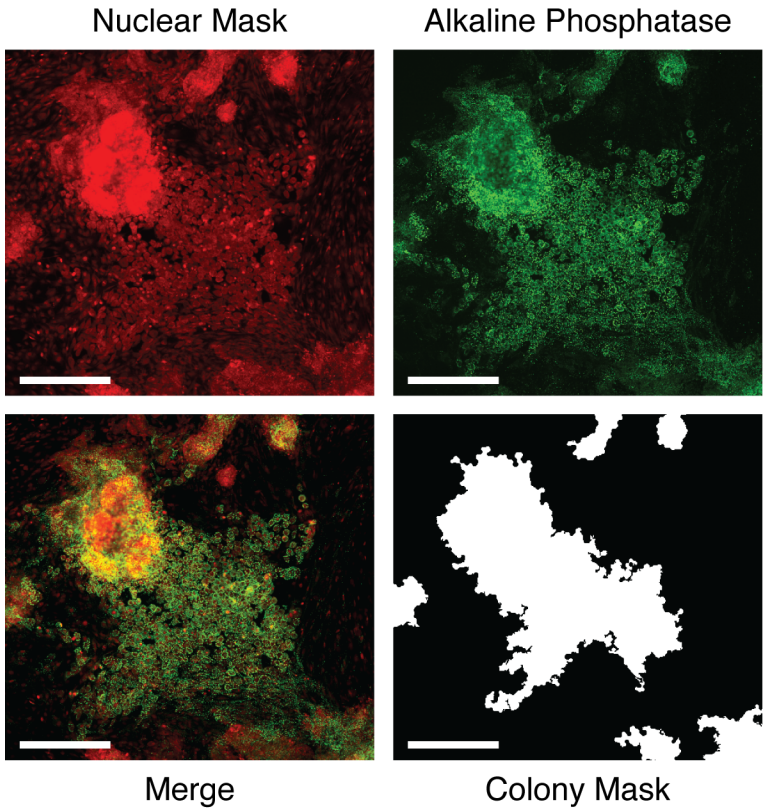

Figure D4. Constitutively-active *ACVR1* condition. In addition to serving as a marker for reprogramming, alkaline phosphatase is also expressed by an osteogenic cell lineage. The minimum colony size measured in the colony mask was 15,000 μm^2. Scale bars are 400 mm.

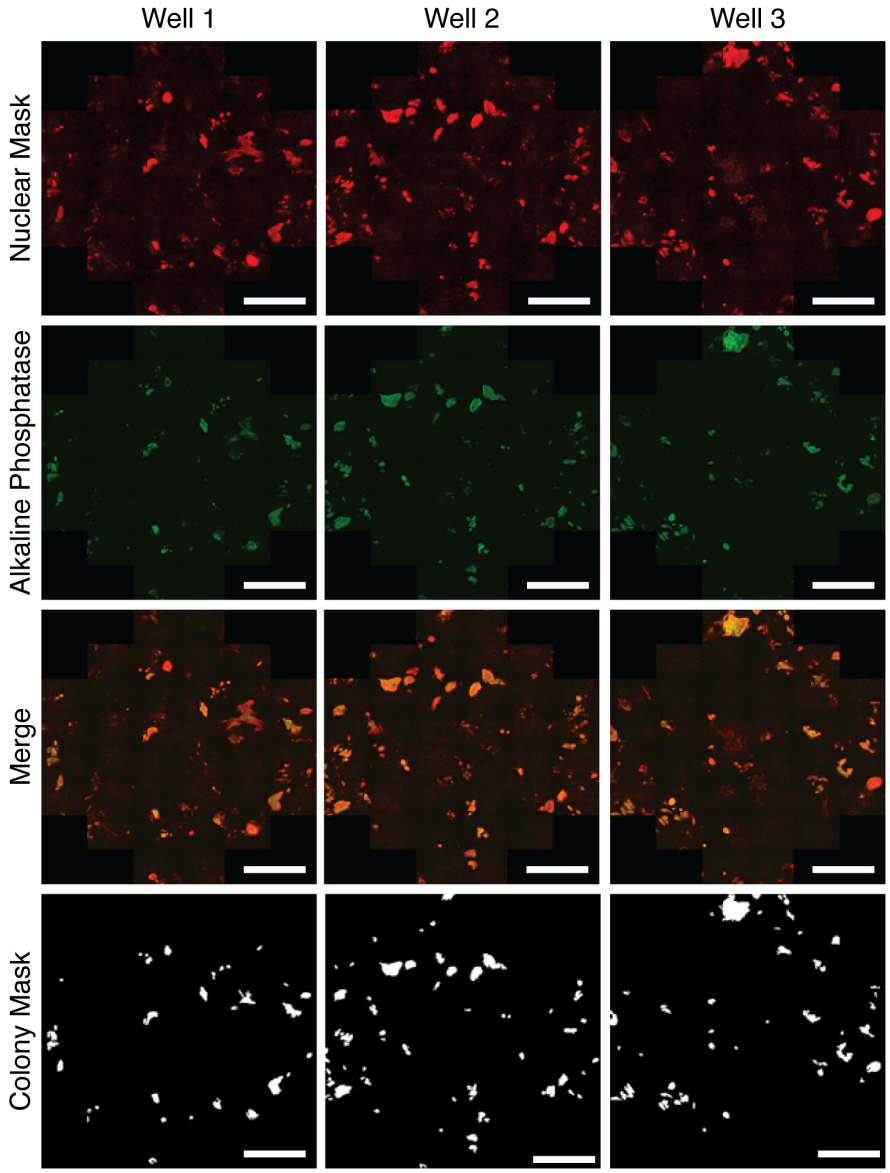

Figure D5. Constitutively-active *HRAS* conditions. The minimum colony size measured in the colony mask was 15,000 μm^2. Scale bars are 3 mm.

APPENDIX E: SUPPLEMENTAL INFORMATION FOR CHAPTER 3

Supplemental Figures

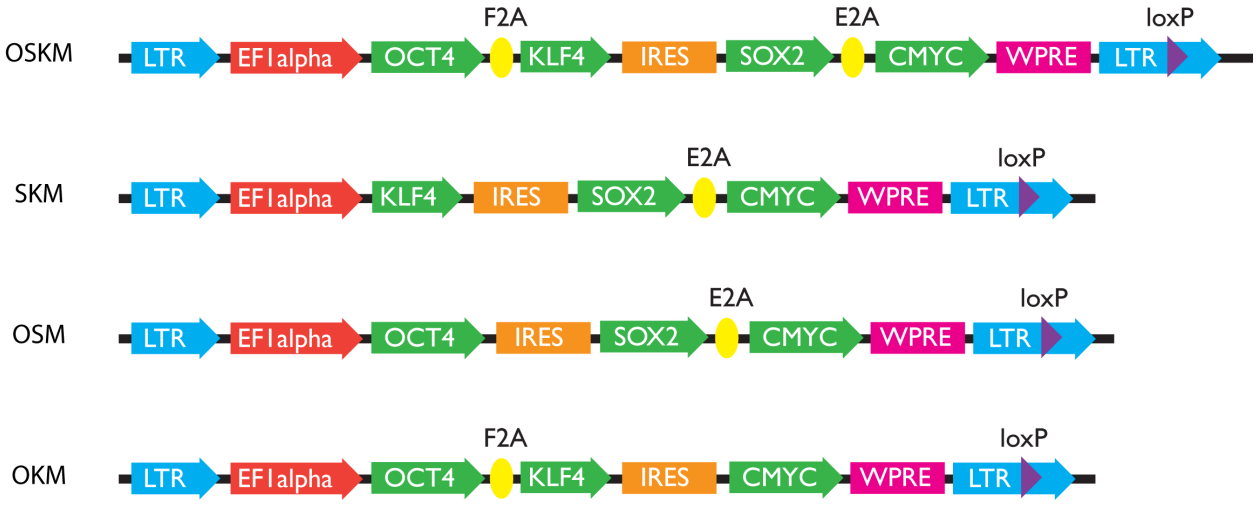

Figure E1. STEMCCA loxP viral vectors. STEMCCA-SKM loxP (SKM), STEMCCA-OSM loxP (OSM), and STEMCCA-OKM loxP (OKM) were modified from the STEMCCA loxP vector (OSKM).

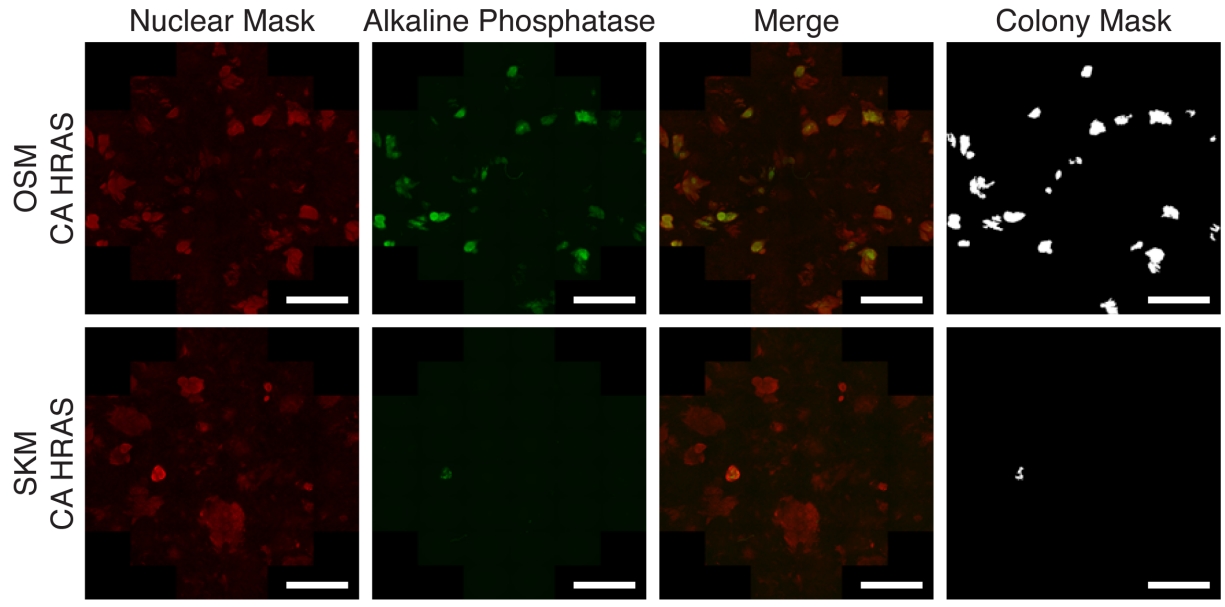

Figure E2. Activated *HRAS* induces alkaline phosphatase positive colonies in the absence of KLF4 but not OCT4. Colonies were infected with OSM or SKM, respectively, and constitutively-active *HRAS*. 10 or 13 days post-infection, respectively, cells were fixed and stained for alkaline phosphatase expression. Cells were analyzed by high-content imaging and analysis. Minimum colony size measured was 31,200 μm^2. Scale bars are 3 mm.

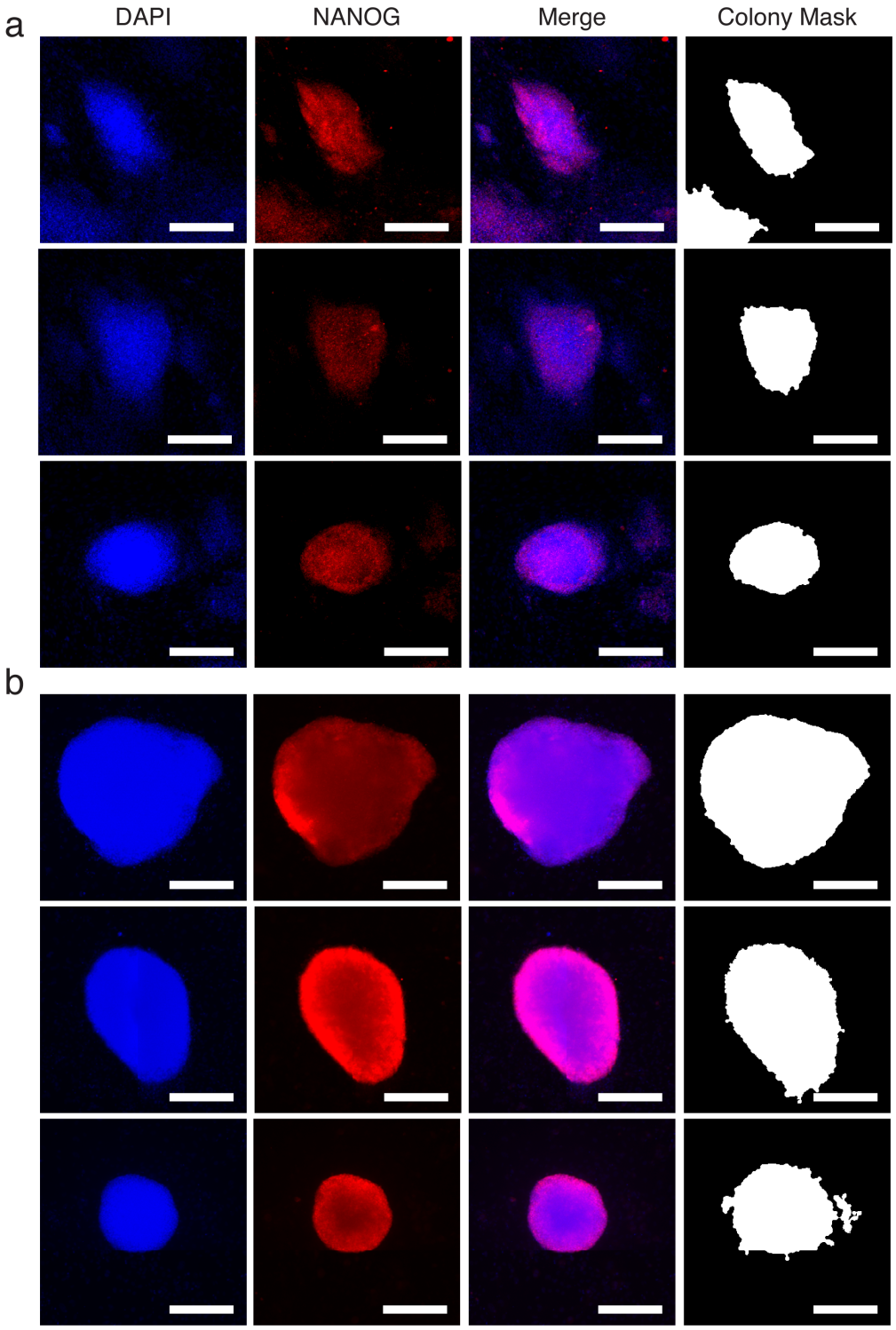

Figure E3. Constitutively-active HRAS induces morphologically different NANOG positive colonies without the *Klf4* or *Oct4* transgene, respectively. (a) Passage 3 MEFs were reprogrammed with OSM and constitutively-HRAS and stained for NANOG expression 8 days post-infection. Three different colonies are shown. (b) Passage 3 MEFs were also reprogrammed with SKM and constitively-active HRAS with the 2i inhibitors (CHIR99021 and PD 0325901) added in serum-free conditions 5 days post-infection. Cells were analyzed for NANOG expression 14 days post-infection. Three different colonies are shown.

Cells were analyzed by high-content imaging and analysis. Minimum colony size measured was 15,000 μm^2. The images were post-processed differently as SKM CA HRAS 2i and OSM CA HRAS had dissimilar colony morphology and expression. Scale bars are 300 μm.

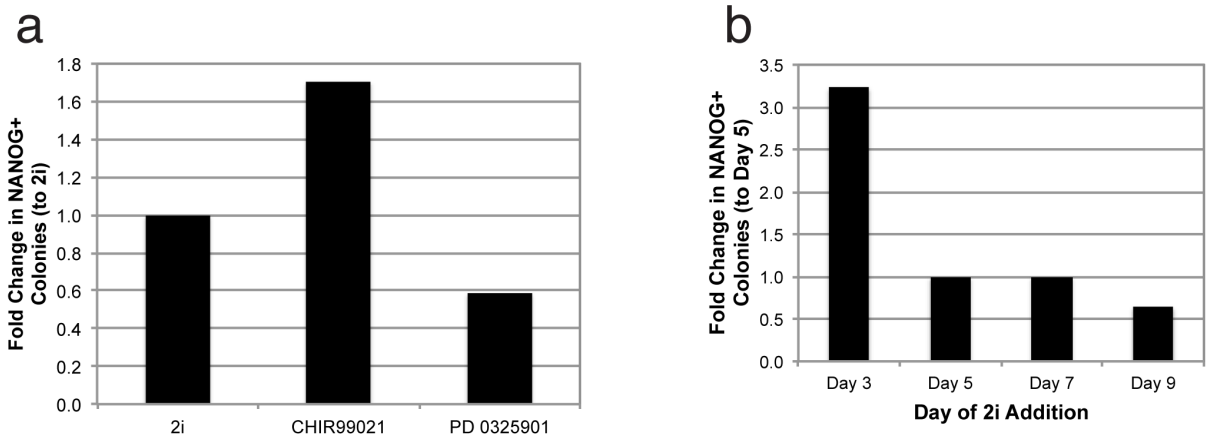

Figure E4. *HRAS*-mediated OCT4 replacement may be improved through the addition of CHIR99021 only or 2i addition earlier in reprogramming. Passage 3 MEFs were reprogrammed with SKM and constitutively-active *HRAS* as previously described. (a) 5 days post-infection CHIR99021 and/or PD 0325901 was added in serum-free medium. (b) 3, 5, 7, or 9 days post-infection, the 2i inhibitors were added to the media. Media and small molecules were changed every other day. Cells were analyzed for NANOG expression 11 days post-infection. Cells were analyzed by high-content imaging and analysis. (N=1) Minimum colony size measured was 15,000 μm^2.

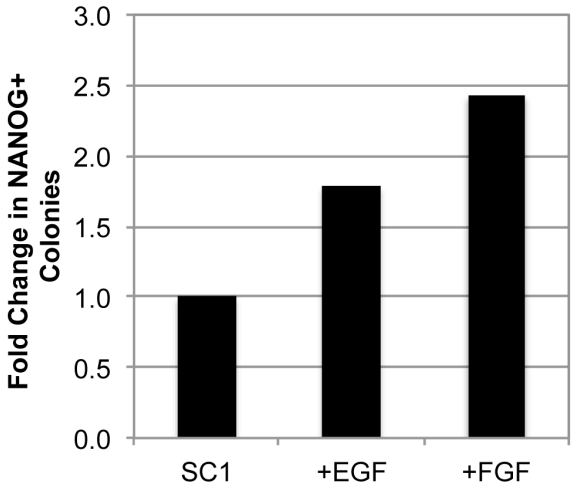

Figure E5. Growth factors may increase the number of NANOG positive colonies in SC1 SKM induced reprogramming. Passage 3 MEFs were reprogrammed with SKM and SC1 was added 3 days post-infection. 5 days post-infection CHIR99021 was added in serum-free media. Medium and small molecules were changed every other day. Cells were analyzed for NANOG expression 9 days post-infection. Cells were analyzed by high-content imaging and analysis. (N=1) Minimum colony size measured was 15,000 μm^2.

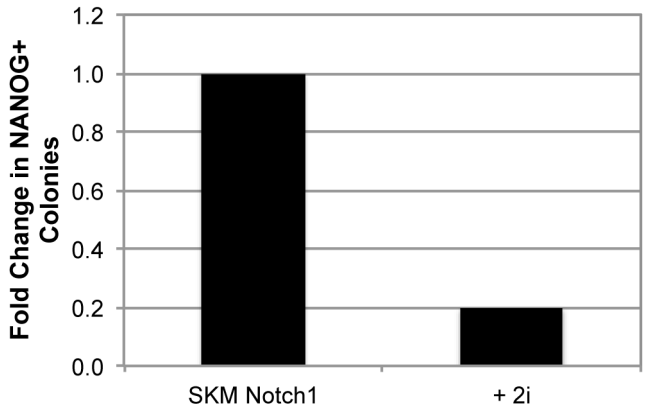

Figure E6. 2i inhibitors hinder constitutively-active *Notch1*-mediated OCT4 replacement. Passage 3 MEFs were reprogrammed with SKM and constitutively-active *Notch1* as previously described. 5 days post-infection CHIR99021 and/or PD 0325901 was added in serum-free medium. Medium and small molecules were changed every day. Cells were analyzed for NANOG expression 12 days post-infection. Cells were analyzed by high-content imaging and analysis. (N=1) Minimum colony size measured was 15,000 μm^2.

Supplemental Tables

Table EI. Genes affecting reprogramming

Group 1 (5)	**Group 2 (12)**
CA *CDC42*	CA *MAP2K3*
CA *NFKBIA*	DN *RHOA*
CA *GNAS*	DN *Akt1*
CA *Notch1*	CA *Camk2a*
CA *Smo*	WT *Camk4*
	CA *CTTNB1*
	CA *Hif1a*
	DN *MAPK3*
	DN *MAPK1*
	CA *GNAI1*
	KD,DN *Gsk3b*
	DN *Gsk3b*

Table EII. Different combinations to replace OSKM

Group 1	**Group 2**	**CA *HRAS***	**FGF**	**CHIR99021 PD 0325901**
MOI 6				
MOI 3	MOI 3			
MOI 3	MOI 3	MOI 1		
MOI 6		MOI 1		
MOI 3	MOI 3		5 ng/μL	3 μM/1 μM
MOI 3	MOI 3	MOI 1	5 ng/μL	3 μM/1 μM

Supplemental Methods

OSKM Replacement Reprogramming

The Group 1 and Group 2 viruses were produced as described in the Methods section. The supernatant was combined, aliquoted, frozen, and titered. 5,000 passage 3 MEFs were plated per condition and after attachment, infected at the MOIs listed in Table EII. The MEF media was changed the following day. The subsequent day, the cells were changed to mouse embryonic stem cell medium. 4 days post-infection the cells were transferred to gelatin-coated plates and passed upon confluency. CHIR99021 and PD 0325901 have been previously described. FGF was used at 5 ng/μL (Peprotech, 100-18B).

APPENDIX F: SUPPLEMENTAL INFORMATION FOR CHAPTER 4

Supplemental Figures

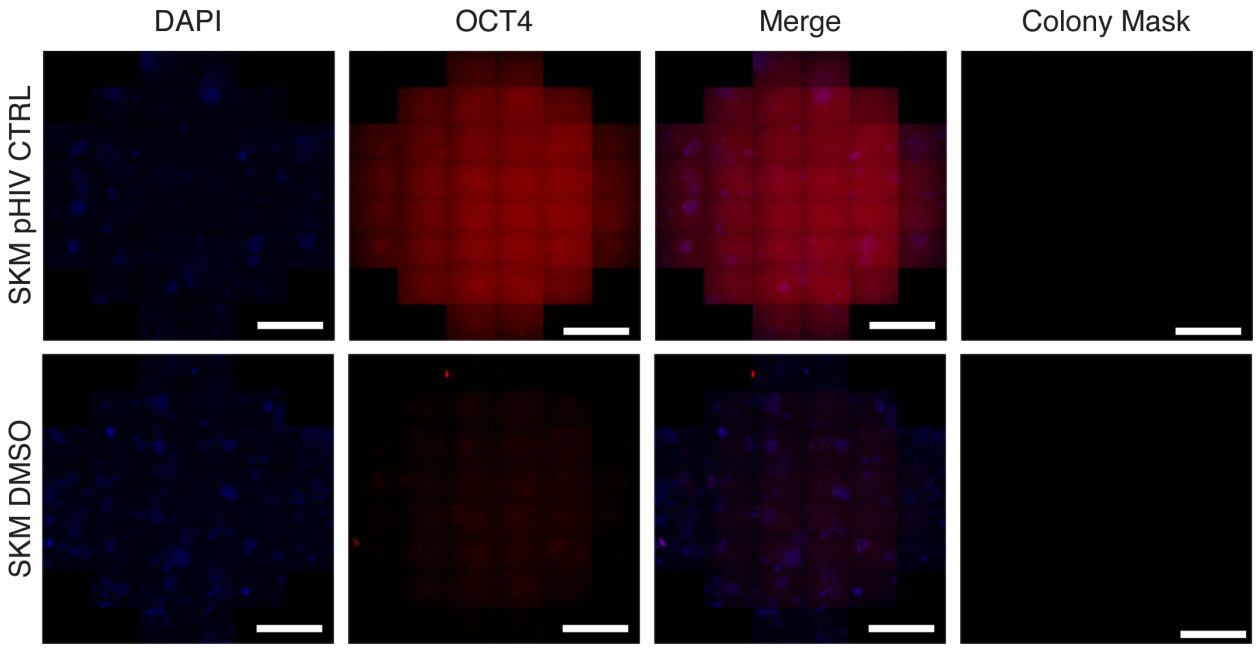

Figure F1. Negative controls have little OCT4 expression. The infection control, pHIV CTRL, and the DMSO only control have no colonies as determined via high-throughput analysis. The minimum colony size measured was 15,000 μm^2. Scale bars are 3 mm.

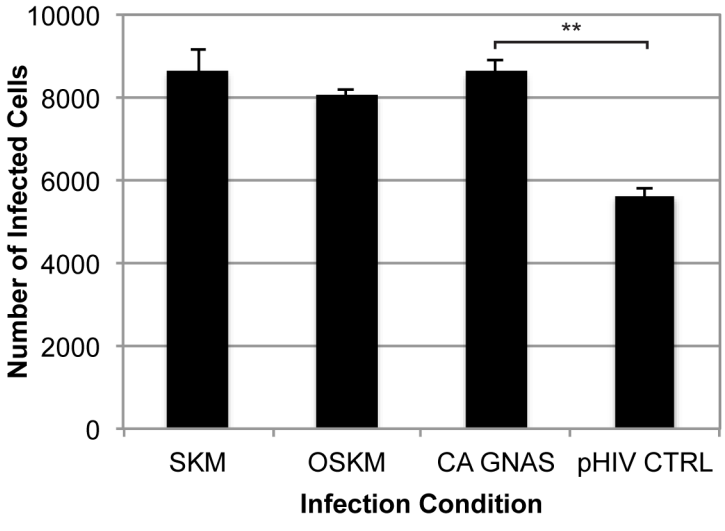

Figure F2. The number of infected cells plated in each condition can be used in determining the efficiency of reprogramming. During the reprogramming efficiency experiment, passage 3 mouse

embryonic fibroblasts were infected with SKM, OSKM, SKM and constitutively-active *GNAS*, or SKM and pHIV CTRL virus. Forty-eight hours post-infection, cells were split onto mitomycin-c treated feeder layers in mESC-FBS media with 022% DMSO. Three wells per condition were plated and fixed eight hours post-passage. The cells were stained for SOX2 expression or SOX2 and GFP, respectively. 80% of the 24 well was imaged by high-content imaging, and the number of infected cells was determined by high-throughput analysis. Statistical significance was measured between SKM-OSKM and constitutively-active *GNAS*-pHIV CTRL using a Student's t-Test (two-tailed, homoscedastic) with ** $p < 0.005$.

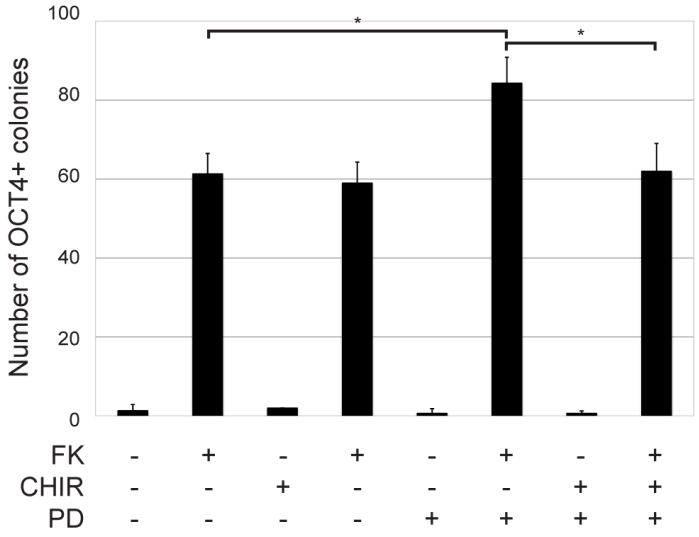

Figure F3. Serum-free conditions and PD 0325901 improve the reprogramming efficiency for OCT4 replacement. All conditions were cultured in KSR-containing medium. The number of OCT4 positive colonies was measured from high-throughput analysis. Statistical significance was measured using a Student's t-Test (two-tailed, homoscedastic) with * $p < 0.05$. Negative controls are $p < 0.005$. The minimum colony size was 15,000 μm^2.

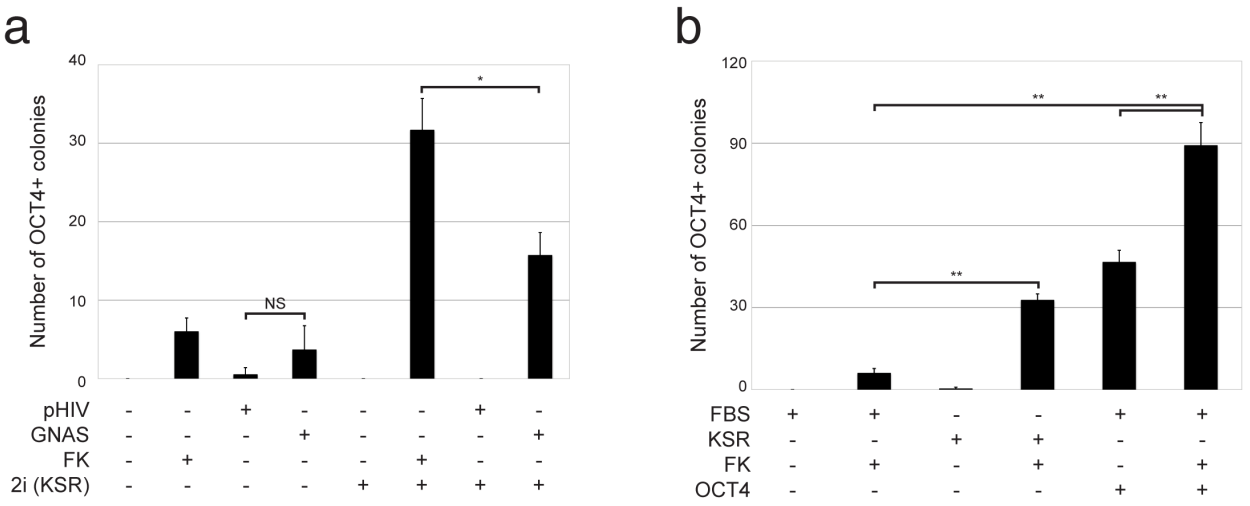

Figure F4. Measuring larger OCT4 colonies results in similar trends in reprogramming efficiency. (a) The number of OCT4 positive colonies measured from high-throughput analysis for constitutively-active *GNAS* and the infection control, pHIV CTRL, and forskolin with SKM. Conditions with and without 2i small molecule inhibitors in serum-free media are shown. (b) The number of OCT4 positive colonies with forskolin, DMSO, and *Oct4* conditions. Statistical significance was measured using a Student's t-Test (two-tailed, homoscedastic) with * $p < 0.05$ and ** $p < 0.005$. Negative controls are $p < 0.005$ unless otherwise noted. The minimum colony size was 30,000 μm^2.

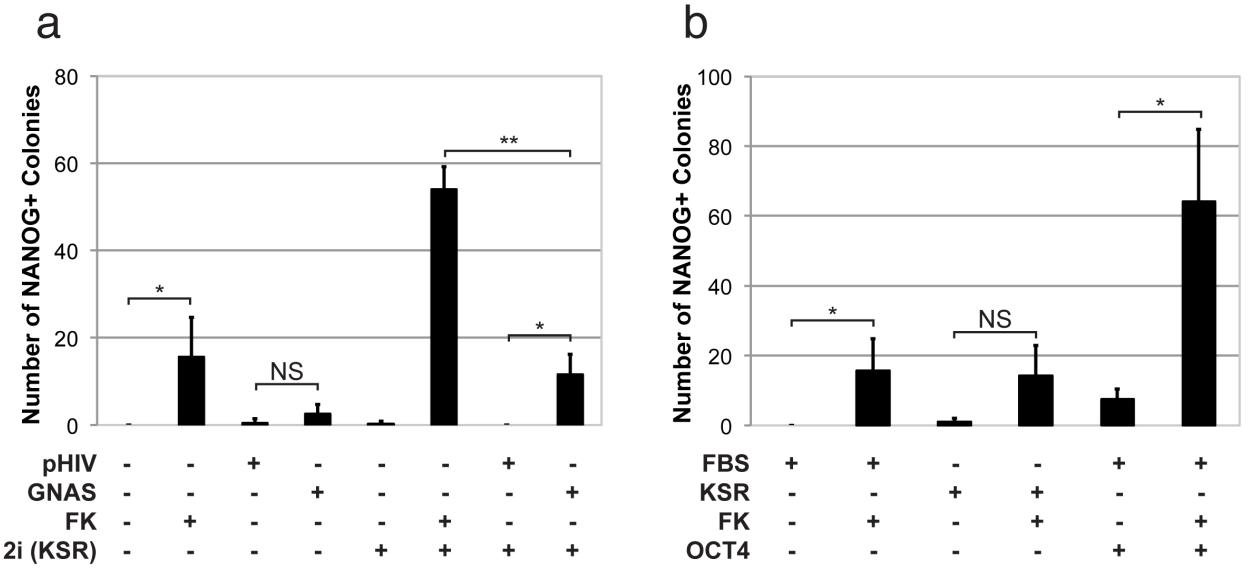

Figure F5. NANOG staining revels similar trends for forskolin conditions, but fewer colonies compared to OCT4 staining. (a) The number of NANOG positive colonies measured from high-throughput analysis for constitutively-active *GNAS* and the infection control, pHIV CTRL and forskolin and SKM only. Conditions with and without 2i small molecule inhibitors in serum-free media are shown. (b) The number of NANOG positive colonies with forskolin, DMSO, and *Oct4* conditions. Statistical significance was measured using a Student's t-Test (two-tailed, homoscedastic) with * $p < 0.05$ and ** $p < 0.005$. Negative controls are $p < 0.005$ unless otherwise noted. The minimum colony size was 15,000 μm^2.

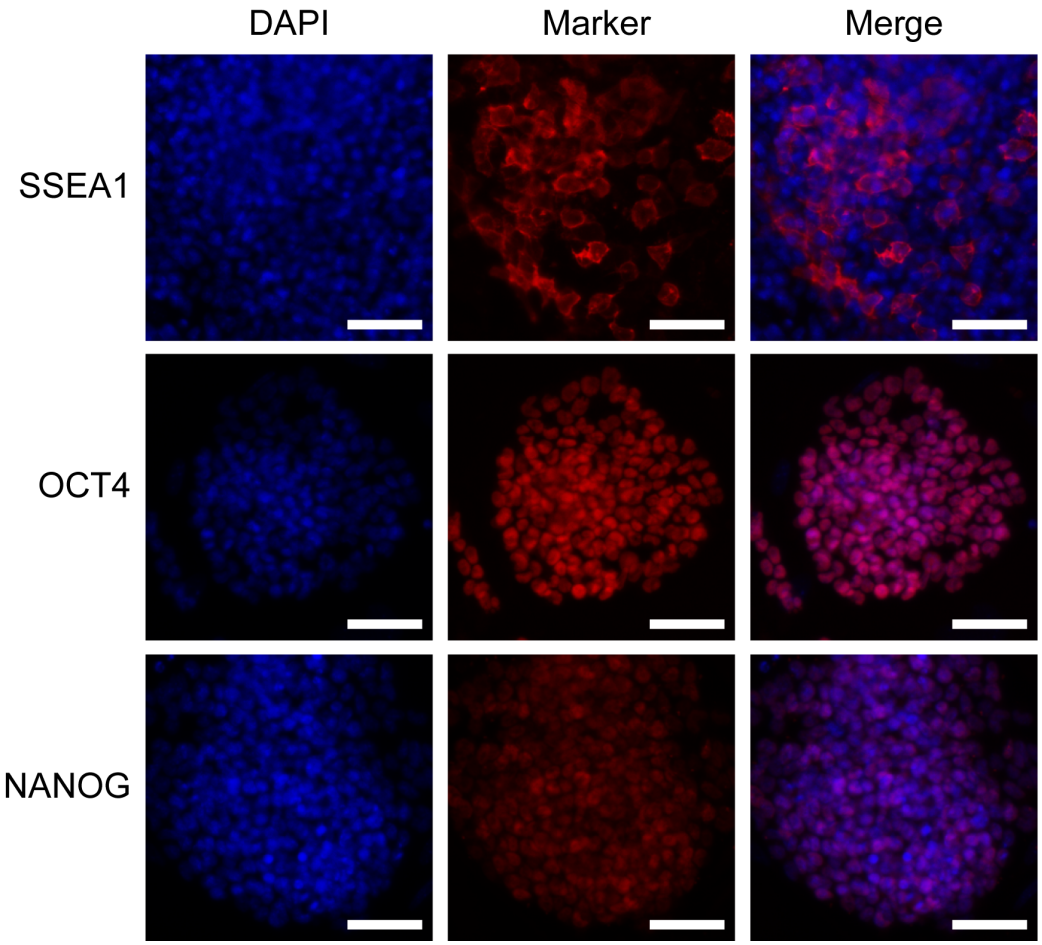

Figure F6. SKM FK 2i-01 cell line expresses pluripotency markers, SSEA1, OCT4, and NANOG. The cell line was imaged seven passages after isolation and four passages in serum containing media without 2i and forskolin. Scale bars are 50 μm.

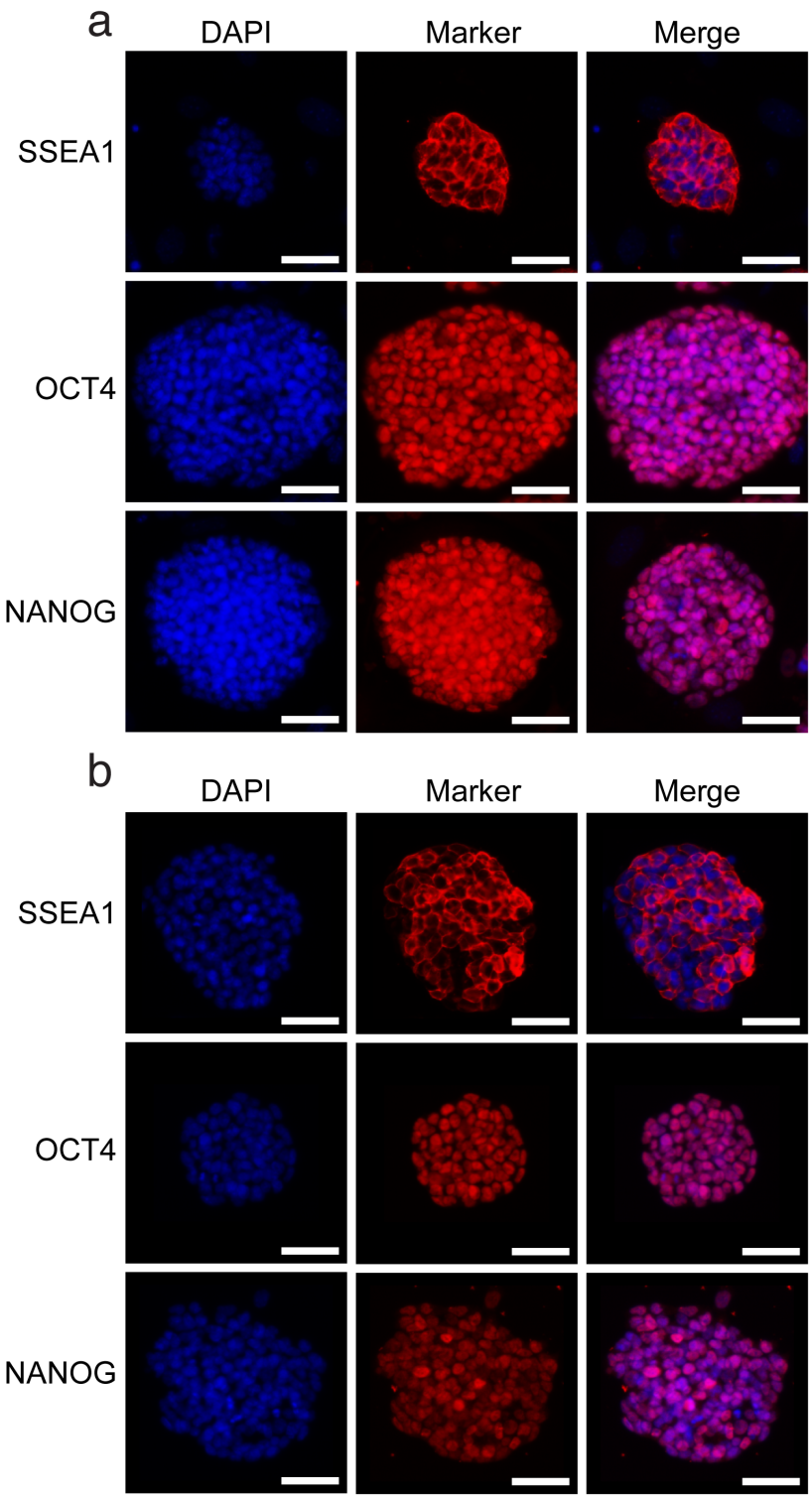

Figure F7. SKM FK 2i-06 cell line expresses pluripotency markers, SSEA1, OCT4, and NANOG in feeder and feeder-free conditions. SKM FK 2i-06 was transitioned to serum without small molecules at two passages post-isolation. (a) SKM FK 2i-06 five passages post-isolation on feeder layers. (b) SKM FK 2i-06 eight passages post-isolation and two passages in feeder free conditions. Scale bars are 50 μm.

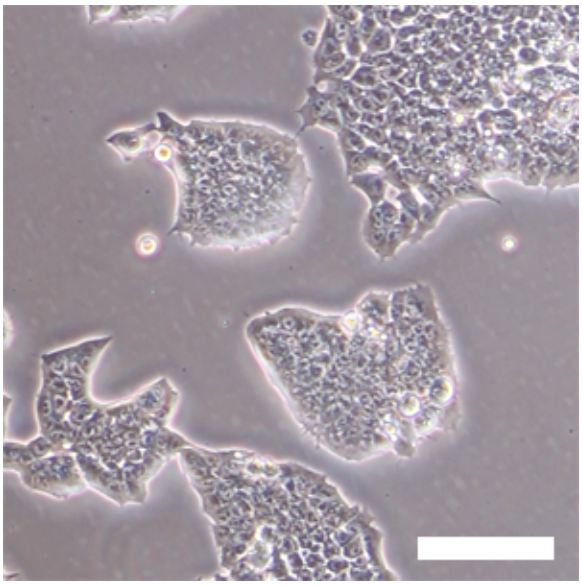

Figure F8. SKM FK 2i-06 maintains embryonic stem cell colony morphology 19 passages after isolation. SKM FK 2i-06 was transferred to feeder free conditions six passages post-isolation. Scale bar is 100 µm.

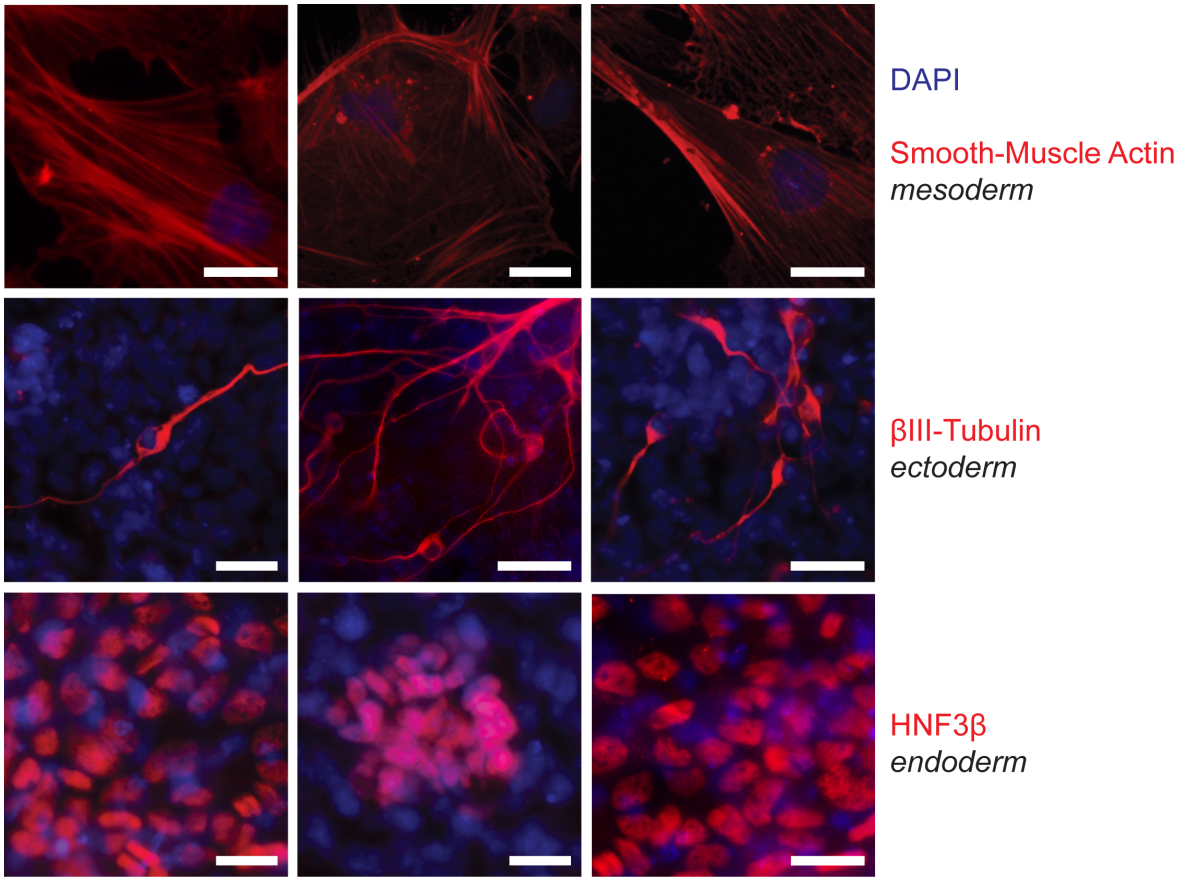

Figure F9. SKM FK 2i-02 produces three germ layers *in vitro*. Images are of different regions expressing smooth-muscle actin, βIII-tubulin, or HNF3β, respectively, in embryoid body outgrowth. Scale bars are 25 µm.

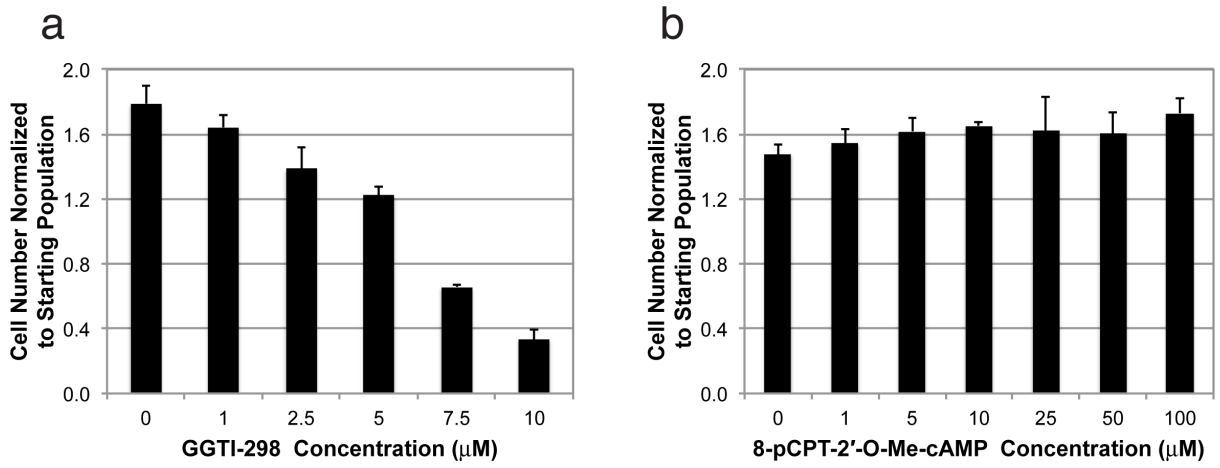

Figure F10. GGTI-298 is toxic to mouse embryonic fibroblasts at higher concentrations. GGTI-298 or 8-pCPT-2'-O-Me-cAMP was added to passage 3 mouse embryonic fibroblasts daily for three days. After 72 hours, the cells were fixed and DAPI was added to visualize the nucleus. High-throughput imaging and analysis was used to count the number of cells in each condition. The number of cells was normalized to the initial number of cells plated.

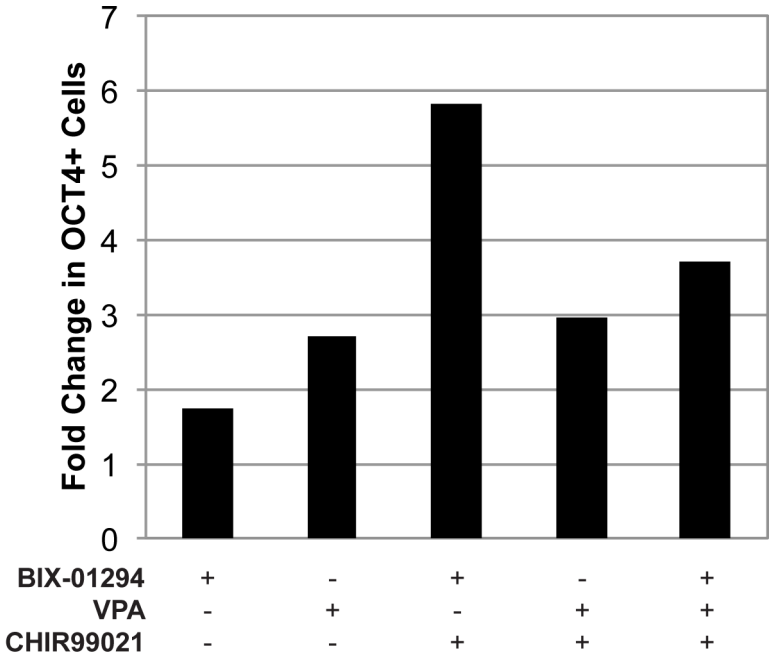

Figure F11. Small molecules increase the number of OCT4 positive cells in adult mouse ear fibroblasts with SKM and forskolin. Each condition is normalized to the control (without forskolin). (N=1) For example, the SKM, forskolin, and BIX-01294 condition is normalized to SKM and BIX-01294 condition. The cells were fixed and stained for OCT4 expression. High-throughput imaging and analysis determined the quantity of OCT4 positive cells. The addition of BIX-01294 and CHIR99021 had the largest increase in the number of OCT4 positive cells.

Supplemental Tables

Table FI. Primers used for qPCR

Gene Name	Primer Sequences	Amplicon Size (bp)	Melting T (°C)	Efficiency (%)	R^2	Water Ct
Internal control						
Hprt[1]	GCTGGTGAAAAGGACCTCT CACAGGACTAGAACACCTGC	249	84.5	91.5, 104.0	0.996, 0.995	37.5
Transgene control						
SKM	CTTTCAGTGCCAGAAGTGTGAC CCCTCACATTGCCAAAAGAC	189	87.5	81.5	0.999	ND
Epithelial genes						
Cdh1[1]	AACAACTGCATGAAGGCGGGAATC CCTGTGCAGCTGGCTCAAATCAAA	246	88.5	74.0	0.996	36.8
Epcam[1]	GCTGGCAACAAGTTGCTCTCTGAA CGTTGCACTGCTTGGCTTTGAAGA	236	89.0	88.0	0.998	ND
Mesenchymal genes						
Cdh2[2]	AATCCCCCCAAGTCCAACATTTC CCGCCGTTTCATCCATACCACAA	189	88.5	88.7	0.999	ND
Slug[2]	CTCCACTCCACTCTCCTTTAC GCTCACATATTCCTTGTCACA	323	93.8	93.8	0.998	41.5
Pluripotency genes						
Oct4[3]	CCAACGAGAAGAGTATGAGGC GTGCTTTTAATCCCTCCTCAG	308	90.5	99.1	0.991	40.8
Klf4[3]	GGCGAGAAACCTTACCACTGT TACTGAACTCTCTCTCCTGGCA	226	90.5	88.9	0.995	41.8
Nanog[3]	CCTCCAGCAGATGCAAGAA GCTTGCACTTCATCCTTTGG	92	83.0	74.8	0.997	ND

ND = Non-detectable

Table FII. Combinations of small molecules for complete factor replacement

		Condition												
Small Molecule	**Concentration**	**1**	**2**	**3**	**4**	**5**	**6**	**7**	**8**	**9**	**10**	**11**	**12**	**13**
± Bay K 8644	2 µM	X			X			X						
2-PCPA	5 µM	X	X	X	X	X	X	X	X	X	X	X	X	X
PD 0325901	1 µM	X	X	X				X	X	X		X		X
CHIR99021	3 µM							X	X	X	X	X	X	X
BIX01294	1 µM	X		X	X		X	X		X	X	X	X	X
VPA	1 mM	X	X	X	X	X	X	X	X	X	X	X	X	X
616452	1 µM		X	X		X	X		X	X				
Kenpaullone	5 µM	X	X	X	X	X	X				X	X	X	X
SC1	300 nM				X	X	X				X	X	X	X
FK	10 µM	X	X	X				X	X	X			X	X

Supplemental Methods

Toxicity Measurements

4,750 passage 3 mouse embryonic fibroblasts were plated in 48 well plates in mouse embryonic stem cell media with GGTI-298 (Santa Cruz Biotech, sc-221673) or 8-pCPT-2'-O-Me-cAMP (Sigma Aldrich, C8988) at various concentrations. The small molecules and media were changed 24 and 48 hours later. 72 hours later, the cells were fixed with 4% paraformaldehyde. The nuclei were stained with DAPI (Invitrogen, 1:2000 dilution). The cells

were imaged with the Molecular Devices ImageXpress Micro and the cell numbers were quantified with MetaXpress software. Cell counts were normalized to the number of initially plated cells.

Mouse Ear Fibroblast Reprogramming

Early passage adult ear fibroblasts were a kind gift of Tim Downing (University of California, Berkeley). The cells were plated into a 24 well plate and a 6 well plate to count the cells after attachment. The following day, the cells were infected with STEMCCA-SKM loxP virus at a calculated MOI of 0.38. Two days post-infection, the cells were plated on mitomycin-c treated feeder layers (GlobalStem, GSC-6101M) with mouse embryonic stem cell medium. Forskolin (10 μM, Enzo Life Sciences, BML-CN100-0010), BIX-01294 (1 μM, Cayman Chemical, 13124), VPA (1 mM, Cayman Chemical, 13033), and CHIR99021 (3 μM, Cayman Chemical, 13122) were added to the respective condition. Media and small molecules were replaced daily. 10 days post-infection, cells were fixed with 4% paraformaldehyde. An anti-Oct4 antibody (Santa Cruz Biotechnology, sc-5279, 1:100 dilution) and a secondary antibody (Invitrogen, A-21235, 1:250 dilution) were used to visualize OCT4 expression. The cells were imaged with the Molecular Devices ImageXpress Micro and the cell numbers were quantified with MetaXpress software. Counts were normalized to their respective negative control.

Complete Factor Replacement with Small Molecules

90,000 passage 3 mouse embryonic fibroblasts were plated in 6 well plates. Two days later, small molecules were added to the serum-containing mouse embryonic stem cell media. ± Bay K 8644 (2 μM, Calbiochem, 196878), 2-PCPA (5 μM, Cayman Chemical, 10010494), BIX-01294 (1 μM, Cayman Chemical, 13124), VPA (1 mM, Cayman Chemical, 13033), 616452 (1 μM, Calbiochem, 616452), kenpaullone (5 mM, Cayman Chemical, 13124), SC1 (300 nM, Cayman Chemical, 10009557), and forskolin (10 μM, Enzo Life Sciences, BML-CN100-0010), were added to the respective conditions. 72 hours later, the media was replaced with serum-free embryonic stem medium and CHIR99021 (3 μM, Cayman Chemical, 13122) and PD 0325901 (1 μM, Cayman Chemical, 13034) were added to the respective conditions. Media was changed daily.

References

1. Samavarchi-Tehrani, P. et al. Functional genomics reveals a BMP-driven mesenchymal-to-epithelial transition in the initiation of somatic cell reprogramming. *Cell Stem Cell* 7, 64-77 (2010).
2. Yang, P. et al. RCOR2 is a subunit of the LSD1 complex that regulates ESC property and substitutes for SOX2 in reprogramming somatic cells to pluripotency. *Stem Cells* 29, 791-801 (2011).
3. Kaji, K. et al. Virus-free induction of pluripotency and subsequent excision of reprogramming factors. *Nature* (2009).

APPENDIX G: SUPPLEMENTAL PROTOCOLS

General Protocol for Reprogramming

Materials

- Glasgow Minimum Essential Medium, With sodium bicarbonate, without L-glutamine, liquid, sterile-filtered, Sigma Aldrich, G5154-500ML
- Dulbecco's Modified Eagle Medium (D-MEM) (1X), liquid (high glucose), Invitrogen, 11960-051
- GlutaMAX™-I Supplement, Invitrogen, 35050-061
- MEM Sodium Pyruvate Solution 100 mM (100X), Invitrogen, 11360-070
- MEM Non-Essential Amino Acids Solution 10 mM (100X), Invitrogen, 11140-050
- Penicillin-Streptomycin, liquid (100 U, 100 μg/mL), Invitrogen, 15140-148
- 2-Mercaptoethanol (55 mM), liquid, Invitrogen, 21985-023
- ESGRO® (LIF), 10^7 units, Millipore, ESG1107
- Thermo Scientific HyClone* ES Cell Screened Fetal Bovine Serum (FBS), Fisher, SH3007003E
- EmbryoMax® 0.1% Gelatin Solution, Millipore, ES-006-B
- CF-1 MEF 7M Mito-C, GlobalStem, GSC-6101M
- Phosphate-Buffered Saline, 1X, Cellgro, 21-040-CV
- Trypsin EDTA 1X, 0.25% Trypsin/2.21 mM EDTA in HBSS without sodium bicarbonate, calcium and magnesium, Cellgro, 25-053-CI

Solutions and Media

MEF medium (250 mL, DMEM, high glucose + 10% FBS + 1% P/S + 1% GlutaMAX)

In tissue culture hood, add DMEM, high glucose to a 0.22 bottle-top filter on orange cap bottle (no vacuum) to cover membrane. Add 2.5 mL of GlutaMAX and Pen/Strep. Add 25 mL FBS. Add remaining DMEM to 250 mL. Vacuum filter, and store at 4°C (good for one month with FBS).

mESC-DMEM based for feeder layers (160 mL, DMEM, high glucose + 15% FBS + 0.5% P/S + 1% GlutaMAX + 1% Sodium Pyruvate + 1% MEM NEAA + 0.18% 2-mercaptoethanol + 1000 U/mL LIF)

In tissue culture hood, add 30 mL DMEM, high glucose to a 0.22 bottle-top filter on orange cap bottle (no vacuum). Add 1.6 mL each of GlutaMAX, sodium pyruvate, and MEM NEAA. Add 0.8 mL of Pen/Strep. Add 290 μL 2-mercaptoethanol. Add 24 mL FBS. Add remaining DMEM (100 mL). Vacuum filter, aliquot media (40mL), and store at 4°C (good for one month with FBS). Add LIF to media in conical vial before adding the media to cells (good for one week with LIF).

mESC-GMEM based for feeder-free (160 mL, DMEM, high glucose + 15% FBS + 0.5% P/S + 1% GlutaMAX + 1% Sodium Pyruvate + 1% MEM NEAA + 0.18% 2-mercaptoethanol + 1000 U/mL LIF)
In tissue culture hood, add 30 mL GMEM, high glucose to a 0.22 bottle-top filter on orange cap bottle (no vacuum). Add 1.6 mL each of GlutaMAX, sodium pyruvate, and MEM NEAA. Add 0.8 mL of Pen/Strep. Add 290 µL 2-mercaptoethanol. Add 24 mL FBS. Add remaining GMEM (100 mL). Vacuum filter, aliquot media (40mL), and store at 4°C (good for one month with FBS). Add LIF to media in conical vial before adding the media to cells (good for one week with LIF).

Reprogramming
Day -1
Plate P3 129 MEFs in TCPS plate (aim for 7,000-10,000+ cells/cm^2)

Day 0
Infect cells with concentrated virus (~MOI of 0.1-0.4)

Day 1
Change media with MEF media (do not tilt plate)
If passing to MEF feeder layers

1. Coat wells with 0.1% gelatin for approximately 20 minutes (just enough to cover surface)
2. Retrieve vial of feeder layers from liquid nitrogen. Loosen cap to remove any liquid nitrogen that has seeped into the vial.
3. Thaw cells by incubating (and agitating) vial in 37°C water bath. Be careful to not submerge cap of the vial under water. Once a small crystal remains, spray the vial down with 70% ethanol, and bring into hood.
4. Gently pipette up and down with a P1000 and add the 1 mL cell suspension to a 50 mL conical vial.
5. Add 10 mL of MEF media slowly and gently down the side of the conical vial. Tap the vial while adding the media to mix the cell suspension/media. This should take approximately 2 minutes.
6. Pipette the cell suspension into a 15 mL conical vial.
7. Spin down cells at 1200 RPM for 2.5 minutes
8. One vial of MEFs is good for 5-10 cm plates or 6-24 well plates. Resuspend the cell pellet in 6 mL (for 24 wells). Add 1 mL cell suspension to 11 mL MEF media in a 15 mL conical vial.
9. Remove the gelatin from the well plate
10. Add 500 µL diluted cell suspension to each well (for 24 well plate)
11. Rock the plate forward/backward – side to side to distribute cells evenly
12. Incubate at 37°C with 5% CO_2

Day 2

1. If not passing to feeder layers, coat wells with 0.1% gelatin for at least 20 minutes at room temperature
2. Pass cells into well plate
    1. Wash the cells with PBS

2. Add trypsin to cover well
3. Incubate for 5-10 minutes at 37˚C
4. Add mESC media to stop trypsin
5. Pipette up and down with P200. Aliquot into microcentrifuge tube. This can be split into three wells if testing in triplicate
6. Mix and pipette 200 µL into well plate with feeder layers or remove gelatin and pipette onto well plate if not using feeder layers
7. Rock plate back and forth, side to side, and place in incubator

Day 4

Change media with respective mESC media (do not tilt plate).

Day 6, 8, 10, etc…

Change media with respective mESC media. Media can be changed every day instead of every other day.

Mouse iPSC Colony Selection

Materials

- Dulbecco's Modified Eagle Medium (D-MEM) (1X), liquid (high glucose), Invitrogen, 11960-051
- GlutaMAX™-I Supplement, Invitrogen, 35050-061
- MEM Sodium Pyruvate Solution 100 mM (100X), Invitrogen, 11360-070
- MEM Non-Essential Amino Acids Solution 10 mM (100X), Invitrogen, 11140-050
- Penicillin-Streptomycin, liquid (100 U, 100 µg/mL), Invitrogen, 15140-148
- 2-Mercaptoethanol (55 mM), liquid, Invitrogen, 21985-023
- ESGRO® (LIF), 10^7 units, Millipore, ESG1107
- Thermo Scientific HyClone* ES Cell Screened Fetal Bovine Serum (FBS), Fisher, SH3007003E
- KnockOut™ Serum Replacement, Invitrogen, 10828-028
- EmbryoMax® 0.1% Gelatin Solution, Millipore, ES-006-B
- CF-1 MEF 7M Mito-C, GlobalStem, GSC-6101M
- Phosphate-Buffered Saline, 1X, Cellgro, 21-040-CV
- Trypsin EDTA 1X, 0.25% Trypsin/2.21 mM EDTA in HBSS without sodium bicarbonate, calcium and magnesium, Cellgro, 25-053-CI
- BD Falcon™ Multiwell Plates. Tissue-culture treated polystyrene, flat bottom, with low-evaporation lid, BD Biosciences
- EVOS xl core microscope, AMG
- 21 G x 1 1/2 in. BD PrecisionGlide™ Needles, BD Biosciences, 305167
- 3 mL BD Luer-Lok Tip Syringes Without Needles, BD Biosciences, 309585
- P20, P200 pipettes
- P200 pipette tips
- Disposable, sterile 15 and 50 mL conical vials
- Disposable, sterile microcentrifuge tubes

Media

mESC (FBS) medium (160 mL, DMEM, high glucose + 15% FBS + 0.5% P/S + 1% GlutaMAX + 1% Sodium Pyruvate + 1% MEM NEAA + 0.18% 2-mercaptoethanol + 1000 U/mL LIF)

In tissue culture hood, add 30 mL DMEM, high glucose to a 0.22 bottle-top filter on orange cap bottle (no vacuum). Add 1.6 mL each of GlutaMAX, sodium pyruvate, and MEM NEAA. Add 0.8 mL of Pen/Strep. Add 290 µL 2-mercaptoethanol. Add 24 mL FBS. Add remaining DMEM (100 mL). Vacuum filter, aliquot media (40mL), and store at 4°C (good for one month with FBS). Add LIF to media in conical vial before adding the media to cells (good for one week with LIF).

mESC (KSR) medium (160 mL, DMEM, high glucose + 15% KSR + 0.5% P/S + 1% GlutaMAX + 1% Sodium Pyruvate + 1% MEM NEAA + 0.18% 2-mercaptoethanol + 1000 U/mL LIF)

In tissue culture hood, add 30 mL DMEM, high glucose to a 0.22 bottle-top filter on orange cap bottle (no vacuum). Add 1.6 mL each of GlutaMAX, sodium pyruvate, and MEM NEAA. Add 0.8 mL of Pen/Strep. Add 290 µL 2-mercaptoethanol. Add 24 mL KSR. Add remaining DMEM (100 mL). Vacuum filter, aliquot media (40mL), and store at 4°C (good for one month

with FBS). Add LIF to media in conical vial before adding the media to cells (good for one week with LIF).

MEF medium (250 mL, DMEM, high glucose + 10% FBS + 1% P/S + 1% GlutaMAX)
In tissue culture hood, add DMEM, high glucose to a 0.22 bottle-top filter on orange cap bottle (no vacuum) to cover membrane. Add 2.5 mL of GlutaMAX and Pen/Strep. Add 25 mL FBS. Add remaining DMEM to 250 mL. Vacuum filter, and store at 4°C (good for one month with FBS).

Protocol
Preparing MEF feeder layers

1. Coat a 48 well plate with 0.1% gelatin for approximately 20 minutes (a few drops – just enough to cover surface).
2. Retrieve vial of feeder layers from liquid nitrogen. Loosen cap to remove any liquid nitrogen that has seeped into the vial.
3. Thaw cells by incubating (and agitating) vial in 37°C water bath. Be careful to not submerge cap of the vial under water. Once a small crystal remains, spray the vial down with 70% ethanol, and bring into hood.
4. Gently pipette up and down with a P1000 and add the 1 mL cell suspension to a 50 mL conical vial.
5. Add 10 mL of MEF media slowly and gently down the side of the conical vial. Tap the vial while adding the media to mix the cell suspension/media. This should take approximately 2 minutes.
6. Pipette the cell suspension into a 15 mL conical vial.
7. Spin down cells at 1200 RPM for 2.5 minutes
8. One vial of MEFs is good for 5-10 cm plates or 6-48 well plates. Resuspend the cell pellet in 6 mL (for 48 wells). Add 1 mL cell suspension to 11 mL MEF media in a 15 mL conical vial.
9. Aspirate 24 wells on the 48 well plate.
10. Add 250 µL/well, doing only 4 wells at a time, and mixing thoroughly between each batch.
11. Repeat Steps 8-9 for the remaining 24 wells.
12. Shake the plate forward/backward – side to side to distribute cells evenly.
13. Incubate at 37°C with 5% CO_2 for at least 24 hours or up to 10 days.

Picking colonies (in the stem cell center – contact Mary West at mwest@berkeley.edu)

1. Spray down the microscope with 70% ethanol. Wipe down the surface with kimwipes.
2. With the video screen down, UV the microscope for 20 minutes.
3. Once the microscope is sterilized, turn on the blower and light for the hood. Wait a few minutes for the airflow to stabilize.
4. Aspirate MEF media off MEF feeder layers from Step 12 and add 200 µL mESC media (FBS or KSR depending on cell type). Incubate at 37°C with 5% CO_2 until the feeder layers are needed.
5. Set up microcentrifuge tubes with trypsin. Add 25 µL trypsin to 10 microcentrifuge tubes. Label the tubes with clone # (1, 2, 3…)
6. Aspirate the media from the mESC/miPS cells.

7. Wash the cells with PBS.
8. Aspirate the PBS and fresh PBS to the cells.
9. Pick as many colonies as you can within 10-15 minutes. To start, find a good colony that is isolated and not close to other colonies. The larger the colony, the easier it is to select. Try for 5 different colonies.
10. Place a 21-gauge needle on a 3 mL syringe barrel. Use the needle to score the area around the colony – this will cut the colony off the MEF feeder layer. Discard the needle, but the syringe barrel can be used with other colonies.
11. Use a P200 pipette to nudge the colony off the plate if it has not detached already.
12. With a P20 pipette set at 20 µL, align the pipette tip to collect the colony. I recommend stabilizing the pipette with the left hand.
13. Check to see if the colony is in the pipette. If it is, pipette the colony into the first microcentrifuge tube with trypsin to break apart the colony. Check to make sure the colony goes into the trypsin and is not attached to the pipette tip. Start a timer.
14. Discard the pipette tip. With a new 21-gauge needle repeat Steps 10-13. Select as many colonies as possible until the timer reaches 10 minutes.
15. Pipette the first colony up and down with a P20 pipette to achieve a single cell suspension.
16. Add 100 µL mESC media to dilute the trypsin.
17. Retrieve the 48 well plate with the MEF feeder layers.
18. Using a P200 pipette set at 200, pipette up and down and add the cell suspension to a well of the 48 well plate. Mark the well with the date and name of the clone.
19. Repeat Steps 15-16, 18 for the remaining colonies.
20. Incubate the clones 37°C with 5% CO_2 changing media daily until colonies are confluent and ready to pass to a new plate.
21. Aspirate the PBS off the plate from which colonies were selected.
22. Add fresh mESC media to plate and incubate at 37°C with 5% CO_2.
23. Allow the plate to recover for 15-30 minutes before selecting more colonies.

Mouse iPS Cell Culturing Protocol

Materials

- Dulbecco's Modified Eagle Medium (D-MEM) (1X), liquid (high glucose), Invitrogen, 11960-051
- GlutaMAX™-I Supplement, Invitrogen, 35050-061
- MEM Sodium Pyruvate Solution 100 mM (100X), Invitrogen, 11360-070
- MEM Non-Essential Amino Acids Solution 10 mM (100X), Invitrogen, 11140-050
- Penicillin-Streptomycin, liquid (100 U, 100 µg/mL), Invitrogen, 15140-148
- 2-Mercaptoethanol (55 mM), liquid, Invitrogen, 21985-023
- ESGRO® (LIF), 10^7 units, Millipore, ESG1107
- Thermo Scientific HyClone* ES Cell Screened Fetal Bovine Serum (FBS), Fisher, SH3007003E
- EmbryoMax® 0.1% Gelatin Solution, Millipore, ES-006-B
- CF-1 MEF 7M Mito-C, GlobalStem, GSC-6101M
- Phosphate-Buffered Saline, 1X, Cellgro, 21-040-CV
- Trypsin EDTA 1X, 0.25% Trypsin/2.21 mM EDTA in HBSS without sodium bicarbonate, calcium and magnesium, Cellgro, 25-053-CI
- BD Falcon™ Multiwell Plates. Tissue-culture treated polystyrene, flat bottom, with low-evaporation lid, BD Biosciences
- P1000 pipette
- P100 pipette tips
- Disposable, sterile 15 mL conical vial

Media

mESC medium (160 mL, DMEM, high glucose + 15% FBS + 0.5% P/S + 1% GlutaMAX + 1% Sodium Pyruvate + 1% MEM NEAA + 0.18% 2-mercaptoethanol + 1000 U/mL LIF)

In tissue culture hood, add 30 mL DMEM, high glucose to a 0.22 bottle-top filter on orange cap bottle (no vacuum). Add 1.6 mL each of GlutaMAX, sodium pyruvate, and MEM NEAA. Add 0.8 mL of Pen/Strep. Add 290 µL 2-mercaptoethanol. Add 24 mL FBS. Add remaining DMEM (100 mL). Vacuum filter, aliquot media (40mL), and store at 4°C (good for one month with FBS). Add LIF to media in conical vial before adding the media to cells (good for one week with LIF).

MEF medium (250 mL, DMEM, high glucose + 10% FBS + 1% P/S + 1% GlutaMAX)

In tissue culture hood, add DMEM, high glucose to a 0.22 bottle-top filter on orange cap bottle (no vacuum) to cover membrane. Add 2.5 mL of GlutaMAX and Pen/Strep. Add 25 mL FBS. Add remaining DMEM to 250 mL. Vacuum filter, and store at 4°C (good for one month with FBS).

mESC Freezing Media (40% ES (FBS) Media, 50% FBS, 10% DMSO) – based on Millipore's ESC freezing conditions

In tissue culture hood, add 4 mL mESC media, 5 mL FBS, and 1 mL DMSO. Mix and store at 4°C until thoroughly chilled. (good for one day).

Protocol

Preparing MEF feeder layers

1. Coat 13-6 cm or 5-10 cm tissue culture dishes with 0.1% gelatin for approximately 20 minutes (just enough to cover surface). The following protocol will be for maintaining iPSCs on 6 cm dishes. Scale appropriately for 10 cm or tissue culture plates.
2. Retrieve vial of feeder layers from liquid nitrogen. Loosen cap to remove any liquid nitrogen that has seeped into the vial.
3. Thaw cells by incubating (and agitating) vial in 37°C water bath. Be careful to not submerge cap of the vial under water. Once a small crystal remains, spray the vial down with 70% ethanol, and bring into hood.
4. Gently pipette up and down with a P1000, and add the 1 mL cell suspension to a 50 mL conical vial.
5. Add 10 mL of MEF media slowly and gently down the side of the conical vial. Tap the vial while adding the media to mix the cell suspension/media and dilute out the DMSO. This should take approximately 2 minutes.
6. Pipette the cell suspension into a 15 mL conical vial.
7. Spin down cells at 1200 RPM for 2.5 minutes
8. Remove the gelatin from the 6 cm dishes. Add 3 mL MEF media gently down the side of the dish.
9. One vial of MEFs is good for 13-6 cm plates. Resuspend the cell pellet in 13 mL. Add 1 mL cell suspension per 6 cm dish.
10. Rock the plate forward/backward – side to side to distribute cells evenly.
11. Incubate at 37°C with 5% CO_2 for at least 8 hours or up to 10 days.

Passing miPSCs in 6cms

1. Wash miPSCs with 2 mL PBS.
2. Aspirate the PBS, and add 385 µL trypsin-EDTA. Accutase can be substituted for trypsin, but the cells must be pelleted after the incubation. Accutase is a different enzyme used on sensitive cell types for passage. Using Accutase may decrease the occurrence of genomic mutations due to the enzymatic passage with trypsin.
3. Incubate the cells in trypsin-EDTA for 2-5 minutes at 37°C until gentle shaking of the plate releases the cells from the plate surface.
4. Pipette up and down with a P1000 (set on 385 µL) to achieve a single cell suspension.
5. Add 1 mL mESC medium. Pipette up and down with a P1000 pipette and collect in a 15 mL tube.
6. Spin down cells at 1200 RPM for 2.5 minutes. This will help remove dying MEF feeder layers.
7. Remove the MEF media from the MEF feeder layers while the cells are being pelleted in the centrifuge. Aspirate off the media and add 4 mL mESC media gently down the side. Label the plate with name, date, cell line, and passage number.
8. miPSCs should be passed every 2-3 days at a passage ratio of 1:10-1:15. I usually resuspend the cells in 3 mL of mESC media and add 200 µL cell suspension to the 6 cm dish (1:15). To be more accurate, cell counts can be done. Plate 9000-1.8x10^4 cells/cm^2 or 1.9-3.8x10^5 cells/6 cm. Once the cells are confluent, which is approximately every 2-3 days, pass the cells.

9. Incubate at 37°C with 5% CO_2 for 2-3 days until confluent. Confluency is when colonies take up 50-60% of the plate and are not touching each other. If the cells are over confluent, cells can be passed at really high passage ratios as mouse ES cells grow best when they are plated as single cells. For the best recovery, count cells as specified in Step 8.

Freezing miPSCs from 6cms

1. Prepare freezing vials by writing cell type, passage number (passage number when thawed, i.e. add one to current passage number), date, and size and number dishes to thaw into (if other than 1) on the vials.
2. Prepare freezing medium. Add 1 mL DMSO to 4 mL of ES (FBS) medium and 5 mL of FBS. This should be cold before being added to the cells. DMSO will incur a heat of mixing, so give at least 20 minutes to cool down at 4°C.
3. Wash miPSCs with 2 mL PBS.
4. Aspirate the PBS, and add 385 µL trypsin-EDTA. Accutase can be substituted for trypsin, but the cells must be pelleted after the incubation. Accutase is a different enzyme used on sensitive cell types for passage. Using Accutase may decrease the occurrence of genomic mutations due to the enzymatic passage with trypsin.
5. Incubate the cells in trypsin-EDTA for 2-5 minutes at 37°C until gentle shaking of the plate releases the cells from the plate surface.
6. Pipette up and down with a P1000 (set on 385 µL) to achieve a single cell suspension.
7. Add 1 mL mESC medium. Pipette up and down with a P1000 pipette and collect in a 15 mL tube.
8. Spin down cells at 1200 RPM for 2.5 minutes. This will help remove dying MEF feeder layers.
9. Resuspend the cells in mESC media. Use a cell count to determine the total number of cells. For each vial, freeze down twice as many cells as you would during normal passage. e.g. freeze 1.8-3.6x10^4 cells/cm^2 or 3.8-7.6x10^5 cells/6 cm.
10. Spin down cells at 1200 RPM for 2.5 minutes.
11. Resuspend the cells in cold freezing media (0.5-1 mL/vial to give the cell counts found in Step 9).
12. Aliquot 0.5-1 mL of cell suspension into one freezing vial.
13. Tighten cap and move to -80°C ASAP – use a freezing container that allows for -1°C/min or Styrofoam container.
14. After 24 hours, move to liquid nitrogen ASAP (move within two weeks).

Immunocytochemistry Protocol (Pluripotency and Differentiation Markers)

Solutions

Internal Marker Blocking Buffer: PBS with 5% serum (from secondary host), 2% BSA, 0.2% Triton X-100. 2% Triton X-100 stock: add 400 µL Triton X-100 to 19.6 mL PBS, mix by pipetting. Weigh out 0.4g BSA. Add 2 mL of 10X Triton X-100, 1 mL appropriate serum (usually goat or donkey), and add PBS to 20 mL. Mix by pipetting. Store blocking buffer at 4°C. Buy serum in 10 mL bottles, thaw, and make 1 mL aliquots in amber tubes. Store aliquoted serum at -20°C.

External Marker Blocking Buffer: PBS with 5% serum, 2% BSA. Weigh out 0.4g BSA. Add 1 mL appropriate serum (usually goat or donkey) and PBS to 20 mL. Mix by pipette. Store blocking buffer at 4°C. Buy serum in 10 mL bottles, thaw, and make 1 mL aliquots in amber tubes. Store aliquoted serum at -20°C.

PBST (0.2%): PBS with 0.2% Triton X-100. Add 2 mL of 10X Triton X-100 to 18 mL PBS. Store at 4°C.

PBST (0.1%): PBS with 0.2% Triton X-100. Add 1 mL of 20X Triton X-100 to 19 mL PBS. Store at 4°C.

Secondary Antibody Buffer: PBS with BSA. Weigh out 0.4g BSA and add PBS to 20 mL. Mix by pipette. Store buffer at 4°C.

Antibodies

Primary and Secondary Antibodies (appropriate dilutions)

Primary antibodies are usually stored at 4°C but can be aliquoted and stored at -20°C. Check manufacturer's suggestions for both storage conditions and dilutions. Secondary antibodies are usually aliquoted and stored at -20°C but can be aliquoted and stored at -80°C. Alexa Fluor antibodies tend to be stable at 4°C for >2 years. Check manufacturer's suggestions for both storage conditions and dilutions.

- Mouse monoclonal IgG2b anti-Oct4, Oct-3/4 (C-10), Santa Cruz Biotechnology, sc-5279, 200 µg/ml, 1 mL, dilute 1:200
- Alexa Fluor® 546 Goat Anti-Mouse IgG (H+L), Invitrogen, A-11003, 2 mg⁄mL, 0.5 mL, dilute 1:500-1:1000 (1:1000 for new antibodies)
- Rabbit polyclonal IgG anti-Nanog, Abcam, ab70482, 1 mg/mL, 100 µL, dilute 1:250
- Alexa Fluor® 594 Goat Anti-Rabbit IgG (H+L), Invitrogen, A-11012, 2 mg⁄mL, 0.5 mL, dilute 1:500-1:1000 (1:1000 for new antibodies)
- Mouse monoclonal IgM anti-Stage-Specific Embryonic Antigen-1, clone MC-480, Millipore, MAB4301, 1 mg/mL, 100 µL, dilute 1:200 **external marker**
- Alexa Fluor® 546 goat anti-mouse IgM (µ chain), Invitrogen, A-21045, 2 mg/mL, 0.5 mL, dilute 1:500-1:1000 (1:1000 for new antibodies)
- Mouse monoclonal IgG2a Anti-α-Smooth Muscle Actin, clone 1A4, ascites fluid, Sigma Aldrich, A2547, 200 µL, dilute 1:500

- Alexa Fluor® 546 Goat Anti-Mouse IgG (H+L), Invitrogen, A-11003, 2 mg⁄mL, 0.5 mL, dilute 1:500-1:1000 (1:1000 for new antibodies)
- Rabbit polyclonal IgG Anti-HNF3β/FOXA2, Millipore, 07-633, 1 mg/mL, 100 µL, dilute 1:500
- Rabbit monoclonal IgG1 Anti-Neuronal Class III β-Tubulin (TUJ1), Covance, MRB-435P, 1 mg/mL, 100 µL, dilute 1:500
- Alexa Fluor® 594 Goat Anti-Rabbit IgG (H+L), Invitrogen, A-11012, 2 mg⁄mL, 0.5 mL, dilute 1:500-1:1000 (1:1000 for new antibodies)

Protocol

For 24 Well Plates

1. Wash the cells with PBS.
2. **Fixation**. Add 500 µL 4% PFA, and incubate at RT for 15 minutes. If the protein is light sensitive (e.g. GFP), cover plate with foil during all incubation steps.
3. Aspirate liquid off well. Add 500 µL fresh PBS. Rock plate to mix. Repeat two more times. If storing overnight to one week, aspirate all liquid off the plate and add 500 µL PBS to cover. Store at 4°C.
4. **Blocking**. Remove all liquid. Add *Appropriate Blocking Buffer*. Incubate for 20 minutes on a belly-button rocker at low speed.
5. **Preparing primary**. Pipette primary antibody gently to mix. Do not remove the few microliters in the bottom of the tube. Dilute primary antibody in *Appropriate Blocking Buffer*.
6. **Primary antibody**. Remove all liquid. Add 200 µL of appropriate primary antibody diluted for 1 hour on belly-button rocker at low speed at RT.
7. Store plates at 4C overnight (not on rocker) or proceed with Step 8.
8. Remove primary antibody. Add 500 µL *PBST (0.2%)* or PBS (for external markers).
9. Remove all liquid. Add 500 µL *PBST (0.1%)* or PBS (for external markers). Incubate plate for 5 minutes on belly button rocker at RT.
10. Remove all liquid. Repeat Step 9 two times.
11. **Preparing secondary**. Spin down secondary antibody briefly. Do not remove the few microliters in the bottom of the tube. Dilute secondary antibody in *Secondary Antibody Buffer*.
12. **Secondary antibody**. Remove all liquid. Add 200 µL of diluted secondary for 2 hours on belly-button rocker at low speed at RT. Cover plate with foil during all incubations after addition of secondary antibody (light sensitive).
13. **Preparing DAPI**. Dilute DAPI in PBS at 1:1000. Vortex to mix completely.
14. Remove all liquid. Add 500 µL fresh PBS. Incubate plate for 5 minutes on belly button rocker at RT.
15. **DAPI**. Remove all liquid. Add 200 µL diluted DAPI. Incubate at RT for 5 minutes on belly-button rocker at low speed. Permeabilization is not necessary for **external markers**.
16. Remove all liquid. Add 500 µL fresh PBS. Incubate plate for 5 minutes on belly button rocker at RT.
17. Repeat Step 16 two more times. Store plates at 4C and image within one week.

Mouse Embryoid Body Differentiation – Hanging Drop Protocol

Note: to increase neuronal differentiation, 5 μM retinoic acid can be added to the media. Add 5 μM retinoic acid on Day 2. On Day 4, change the media (50% media change) with retinoic acid. On Day 6, pipette individual embryoid bodies well dishes as in the protocol. Use a 5 mM (1000X) retinoic acid stock.

Materials

- Dulbecco's Modified Eagle Medium (D-MEM) (1X), liquid (high glucose), Invitrogen, 11960-051
- GlutaMAX™-I Supplement, Invitrogen, 35050-061
- MEM Sodium Pyruvate Solution 100 mM (100X), Invitrogen, 11360-070
- MEM Non-Essential Amino Acids Solution 10 mM (100X), Invitrogen, 11140-050
- Penicillin-Streptomycin, liquid (100 U, 100 μg/mL), Invitrogen, 15140-148
- 2-Mercaptoethanol (55 mM), liquid, Invitrogen, 21985-023
- ESGRO® (LIF), 10^7 units, Millipore, ESG1107
- Thermo Scientific HyClone* ES Cell Screened Fetal Bovine Serum (FBS), Fisher, SH3007003E
- EmbryoMax® 0.1% Gelatin Solution, Millipore, ES-006-B
- Phosphate-Buffered Saline, 1X, Cellgro, 21-040-CV
- Trypsin EDTA 1X, 0.25% Trypsin/2.21 mM EDTA in HBSS without sodium bicarbonate, calcium and magnesium, Cellgro, 25-053-CI
- BD Falcon™ 100 mm x 15 mm standard style dish, BD Biosciences, 351029 (not TC-treated, used for bacterial culture)
- BD Falcon™ 48-well Multiwell Plate. Tissue-culture treated polystyrene, flat bottom, with low-evaporation lid, BD Biosciences, 353078
- Corning Tissue Culture Dishes, Polystyrene, Sterile, Corning, 430196/430293
- EVOS xl core microscope, AMG (*optional*)
- P50 or P200 multichannel pipette
- 25 mL or smaller reservoirs for multichannel pipette
- Disposable, sterile 15 and 50 mL conical vials
- Hemacytometer
- Retinoic Acid, All Trans, Enzo Life Sciences, BML-GR100-0500

Media

mESC medium (160 mL, DMEM, high glucose + 15% FBS + 0.5% P/S + 1% GlutaMAX + 1% Sodium Pyruvate + 1% MEM NEAA + 0.18% 2-mercaptoethanol + 1000 U/mL LIF)

In tissue culture hood, add 30 mL DMEM, high glucose to a 0.22 bottle-top filter on orange cap bottle (no vacuum). Add 1.6 mL each of GlutaMAX, sodium pyruvate, and MEM NEAA. Add 0.8 mL of Pen/Strep. Add 290 μL 2-mercaptoethanol. Add 24 mL FBS. Add remaining DMEM (100 mL). Vacuum filter, aliquot media (40mL), and store at 4°C (good for one month with FBS). Add LIF to media in conical vial before adding the media to cells (good for one week with LIF).

EB medium (160 mL, DMEM, high glucose + 15% FBS + 0.5% P/S + 1% GlutaMAX + 1% Sodium Pyruvate + 1% MEM NEAA + 0.18% 2-mercaptoethanol)
Use the mESC aliquots without LIF.

Protocol

1. **Day 0**. Coat 10cm dish with 0.1% gelatin for approximately 20 minutes.
2. Wash mESCs/miPSCs with PBS.
3. Dissociate confluent mESCs/miPSCs by incubating the cells in trypsin-EDTA for 2-5 minutes at 37°C.
4. Pipette up and down with a P1000 to achieve a single cell suspension.
5. Add 1 mL EB medium. Pipette up and down and collect in a 15 mL tube.
6. Spin down cells at 1200 RPM for 2.5 minutes
7. Resuspend the cell pellet in 10 mL of EB media.
8. Incubate the cells on the gelatin-coated dish for 1 hour to remove the remainder MEF feeder layer. Place the cells on a low movement shelf in the 37°C with 5% CO_2 incubator.
9. Gently collect the mESCs that have not attached to the plate. Spin down and resuspend in 5 mL EB media. Count cells.
10. Make a $2.25x10^4$ cells/mL cell suspension (5 mL for 2-15 cms). This is about 2% of a confluent 6 cm. The cell count and adjustment of cell concentration can be done before Step 7; however, excess cells should be plated initially due to attachment of MEFs (recommend $3x10^4$ cells/mL).
11. Add the cell suspension to a reservoir.
12. Add 10 mL PBS into a 15 cm plate.
13. Carefully flip lid of 15 cm over and set down on the hood surface such that nothing will pass over the lid or the open dish.
14. With the multichannel pipette set on 20 µL. Attach 6 pipettes and pipette 20 µL drops over the top of the lid. You should be able to get 6-8 rows of 12 drops and 12 drops at the top and bottom of the lid. Carefully turn the lid over slowly. Place on top of the bottom of the dish filled with PBS.
15. Incubate at 37°C with 5% CO_2 for 2 days with no movement (leave a note on the shelf in the incubator).
16. **Day 2**. Using a P200 pipette and a 15 mL conical vial collect the EBs. With the pipette set at 200 µL, pull up approximately 25-50 µL, add a little of the media to a drop, pipette up and down once and pull up as much of the drop as possible. Continue with as many drops as you can before you reach the maximum volume in the tip. Aliquot the tip into the 15 mL conical vial.
17. Repeat Step 16 using changing out tips every time fresh media is needed. Collect all the drops on 2-15 cms.
18. Add 5-6 mL fresh media to the collected embryoid bodies with the Pipet-Aid set on slow. The total media should be approximately 10 mL.
19. Add the embryoid body suspension into a bacterial-grade sterile 10 cm dish. The embryoid bodies will not attach to the plate and will be able to continue to proliferate and differentiate in suspension. At this stage, it will be difficult to see the embryoid bodies without the use of a microscope.

20. Incubate at 37°C with 5% CO_2 for 3 days. The embryoid bodies can be cultured longer in suspension if desired.
21. **Day 5**. Coat a 24 or 48 well plate with 0.1% gelatin for approximately 20 minutes.
22. The embryoid bodies should be apparent without the use of a microscope. However, if the embryoid bodies are too difficult to see, a microscope can be used to aid in the section. Refer to the "Mouse iPSC Colony Selection" protocol for more information on using the microscope.
23. Remove the gelatin from the 24 or 48 well plate, and add 250 or 100 µL EB medium per well, respectively. With a P20 pipette set at 20 µL, pipette individual embryoid bodies into the 24 or 48 well plate. To do this, hold the lid in the left hand and carefully place the tip of the pipette near an embryoid body. Try to capture the embryoid body in the pipette tip. If no embryoid body or multiple embryoid bodies are in the tip, pipette out the liquid and try again.
24. Repeat Step 22 until embryoid bodies have been collected.
25. Swirl the plate such that most of the embryoid bodies are in the center of the well.
26. Incubate at 37°C with 5% CO_2 for 1 day.
27. **Day 6**. Change the medium by aspirating with the plate flat. Add media gently down the side of the well with the Pipet-Aid set on slow. Use 0.3 mL/24 well and 0.1 mL/48 well.
28. Repeat media changes every other day. Check the plates for differentiation.
29. **Day 12**. Check the wells for cardiomyocyte differentiation.
30. Fix the EBs when all three germ layers are present. Stain with antibodies against endodermal, ectodermal, and mesodermal markers.